

# Advancing Image Super-resolution Techniques in Remote Sensing: A Comprehensive Survey

Yunliang Qi<sup>a,1</sup>, Meng Lou<sup>b,1</sup>, Yimin Liu<sup>a,\*</sup>, Lu Li<sup>a,\*</sup>, Zhen Yang<sup>c</sup>, Wen Nie<sup>a</sup>

<sup>a</sup>*Space based Computing Systems Research Center, Zhejiang Lab, Hangzhou, 311100, Zhejiang, China*

<sup>b</sup>*Department of Computer Science, The University of Hong Kong, Hong Kong SAR, China*

<sup>c</sup>*School of Information Science and Engineering, Lanzhou University, Lanzhou, 730000, Gansu, China*

## Abstract

Remote sensing image super-resolution (RSISR) is a crucial task in remote sensing image processing, aiming to reconstruct high-resolution (HR) images from their low-resolution (LR) counterparts. Despite the growing number of RSISR methods proposed in recent years, a systematic and comprehensive review of these methods is still lacking. This paper presents a thorough review of RSISR algorithms, covering methodologies, datasets, and evaluation metrics. We provide an in-depth analysis of RSISR methods, categorizing them into supervised, unsupervised, and quality evaluation approaches, to help researchers understand current trends and challenges. Our review also discusses the strengths, limitations, and inherent challenges of these techniques. Notably, our analysis reveals significant limitations in existing methods, particularly in preserving fine-grained textures and geometric structures under large-scale degradation. Based on these findings, we outline future research directions, highlighting the need for domain-specific architectures and robust evaluation protocols to bridge the gap between synthetic and real-world RSISR scenarios.

**Keywords:** Remote sensing images, Image super-resolution, Machine learning

## 1. Introduction

Image super-resolution (SR) involves reconstructing high-resolution (HR) images from low-resolution (LR) images [1]. As a fundamental computer vision task, SR has far-reaching applications in various domains, including remote sensing [2], medical imaging [3], and security investigation [4]. However, remote sensing images (RSI) often suffer from limited spatial resolution due to sensor constraints, such as resolution, cost, orbit altitude, and transmission bandwidth. Despite these limitations, high-quality HR images are essential for real-world remote sensing applications. To address this challenge, remote sensing image super-resolution (RSISR) aims to enhance the detailed information of RSI by generating HR images from LR images, as shown in Fig. 1. RSISR has been extensively applied in land cover mapping [5], agricultural monitoring [6], disaster assessment [7], and urban monitoring [8].

Typically, RSISR approaches are categorized as single-frame or multi-frame based on input count. Single-frame methods utilize a single LR image to reconstruct a HR output, whereas multi-frame techniques exploit multiple LR observations from diverse perspectives or spectral bands to enhance reconstruction fidelity. Multi-frame SR benefits from complementary information across temporal, multi-view, or multi-sensor data, enabling improved recovery of fine details and high-frequency components. However, practical deployment is constrained by the limited availability of multi-temporal or multi-sensor imagery [9].

and the computational complexity of accurate image registration. Satellite-based applications, for instance, face challenges in acquiring multi-temporal data due to long revisit intervals. Consequently, several studies [10, 11, 12, 13] have focused on single-frame RSISR to circumvent these limitations. Motivated by these considerations, this survey primarily examines single-frame RSISR methodologies.

RSISR has been an active research area for over three decades, with a plethora of algorithms proposed to date. As illustrated in Fig. 2, the number of publications on RSISR methods has experienced a rapid surge in recent years. Early RSISR approaches can be broadly categorized into three paradigms: interpolation-based methods [14, 15], transform domain-based methods [16, 17], and reconstruction-based methods [18]. Interpolation-based methods offer the advantages of low computational complexity and real-time implementation, but their performance is often limited by the quality of the LR images, making it challenging to recover high-frequency details and real structures. In contrast, reconstruction-based methods can better preserve the perceptual properties of LR images [9], but they often suffer from high computational complexity and dependence on the detail preservation of LR images. Transform domain-based methods, on the other hand, transform the image into another domain (e.g., wavelet domain or sparse representation domain) and perform HR reconstruction by enhancing high-frequency components. Various transform domain-based methods have been proposed, including wavelet domain-based methods [16, 19], sparse representation methods [20, 18, 21], and hybrid methods [22].

In recent years, the rapid development of artificial intelli-

\*Corresponding author: Lu Li and Yimin Liu.

Email address: [lilu@zhejianglab.org](mailto:lilu@zhejianglab.org) (Lu Li)

<sup>1</sup>Contributed equally to this work.

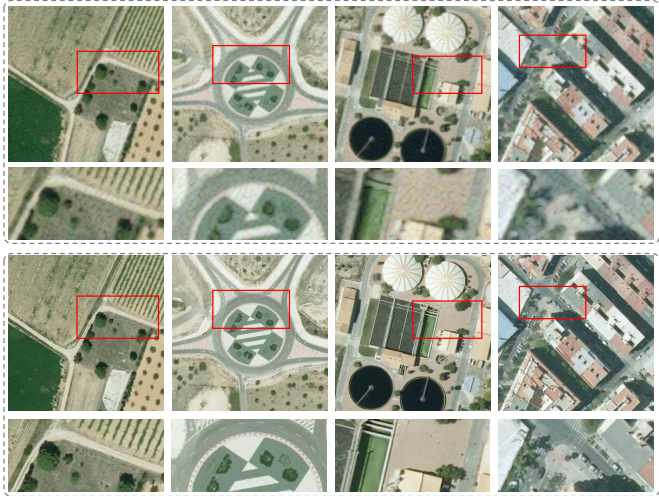


Figure 1: The benefit of remote sensing images super-resolution. The first row shows the low-resolution images, while the second row shows the results of 4x super-resolution using the SRCNN method [32, 33]. As can be seen, the super-resolution images contain richer details and texture information.

gence (AI) has led to the widespread adoption of deep learning techniques in RSISR. A plethora of deep learning-based RSISR methods have emerged, leveraging various models such as convolutional neural networks (CNNs) [23, 24], generative adversarial networks (GANs) [25, 26, 27], Transformers [28, 29, 30], and Mamba [31] to perform RSISR tasks.

Despite the numerous papers on RSISR methods published annually, there is a scarcity of comprehensive survey papers that thoroughly summarize these algorithms. While several excellent survey papers on RSISR exist [9, 14, 34, 35, 36, 2, 37, 38, 25], they remain limitations and challenges. For instance, early review papers primarily focused on conventional RSISR algorithms [9, 14], which are insufficient to meet current needs due to the lack of investigation of deep learning methods. Additionally, some surveys only cover specific types of methods, such as deep learning-based methods [35, 36, 2, 38] and GAN-based methods [25]. Liu et al. [34] conducted an excellent survey on RSISR, but it was published in 2021 and does not cover algorithms published from 2022 to 2025.

In this paper, we address these gaps by presenting a detailed, comprehensive, and systematic review of RSISR methods developed over the past two decades, covering more than 300 references. Meanwhile, the background, taxonomy, recent development characteristics, datasets and evaluation metrics in RSISR are also summarized in detail. In summary, the main contributions of this paper lie in the following aspects:

- *A comprehensive review of RSISR methods.* We conduct a thorough survey on the development of RSISR algorithms in the past two decades, including methods, datasets, and evaluation metrics. For a clearer discussion, various RSISR algorithms are classified into different categories, and their representative algorithms are introduced in detail. To the best of our knowledge, this is the most

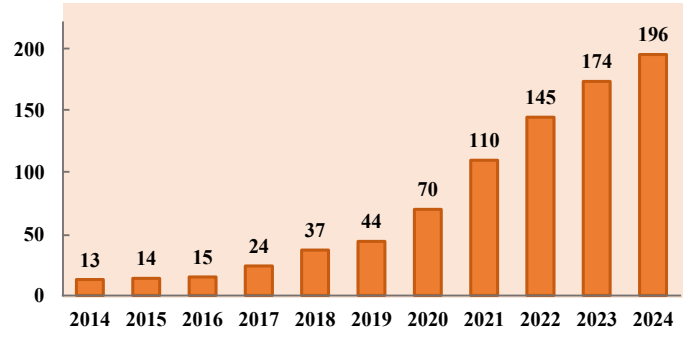


Figure 2: The number of papers about SR algorithms for RSI since 2014 (according to Web of Science).

comprehensive review of RSISR methods to date.

- *A systematic summary of the development characteristics of RSISR methods.* Recent development features are summarized based on an in-depth survey of more than 300 RSISR papers. Further, development trends and challenges can be extrapolated.
- *A detailed discussion of future prospects.* Based on a comprehensive investigation and practical experience, future prospects of RSISR methods are discussed. These insights are expected to encourage further exploration of fundamental challenges and inspire broader engagement in this rapidly evolving field.

The rest of paper is organized as follows. Section 2 introduces the background and taxonomy of RSISR methods. Section 3 and 4 elaborate on the supervised and unsupervised RSISR methods respectively, followed the recent development characteristics of the RSISR field in Section 5. Then, Section 6 analyzes the summary of datasets and evaluation metrics. Next, Section 7 discusses the performance evaluation methods for RSISR. and Section 8 discusses future prospects. Finally, Section 9 concludes this paper.

## 2. Background and Taxonomy

This section first elaborates on the image modeling background of the RSISR solution to better understand the mechanism of RSISR. Then, the category structure of the RSISR method in this paper is introduced.

### 2.1. Background of RSISR

RSISR has evolved over two decades, encompassing diverse technical branches such as multispectral image super-resolution (MSISR) [39], hyperspectral image super-resolution (HSISR) [40] and pan-sharpening [41]. RSISR has emerged as a critical research field due to the inherent resolution limitations of satellite and aerial imaging systems, which directly affect the performance of downstream applications such as land-use monitoring [5], disaster assessment [7], and urban monitoring [8].

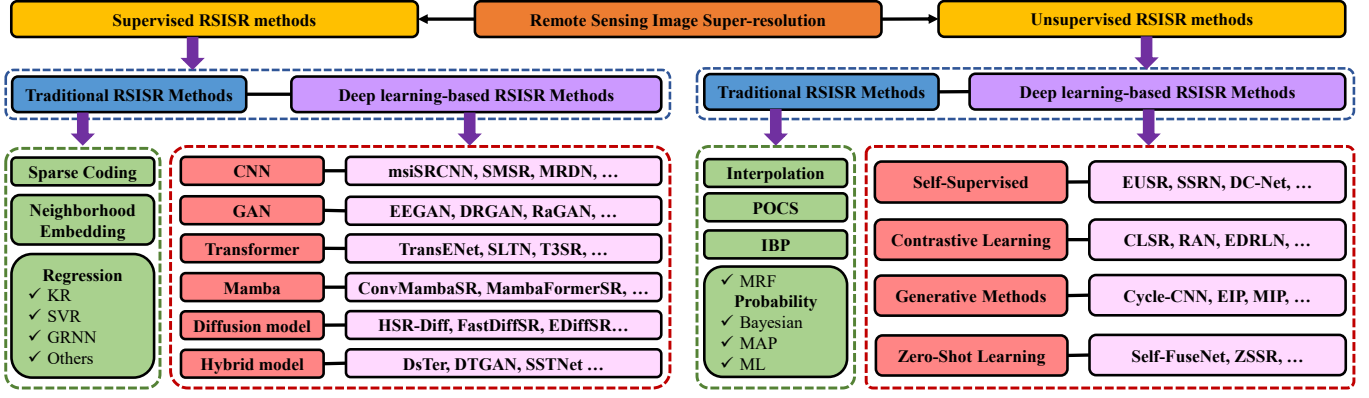


Figure 3: Taxonomy of the existing RSISR methods.

Generally speaking, the process of RSI acquisition can be understood as a sequence of degradation operations involving blurring, downsampling, and noise. Specifically, RSI acquisition can be modeled as follows:

$$I_{LR} = \mathcal{D}(\mathcal{B}(I_{HR})) + \mathcal{N} \quad (1)$$

where  $\mathcal{B}$  is the blurring operator, which represents the blurring factor introduced by the optical system, such as low-pass filtering,  $\mathcal{D}$  represents the downsampling operator of the corresponding sensor resolution, and  $\mathcal{N}$  represents the noise disturbance in the imaging process.  $I_{HR}$  and  $I_{LR}$  are the corresponding HR image and LR image of the same target scene, respectively. It can be seen from Eq.(1) that the RSISR task is a process of inversely solving RSI-degraded imaging, which is an ill-posed problem because different HR images may obtain the same LR image after passing through a specific imaging model.

## 2.2. Taxonomy of RSISR Algorithms

RSISR algorithms can be classified in different ways. Based on the latest trends in image processing, this paper conducts a comprehensive survey of RSISR algorithms from unsupervised and supervised perspectives. Fig. 3 shows a taxonomy of existing RSISR methods in this paper. Specifically, unsupervised methods and supervised methods can be grouped into traditional methods and deep learning based methods, respectively. It should be mentioned that most existing traditional RSISR methods are unsupervised, which mainly focus on the intrinsic structural characteristics and prior knowledge of the image. In addition, most deep learning-based RSISR methods are supervised, which mainly rely on large-scale labeled data to learn more complex mapping. Furthermore, supervised traditional methods can be divided into sparse coding-based, neighborhood embedding-based and regression-based methods, while unsupervised traditional methods can be divided into interpolation-based, Projection onto Convex Sets (POCS)-based, Iterative Back Projection (IBP)-based and probability-based methods. According to the type of adopted model, supervised deep learning methods can be divided into CNN-based, GAN-based, Transformer-based, Diffusion-based, Mamba-based and hybrid model-based methods. In contrast,

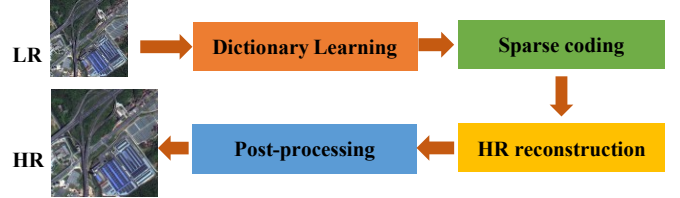


Figure 4: RSISR framework based on sparse representation.

unsupervised deep learning methods can be divided into self-supervised learning, contrastive learning, generative methods, and zero-shot learning methods. An overview of representative RSISR methods is given in Table 1.

## 3. Supervised RSISR Methods

Benefiting from machine learning methods, supervised learning-based methods are outperforming traditional methods. Generally, the supervised SR algorithms require training with HR-LR image pairs to learn the mapping relationship from LR images to HR images. This section surveys the supervised RSISR algorithms in detail from two aspects: traditional methods and deep learning-based methods.

### 3.1. Traditional RSISR Methods

#### 3.1.1. Sparse coding-based methods

Sparse coding is a learning-based method that represents a signal via an over-complete dictionary with a small number of non-zero coefficients. To the best of our knowledge, Yang et al. [115, 116] proposed the first sparse coding-based SR method, which mainly consists of three algorithmic steps: dictionary learning, sparse coding and HR reconstruction, as shown in Fig. 4. Specifically, an over-complete dictionary is first learned from the training patches, then the test patches are represented by sparse coefficients, and finally the weighted coefficients are used to reconstruct the HR image.

Some studies based on sparse representation have been conducted to reconstruct the HR images in remote sensing. For

Table 1: An overview of representative RSISR methods. Only peer-reviewed methods are summarized in this table.

Name/Reference	Year	Category	Image type	Innovations	Supervised		Deep Learning	Code
					Yes	No	Yes	
NeedFS [42]	2009	Neighbor embedding	Natural	Edge-aware feature-selected neighbor embedding	✓		✓	
Zhang et al. [43]	2011	POCS	Optical	Global weighted projection convex set optimization	✓		✓	
He et al. [20]	2012	Sparse coding	SAR	Coherence-optimized coupled multi-dictionary	✓		✓	
Zhou et al. [44]	2012	Interpolation	Natural	Multisurface maximum a posteriori fusion	✓		✓	
ANR [45]	2013	Neighbor embedding	Natural	Anchored collaborative coding super-resolution	✓		✓	✓ (Matlab)
DGNE [46]	2014	Neighbor embedding	Natural	Dual-geometric neighbor embedding	✓		✓	
Ma et al. [47]	2014	Kernel regression	Optical	Robust locally weighted kernel regression with Taylor approximation	✓		✓	
SVR-SRM [48]	2014	SVR	Hyperspectral	Example-based support vector regression	✓		✓	
JOR [49]	2015	Regression	Natural	Adaptive multi-regressor ensemble selection	✓		✓	✓ (Matlab)
SRCCNN [32]	2015	CNN	Natural	End-to-end convolutional super-resolution	✓		✓	✓ (Matlab)
SSME [50]	2016	Sparse coding	Optical	Geometric regularities embedding	✓		✓	
GRNN-SMUFI [51]	2016	GRNN	Optical	First application in urban flood super-resolution mapping	✓		✓	
Liu et al. [52]	2016	POCS	Infrared	Variable thresholds and contrast constraints via visual mechanism	✓		✓	
LGCNet [53]	2017	CNN	Optical	Multifork-structured local-global CNN prior integration	✓		✓	
Haut et al. [54]	2018	Self-Supervised	Optical	Unsupervised convolutional generative super-resolution	✓		✓	
Solanki [55]	2018	Interpolation	Optical	Wavelet-enhanced edge-directed artifact-free super-resolution	✓		✓	
Irmak [56]	2018	Probability theory	Hyperspectral	Quadratic optimization in abundance map domain	✓		✓	
EEIBP [57]	2018	IBP	Natural	Hybrid spline-adaptive evolutionary ibp optimization	✓		✓	
CSAE [18]	2019	Sparse coding	Optical	Coupled sparse autoencoder mapping	✓		✓	
EEGAN [58]	2019	GAN	Optical	Edge-enhanced GAN with noise purification and mask processing	✓		✓	
FSVMGRNN [59]	2019	GRNN	Optical	Combination of SVM and GRNN	✓		✓	
DRSEN [60]	2019	CNN	Optical	Residual squeeze-excitation channel attention				
Haut et al. [61]	2019	CNN	Optical	Visual attention mechanism				
MPSR [62]	2019	CNN	Optical	Multi-perception attention with adaptive hierarchical fusion				
RSMAP [63]	2019	SAR	Rayleigh-based sparse Bayesian deconvolution					✓
CA-FRN [64]	2020	CNN	Optical	Parameter-efficient channel-attentive recursive fusion	✓		✓	✓ (Pytorch)
MSAN [65]	2020	CNN	Optical	Multiscale activation fusion with scene-adaptive	✓		✓	
NLCSR [66]	2020	CNN	Optical	Non-local global context with multi-scale channel-spatial attention				
CDGANs [67]	2020	GAN	Optical	Coupled-discriminator GAN with dual-path adversarial learning				
EUSR [68]	2020	Self-Supervised	Optical	Dense skip-connection efficient unsupervised super-resolution				
DSSR [69]	2021	CNN	Optical	Dense multi-prior attention with chain optimization				
MHAN [61]	2021	CNN	Optical	High-order attention with frequency-aware refinement				
CGAN [70]	2021	GAN	Optical	Cascade generative adversarial networks with scene-content constraints				
MIP [71]	2021	Generative method	Optical	Unsupervised migration prior generative super-resolution				
Cycle-CNN [72]	2021	Generative method	Optical	Unsupervised cycle convolutional super-resolution				
EIP [73]	2021	Generative method	Optical	Enhanced latent prior generative super-resolution				
SSRN [74]	2021	Self-Supervised	Hyperspectral	Self-supervised spectral-spatial residual fusion				
Wang et al. [75]	2021	POCS	Hyperspectral	Gradient interpolation and adaptive iteration termination				
FeNet [76]	2022	CNN	Optical	Attention-guided lightweight lattice hierarchical fusion				
Zhang et al. [77]	2022	CNN	Optical	Blur-noise-degradation-modeled RBAN with adversarial UNet				
Fusformer [78]	2022	Transformer	Hyperspectral	Transformer-based spatial residual estimation				
TransENet [79]	2022	Transformer	Optical	Transformer-based multistage enhancement fusion				
MA-GAN [26]	2022	GAN	Optical	Multi-attention GAN with pyramid-convolutional mechanisms				
Mutai et al. [80]	2022	IBP	Optical	Wavelet-GAN with pyramid-edge-preserving fusion				
Ye et al. [81]	2022	Probability theory	Hyperspectral	Bayesian fusion for high-resolution hyperspectral imaging				
JASISR [82]	2023	Sparse coding	Optical	Adaptive joint local-nonlocal strategy				
HAUNet [83]	2023	CNN	Optical	Hybrid-attention U-Net with cross-scale lightweight interactionh				
HSR-Diff [84]	2023	Diffusion model	Hyperspectral	Conditional Diffusion HSI-MSI Progressive Denoising				
ESSAformer [85]	2023	Transformer	Hyperspectral	Efficient spectral-correlation kernel attention with linear complexity				
FSSBP [86]	2023	IBP	Multispectral	Spatial-spectral consistent back-projection fusion				
RAN [87]	2023	Contrastive learning	Optical	Contrastive region-aware graph super-resolution				
CLSR [88]	2023	Contrastive learning	Optical	Contrastive semi-supervised multi-modal super-resolution				
DRSR [89]	2023	Self-Supervised	Hyperspectral	Self-supervised degradation-guided adaptive super-resolution				
SelfS2 [39]	2023	Self-Supervised	Multispectral	Self-supervised spectral-spatial deep prior				
Self-FuseNet [90]	2023	Zero-Shot learning	Optical	Forward self-fusion single-image super-resolution				
Cha et al. [91]	2023	Zero-Shot learning	Optical	Meta-learning multi-task zero-shot super-resolution				
TSFNet [92]	2024	CNN	Optical	Two-stage spatial-frequency adaptive degradation disentanglement				
SCDM [93]	2024	Diffusion model	Hyperspectral	Spectral-cascaded Diffusion Model with Image Condition Guidance				
FastDiffSR [94]	2024	Diffusion model	Optical	Fast Conditional Diffusion with Residual Attention Efficiency				
LWTDM [95]	2024	Diffusion model	Optical	Lightweight Cross-Attention Diffusion				
SDP [40]	2024	Diffusion model	Hyperspectral	Unsupervised Spectral Diffusion Prior MAP Integration				
SSDiff [96]	2024	Diffusion model	Optical	Spatial-spectral diffusion with frequency-modulated alternating fusion				
EVADM [97]	2024	Diffusion model	Optical	Variance-aware spatial attention enhanced efficient diffusion				
EDiffSR [98]	2024	Diffusion model	Optical	Efficient diffusion with simplified attention and prior enhancement				
SRDSRN [99]	2024	GAN	Optical	Stratified dense sampling residual attention with chain training				
RGTGAN [27]	2024	GAN	Optical	Gradient-assisted GAN with deformable convolution				
ESTNet [100]	2024	Transformer	Optical	Efficient swin transformer with channel-group attention				
TTST [29]	2024	Transformer	Optical	Top-k token selective transformer with multi-scale context				
SymSwin [101]	2024	Transformer	Optical	Symmetric multi-scale Swin transformer with wavelet loss				
TTSR [102]	2024	Transformer	Optical	Local-global deformable transformer with terrain-optimized loss				
LSSwinSR [103]	2024	Transformer	UAVs	Swin transformer with semantic segmentation validation				
ConvMambaSR [104]	2024	Mamba	Optical	State-space and CNN integrated global-local fusion				
FreMamba [105]	2024	Mamba	Optical	Frequency-Mamba Fusion Framework				
MambaFormerSR [31]	2024	Mamba	Optical	Light Mamba-Transformer SR Fusion				
EDRLN [106]	2024	Contrastive learning	Optical	Contrastive degradation-aware efficient super-resolution				
TransCycleGAN [107]	2024	Generative method	Optical	Transformer-integrated unpaired CycleGAN super-resolution				
TM-GAN [108]	2024	Hybrid	RGB-D	Transformer-based multi-modal generative adversarial network				
Sharifi et al. [109]	2025	Transformer	Optical	Multihead integrated spatial-channel attention				
IRR-DiffSR [110]	2025	Diffusion model	Optical	Image reconstruction representation-guided efficient diffusion				
SGDM [111]	2025	Diffusion model	Optical	Semantic-guided diffusion with imaging characteristic decoupling				
DRGAN [112]	2025	GAN	Optical	Dynamic-convolution self-attention dense GAN				
Guo et al. [113]	2025	Probability theory	SAR	Structured Bayesian modeling for moving radar imaging				
VIT-ISRGAN [114]	2025	Hybird	Multispectral	Vision transformer with spatial-spectral attention				

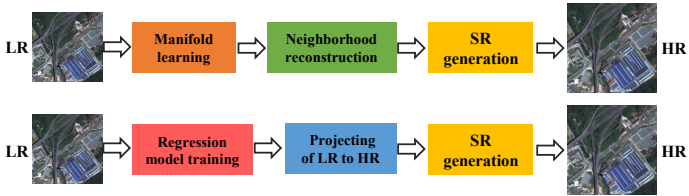


Figure 5: Two different RSISR framework. **Top row**: NE-based methods; **Bottom row**: regression-based methods.

example, Zheng et al. [117] proposed an improved sparse representation method for joint RSISR and denoising. Specifically, they employed Batch Orthogonal Matching Pursuit (Batch-OMP) for LR encoding and achieving HR patch reconstruction via jointly-trained LR-HR dictionaries with sparse representation consistency. In addition, Zhang et al. [118] divides the over-complete dictionary into the primitive dictionary pair and the residual dictionary pair. The former is used to generate the initial HR image from the LR image, and the latter is learned to reconstruct the residual loss information. Similar work in Gou et al. [119] was performed to improve performance, which presented a non-local paired dictionary learning model involving an estimated dictionary and a residual dictionary. Considering that the sparse coefficients of the observed images of LR and HR images can hardly be kept consistent, Shao et al. [18] proposed a novel coupled sparse autoencoder (CSAE) to learn the mapping relationship between LR and HR images. Besides, Deka et al. [82] proposed an adaptive joint sparse representation-based method for RSISR. The main novelty is that its dictionary learning and sparse reconstruction only depend on the input LR images. A sparse structural manifold embedding (SSME) method proposed by Wang and Liu [50] incorporated the geometric properties of images into the neighbors calculation to recover the structure and edge detail information of HR images.

Although sparse representation-based methods are effective in RSISR tasks, they still face many challenges, such as low computational efficiency, high dependence on dictionaries and low robustness. In addition, with the massive increase in remote sensing data, the real-time requirements of RSISR are becoming increasingly higher, which greatly limits the development of sparse representation methods.

### 3.1.2. Neighborhood Embedding-based

Neighborhood embedding (NE) based methods consider that small patches of LR and HR images form low-dimensional non-linear manifolds with uniform local geometry [120]. That is, as long as the number of samples is sufficient, the corresponding image in the HR domain can be reconstructed by weighted averaging the neighbors in the LR domain using the same weights. Generally, NE-based RSISR method consists of the following three steps: manifold learning, LR neighborhood reconstruction, and super-resolution generation, as shown in Fig. 5 (top row). Specifically, manifold learning calculates the reconstruction error by neighborhood weighting for HR and LR manifolds

from a specific training set and performs a minimization optimization. Given a patch  $p_i$  from the neighborhood  $N_i$ , the reconstruction error  $\varepsilon$  of HR or LR manifolds can be expressed as:

$$\varepsilon_i = \|p_i - \sum_{p_j \in N_i} \mathbf{w}_{i,j} \cdot p_j\|_2 \quad (2)$$

where  $p_j$  is an element from the neighborhood  $N_i$  and  $\mathbf{w}_{i,j}$  is the reconstruction weight matrix. For Eq. (2), the following constraints hold:  $\sum \mathbf{w}_{i,j} = 1$  and  $\mathbf{w}_{i,j} = 0$  for any  $p_j \notin N_i$  apply to  $\mathbf{w}_{i,j}$ . Furthermore, LR neighborhood reconstruction step only computes the neighborhood reconstruction weights for the LR image, representing the LR patch as a neighborhood weighted sum based on Eq. (2). Finally, super-resolution generation is performed using the LR reconstruction weights to generate high-resolution patches in the HR manifold, ensuring that the local geometric structure is preserved.

To the best of our knowledge, Chang et al. [121] first proposed the NE-based single image super-resolution method, which employed local linear embedding (LLE) [120] and achieved a good super-resolution performance. Specifically, they perform local compatibility and smoothness constraints between patches in the target HR image via overlap, demonstrating the flexibility and effectiveness of the proposed method. In some studies, feature extraction strategies are utilized to improve performance. For example, Chan et al. [42] proposed a NE-based super-resolution method by combining edge detection and feature selection, named NeedFS, which performs a specific selection of training patches based on joint features and edge detection. In addition, Xu et al. [122] proposed a two-direction self-learning SR method based on a random oscillation+horizontal propagation+vertical propagation strategy. Bevilacqua et al. [123] proposed a low-complexity SR method based on nonnegative NE, which utilized a compact and efficient feature representation strategy to reduce the algorithmic complexity. A work by Timofte et al. [45] combines sparse dictionary learning and anchored neighborhood regression for fast super-resolution tasks. In particular, they used global collaborative coding to reduce the super-resolution map to a pre-computed projection matrix, which is extremely effective in improving the algorithm speed. Yang et al. [46] proposed a dual-geometric neighbor embedding (DGNE) method for SR task, which employed the multiview features and local spatial neighbors to find manifold embedding for image.

NE-based RSISR methods take into account local neighborhood information and can effectively restore high-frequency information of the image, especially in details such as textures and edges. In addition, it retains the structural information of the image and can better avoid over-smoothing. Compared with deep learning methods, the NE-based methods have lower computational complexity and are suitable for resource-constrained environments, especially for large-scale remote sensing data processing. Although the NE-based methods are effective in RSISR, it has obvious disadvantages. For example, NE-based methods focus on the local neighborhoods, and its performance may degrade when processing global information in a larger range. In addition, the choice of neighborhood size has a great

impact on the super-resolution results. Specifically, an inappropriate neighborhood size may lead to information loss or overfitting.

### 3.1.3. Regression-based

The regression-based RSISR methods learn the function mappings between LR and HR images, which regards super-resolution as a regression problem. More specifically, these methods usually extract features from LR images based on paired datasets to train regression models, and then use the trained models to predict and reconstruct HR images. Typically, regression-based methods consist of three main steps: regression model training, projecting of LR images to HR image space, and final super-resolution result generation, as shown in Fig. 5 (bottom row).

In the past two decades, various regression-based super-resolution methods have been proposed, including kernel regression-based methods [124, 48, 125, 126], Bayesian networks [127, 128], and deep neural network methods [129, 130]. Considering the taxonomy rules of RSISR methods in this paper, the survey of deep learning-based RSISR methods are missing in this section, which can be found in the corresponding sections later. Specifically, the detailed investigations on these types of RSISR methods are as follows:

**Kernel Regression.** In 2010, Kim and Kwon [131] representatively proposed a super-resolution method based on kernel ridge regression (KRR), which uses the  $\ell^2$ -norm to train and optimize the mapping regression function. KRR is one of the simplest mapping functions for SR tasks. Furthermore, more complex super-resolution schemes have been proposed [132]. In addition, Zhou et al. [125] proposed a novel single image super-resolution method that uses kernel hill regression to connect LR image patches based on HR coding coefficients. A non-local steering kernel regression (NLSKR) method was used by Zhang et al. [133] to perform single image super-resolution tasks, which designed an effective regularization term based on the complementary properties of local structural regularity and non-local self-similarity of images, aiming to preserve sharp edges and produce fine details in the generated images. Similar works can also be found in their previous studies [134]. In RSISR task, a recent work proposed a new synthetic aperture radars (SARs) images SR method by Kanakaraj et al. [135] which extended kernel regression to the adaptive importance sampling unscented Kalman filter (AISUKF) framework to deal with speckle noise. Besides, a robust locally weighted regression method proposed by Ma et al. [47] also uses the kernel regression to perform RSISR task.

**Support Vector Regression (SVR).** As a kernel regression method, the SVR-based RSISR method has also been widely studied. More concretely, SVR methods involve using high-dimensional feature space to find nonlinear mappings, which is widely used for RSISR tasks and achieves good performance. For example, Zhang et al. [124] proposed a SVR-based RSISR method that learns prior knowledge between HR and LR images. In particular, bilinear interpolation is employed in their method to upsample to the same resolution and preserve high-frequency information. Besides, Zhang et al. [48] proposed an

SVR-based super-resolution mapping method (SVR\_SRM) for the land cover map. Specifically, SVR\_SRM learns the non-linear relationship between coarse-resolution pixels and corresponding labeled sub-pixels to generate fine-resolution land cover maps from the selected best matching training data. However, SVR\_SRM method is sensitive to fraction errors, resulting in many linear artifacts and speckles in the super-resolution results. To this end, Zhang et al. [136] again proposed an improved SVR\_SRM method, which mainly used the back-projection operation and the local smoothness prior model to improve the performance of RSISR.

**General Regression Neural Network (GRNN).** General Regression Neural Networks (GRNN) is a memory-based neural network model [137], which has been used in some studies to improve the performance of RSISR. For example, Li et al. [51] proposed a new GRNN-based method for super-resolution mapping of urban flooding (SMUF) in remote sensing images. In the GRNN-SMUF method [51], a local SMUF model is constructed based on GRNN to describe the relationship between the sub-pixel distribution within a mixed pixel and the scores of the eight neighboring pixels of the mixed pixel. In 2019, Li et al. [59] once again proposed a new SMUF method based on support vector machine and general regression neural network, and named it FSVMGRNN-SMUF. Different from GRNN-SMUF, the FSVMGRNN-SMUF method uses a combination of several SVMs to build a local SMUF model and achieves better performance.

**Other Regression Methods.** In addition to the above-mentioned regression-based methods, some other regression-based RSISR approaches have also been proposed. For example, Yang et al. [138] trained several simple mapping functions to perform super-resolution tasks. In addition, Dai et al. [49] proposed an adaptive optimal regressor selection method for the super-resolution task, which selects the most appropriate regressor for each input patch, which jointly produces the minimum super-resolution error for all training data. Yang et al. [139] proposed a soft-assignment based multi-regression method for RSISR, which reconstructs a high-resolution (HR) patch through a dictionary corresponding to its K-nearest training patch clusters. Gao et al. [140] proposed a self-dictionary regression based method for hyperspectral image super-resolution.

In summary, traditional supervised SR research work mainly focused on the period before 2016, which was attributed to the fact that deep learning methods had not been fully explored before that time. Generally speaking, the calculation of conventional supervised SR methods is relatively simple and suitable for application scenarios with limited hardware resources. Nevertheless, they rely heavily on the relationship between local pixels, which cannot fully extract deep features and high-level semantic information of images, resulting in suboptimal performance. In addition, in high super-resolution (such as  $\times 4$  or  $\times 8$ ) reconstruction tasks, these conventional methods often fail to recover sufficient details, resulting in blurry or distorted results. For example, regression-based methods are easily affected by noise, resulting in a decrease in reconstruction quality.

### 3.2. Deep learning-based RSISR Methods

As mentioned above, conventional supervised RSISR methods have many shortcomings, such as the inability to extract deep features and high-level semantic information of images. In addition, these methods often rely on manually designed feature extractors, which cannot automatically learn complex patterns and structures in images. With the rapid development of artificial intelligence (AI) technology, deep learning has attracted widespread attention, and a large number of deep learning-based RSISR methods have been studied, which can perform end-to-end training on a large amount of data and automatically learn the details and high-level semantics of images to overcome the shortcomings of traditional methods.

In this section, supervised deep learning-based RSISR methods are surveyed and discussed in detail from the perspectives of CNN-based, GAN-based, Transformer-based, Mamba-based, and hybrid methods. More specifically, in order to provide a comprehensive and in-depth discussion of the methods in this category, we conducted a detailed discussion of the literatures up to 2025.

#### 3.2.1. CNN-based RSISR

The prototype of convolutional neural network (CNN) originated from LeNet-5 proposed by LeCun et al. [141], which was the first CNN model to be successfully applied to visual recognition. Since 2012, benefiting from the rapid development of computing resources and hardware technologies such as GPU, CNN had been widely studied and many CNN models had been proposed, such as AlexNet [142], VGG [143] and ResNet [144], etc. These CNN architectures are widely used in computer vision tasks such as image segmentation [145], object detection [146] and image enhancement [147], etc.

In recent years, CNN-based super-resolution methods have been widely studied. Dong et al. [32, 33] first applied CNN to the super-resolution task and achieved good performance. In addition, benefiting from the great success of deep learning, many CNN-based RSISR methods have also been proposed. To the best of our knowledge, Leibel and Korner [148] proposed the first CNN-based RSISR method, namely msiSRCNN, which utilizes remote sensing data (Sentinel-2 images) to train and fine-tune SRCNN [32, 33], as shown in Fig. 6. Specifically, they fine-tuned SRCNN based on the luminance component of the YCbCr color space of remote sensing images and performed performance evaluation.

**Multi-Scale Features.** Many studies utilized multi-scale features to improve the performance of RSISR. For example, Fu et al. [149] proposed a multi-scale CNN framework (RSCNN) for the RSISR task. Specifically, RSCNN employed convolution kernels of different sizes to extract multi-scale features of images and improved the reconstruction performance of HR images. The idea of extracting multi-scale features based on convolution kernels of different sizes is also involved in these works [150, 151]. A multi-scale residual neural network (MRNN) proposed by Lu et al. [152] also uses complementary features in the patches of different sizes from LR satellite images. Dong et al. [153] proposed a second-order multi-scale super-resolution network (SMSR) for RSISR. In addition,

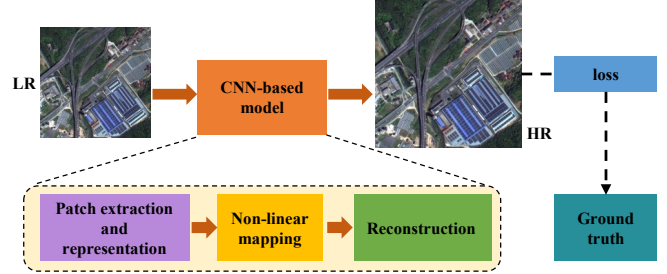


Figure 6: The schematic diagram of the SRCNN-based RSISR method [148].

Wang et al. [154] proposed an adaptive multi-scale fusion network (AMFFN) for RSISI. Specifically, several adaptive multi-scale feature extraction (AMFE) modules and the squeeze-and-excited adaptive gating modules are utilized for feature extraction and fusion. In the work of Huan et al. [155], a symmetric multi-scale super-resolution network (AMSSRN) was designed to fully extract and utilize image features. Specifically, they proposed a residual multi-scale block (RMSB) and a residual multi-scale erosion block (RMSDB) to extract shallow and deep features of the image. Multi-scale feature representation is also involved in the RSISR work of Jiang et al. [156], who proposed a deep distillation recurrent network (DDRN) that performs multi-path feature sharing through ultra-dense residual blocks (UDBs) and multi-scale purification unit (MSPU). Besides, DeepNESRM method [157] uses multi-level feature fusion CNN to eliminate score errors while combining multi-scale information to optimize the mixed pixel problem. On the other hand, residual connections play an important role in solving the gradient vanishing problem of deep networks and are widely used in RSISI tasks. For example, Huan et al. [158] proposed a new pyramidal multi-scale residual network (PM-SRN) for RSISR, which adopts hierarchical residual-like connections to improve the performance. Deeba et. al [159] proposed a transferred wide residual deep neural network model for RSISR, which reduces the memory cost of the network by increasing the width of the residual network and reducing its depth. In addition, Ye et al. [160] proposed a lightweight RSISR framework, which involves a novel multi-scale residual attention information distillation group to extract richer regional features. More specifically, they adopted a high- and low-frequency separation reconstruction strategy to enhance the high-frequency details of the image. Considering that most CNN methods ignore low-weight background features, Wu et al. [161] proposed a background-based multi-scale feature enhancement network (BMFENet) for RSISR, which constructs a large kernel feature supplement block (LFSB) to generate background feature weights for enhancing the attention of ignored information. Similar work includes the multiscale residual dense network (MRDN) proposed by Kong et al. [162] and the dual-path feature reuse multi-scale network (DFMNet) proposed by Xiao et al. [163].

**Attention mechanism.** With the remarkable achievements of deep learning in computer vision tasks, the attention mechanism has been widely studied, which dynamically weights in-

put features to enhance the network's ability to focus on important information while suppressing irrelevant or redundant information. In recent years, many researchers have applied the attention mechanism to the RSISR task and achieved remarkable success. Gu et al. [60] proposed a Deep Squeeze and Excitation Network (DRSEN) for the RSISR task, which involves a Residual Squeeze and Excitation Block (RSEB) to fuse the input of the current block and its internal features, and model the interdependencies and relationships between channels. Besides, Dong et al. [62] proposed a multi-perception attention network (MPSR) for RSISR, which combines an enhanced residual block (ERB) and a residual channel attention group (RCAG) to more effectively perform weighted fusion of multi-level information. A channel-attention-based fused recurrent network (CA-FRN) proposed by Li et al. [64] performs sufficient attention on high-frequency information.

Similar RSISR methods include Haut et al. [61], which focuses on valuable high-frequency information and ignores uninformative low-frequency features based on the attention mechanism. Considering the necessity of describing remote sensing images from multiple scenes, Zhang et al. [65] proposed a multi-scale attention network (MSAN) for RSISR, which employs a scene-adaptive super-resolution strategy to more accurately describe the structural characteristics of different scenes. In addition, Chen et al. [164] proposed a novel residual split attention network (RSAN) for RSISR, which can simultaneously maintain the overall structure and local details of the image, as shown in Fig. 5 (a). Recently, the research on digital elevation model super-resolution (DEM-SR) has also been carried out, which is of great significance for accurately providing remote sensing geographic information. For example, Chen et al. [165] proposed an integrating attention mechanism (IAM) network method for DEM-SR, which can well capture long-range geographic feature dependencies and local context information, as shown in Fig. 5 (b). In order to solve the problem of limited global receptive field in RSISR, some studies have been performed. For instance, Wang et al. [66] proposed a non-local up-down convolutional attention network (NLASR), which mainly designed a feature enhancement module (NLEB) to model spatial long-range dependencies. Wang et al. [83] proposed a hybrid attention U-type network (HAUNet) for the RSISR task to fuse multi-scale global semantic information. In addition, some research works are devoted to solving the problem of high- and low-frequency information aliasing in CNN-based RSISR methods. For example, Peng et al. [166] designed a gated convolution unit to separate the frequency domain information flow, and further proposed a pre-training of gated convolution neural network (PGCNN) for RSISR. Besides, Zhao et al. [167] used a structure-texture dual preservation strategy to constrain edge generation. Zhang et al. [77] further proposed a residual balanced attention network (RBAN) and combined adversarial training to improve the authenticity of high-frequency textures. Aiming at the large-scale super-resolution reconstruction of remote sensing images, Gao et al. [69] proposed a dense sampling super-resolution network (DSSR) RSISR method, which introduced a dense sampling mechanism, a wide feature attention module and a chain training strategy to improve the net-

work performance. For multi-level feature fusion, Wang et al. [168] proposed a multi-scale spatial-spectral network (M3SN) method, which couples 3D convolution with spectral attention, aiming to deeply mine shallow and deep spatial-spectral features in hyperspectral image super-resolution tasks, thereby improving reconstruction performance. With similar motivations, Chen et al. [169] proposed a residual aggregation-segmentation attention fusion network (RASAF) to achieve cross-channel interaction for RSISR.

On the other hand, some attention-based strategies have been studied to improve the local detail recovery capability of RSISR methods. For example, Ma et al. [170] proposed a dense channel attention mechanism to enhance high-frequency feature reuse. Patnaik et al. [171] combined multi-scale residual attention to capture fine-grained texture for RSISR, and Zhang et al. [172] introduced hybrid high-order attention (HOA) to mine deep statistical associations. In addition, Huang et al. [173] proposed a deep residual dual attention network (DR-DAN) method, which introduced a residual dual attention module (RDAB) and a local multi-level fusion module to fuse global and local information. Wang et al. [76] proposed a lightweight feature enhancement network (FeNet) for RSISR, which constructed a lightweight lattice block (LLB) and used channel separation and weight sharing to reduce the computation amount. In the field of lightweight research, Wang et al. [174] proposed a feedback ghost residual dense network (FGRDN), which introduces a spatial-channel attention module (SCM) to extract key features and reduces redundant parameters through feedback mechanism and Ghost module. The enhanced residual convolutional neural network (ERCNN) proposed by Ren et al. [175] also uses a feature attention module, which enhances the discriminative learning ability across feature maps and combines a dual-brightness scheme to optimize high-frequency recovery.

**Transform domain.** In recent years, some studies have combined CNN with transform domain to perform RSISR, which utilizes the frequency band decomposition capability of domain transform (such as wavelet transform and Fourier transform) and the feature modeling advantages of deep learning to improve the reconstruction performance. For example, Wang et al. [176] proposed a RSISR method combining wavelet multi-scale decomposition with multi-branch CNN. Specifically, they trained the network independently and predicted sub-images in different directions and frequency bands respectively, and then synthesized high-resolution aerial images through inverse wavelet transform, which verified the applicability of frequency domain modeling for complex scenes. Two studies in 2019 further deepened the frequency domain framework in RSISR. Ma et al. [16] proposed a recursive residual network (Recursive Res-Net) to predict high-frequency components, innovatively replaced low-frequency subbands with low-resolution images to preserve details, and optimized network efficiency by removing batch normalization layers. In addition, Yang et al. [177] proposed a multi-scale wavelet 3D convolutional neural network (MW-3D-CNN) for hyperspectral image super-resolution, which uses three-dimensional convolution to extract spatial spectral features and uses L1 loss to optimize multi-subband wavelet coefficient prediction, realizing joint spatial-

spectral reconstruction of hyperspectral data. Furthermore, the work of Aburaed et al. [178] also verified the effectiveness of wavelet analysis for reconstructing high-frequency details. In 2021, Deeba et al. [179] proposed a fast wavelet super-resolution framework (FWSR), which accelerates image restoration through approximate sub-band input and sub-pixel layer, and enhances the ability to retain high-frequency features. Sandana et al. [180] proposed a CNN combining wavelet and multi-wavelet transform (CWM-CNN), which integrates discrete wavelet and multi-wavelet transform to extract shallow features, and combines a compact three-layer CNN to achieve parameter-efficient high-resolution reconstruction. Recently, Wang et al. [92] proposed a two-stage joint space-frequency network (TSFNet) to address the problem of large-scale super-resolution. Specifically, they designed an amplitude-guided phase adaptive filtering module (AGPF) to decouple frequency domain degradation features, and achieved progressive detail optimization through cross-stage feature fusion, achieving good performance in maintaining structural integrity.

**Spatial-Spectral Joint Modeling.** In recent years, some studies have focused on joint spatial-spectral modeling to achieve higher quality reconstruction by fusing the spatial context and spectral correlation of images. For example, early work [181] employed CNN to directly learn the mapping from low-resolution bands to high-resolution bands end-to-end based on the inherent resolution differences of Sentinel-2 multi-bands (10m/20m/60m), while implicitly utilizing the spatial features of high-resolution bands to guide the reconstruction of low-resolution bands. Yin et al. [182] proposed a DeepRivSRM method for RSISR. Specifically, they extracted the river spectral features in mixed pixels by spectral unmixing, and then combined the spatial context for super-resolution mapping. To further enhance physical consistency, some studies have injected explicit physical model constraints. For example, Arun et al. [183] proposed a collaborative unmixing framework based on sparse coding for RSISR, which jointly optimized the sparse dictionary and spectral reconstruction, and fused the spatial-spectral prior through the encoding-decoding architecture to ensure spectral fidelity. In addition, Wagner et al. [184] employed a deep residual network (ResNet) to fuse shallow spectral features with deep spatial features via jump connections to achieve end-to-end spectral-spatial joint optimization. Vasilescu et al. [185] innovatively embedded the modulation transfer function (MTF) of the sensor into the multi-objective loss function to simulate the sensor degradation process and force the network to learn the physical consistency of the inverse mapping. In addition, they combined high-frequency detail alignment loss (such as 10m band gradient matching) to improve the accuracy of spatial detail reconstruction. In the recent work of Chen et al. [186], a spatial-spectral attention module (DSSA) combined with a dilated convolution method was proposed to extract global spatial features, and the 3D Inception module was used to mine multi-scale spectral information to solve the problem of spectral-spatial information imbalance in hyperspectral images. In addition, Mei et al. [187] proposed two end-to-end joint optimization framework for RSISR, namely simultaneous spatial-spectral joint SR (SimSSJSR) and separated spa-

tial-spectral joint SR (SepSSJSR). Specifically, spectral unmixing, regularized deconvolution, and endmember similarity constraints are employed to ensure spectral consistency. Müller et al. [188] performed panchromatic band (PAN) and multispectral band fusion, which used CNN training to improve the spatial resolution of multispectral satellite images.

**Local-Global Feature Fusion.** This type of methods usually captures the local detail features and global prior information of remote sensing images, and uses multi-scale feature fusion mechanism to improve the quality of super-resolution reconstruction. For example, the local-global combined networks (LGCNet) proposed by Lei et al. [53] adopts a multi-branch structure to achieve multi-level representation learning. Besides, Xu et al. [189] proposed a deep memory connected network (DMCN) for RSISR, which achieves feature integration by building local-global memory connections. These studies all emphasize the integration of scene-level semantic information while maintaining local texture details. They generally introduce spatial downsampling units to optimize computational efficiency and balance model complexity and performance by compressing the size of feature maps.

**Others CNN-based Methods.** In addition to the above-mentioned CNN-based methods, some other CNN-based RSISR approaches have also been proposed. For example, Chang and Luo [190] proposed a bidirectional ConvLSTM network, which reuses local low-level features through a recursive inference block and combines a bidirectional ConvLSTM layer to adaptively select complementary information. Zhu et al. [191] proposed a degradation model based on satellite imaging and ground post-processing to improve the SR performance of real satellite images. Deeba et al. [192] proposed the Wide Remote Sensing Residual Network (WRSR), which optimizes the efficiency of single-image super-resolution by increasing the width of the residual network, reducing the depth, and using weight normalization to reduce memory costs. Wei and Liu [193] introduced dilated convolution into residual dense blocks while keeping parameters and receptive fields unchanged, and combined them with cloud services to optimize remote sensing image reconstruction. In addition, Zhao et al. [194] utilized super-Laplacian gradient prior to constrain SR reconstruction and enhanced geometric structure recovery through second-order supervision. Some recent studies have used multimodal fusion to improve performance. For example, the DeepOSWSRM method proposed by Yin et al. [195] fuses Sentinel-1 SAR and Sentinel-2 optical images to solve the cloud occlusion problem and further generate high-resolution water distribution maps. In addition, Dai et al. [196] utilized the polarization information and spatial features of polarimetric SAR to extract and fuse polarization context features through a dual-branch architecture to improve the super-resolution performance of PolSAR images.

### 3.2.2. GAN-based RSISR

In 2017, Ledig et al. [197] first applied generative adversarial networks (GANs) to image super-resolution. Since then, many GAN-based RSISR methods have been proposed, and GAN-based methods have become one of the most important types of

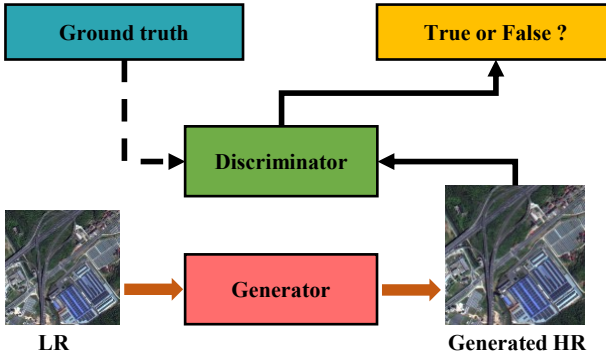


Figure 7: The schematic diagram of the GAN-based RSISR method.

RSISR methods. In general, The GAN-based RSISR methods consist of generators and discriminators. The generator reconstructs the LR image into an HR image, and the discriminator determines whether the image is a true HR (GT HR). Specifically, a two-stage training strategy is adopted in this type of methods. First, the generator is frozen to train the discriminator, thereby enhancing its discrimination ability. Then the discriminator is frozen to train the generator, and the generation result is continuously optimized through adversarial feedback. At the same time, reconstruction loss and perceptual loss are used to improve image structure restoration and visual quality.

**Network architecture optimization.** Some studies improve the generator and discriminator structures to enhance feature extraction and reconstruction capabilities. For example, Ma et al. [198] reduced the computational burden by removing the batch normalization layer, and used transfer learning to alleviate the problem of insufficient data. Subsequently, in their follow-up research, the DRGAN method [199] designed a dense residual generator and combined it with Wasserstein GAN to improve training stability. Guo et al. [70] proposed a cascaded GAN method for RSISR, which introduced scene constraints and edge enhancement modules to improve performance. In addition, Wang et al. [200] innovatively constructed a two-dimensional matrix topology structure to significantly increase the connection density of the network for RSISR. The EEGAN method [58] proposed a dual-branch network structure to suppress noise through an edge enhancement subnet. Furthermore, the TDRRDB-EEGAN method [201] improved the edge purification module of EEGAN and combined the intermediate image with the enhanced edge to generate clear results. Pang et al. [202] replaced the generator with ResNet-50 and inserted a fully connected layer in the discriminator, significantly improving the quality of super-resolution images while maintaining the reconstruction speed. Liu et al. [203] proposed a cascaded conditional Wasserstein GAN combined with residual dense blocks to optimize gradient propagation. Guo et al. [204] designed a multi-level dense network and matrix mean discriminator to optimize the reconstruction of real aerial images. Similarly, Sustika et al. [205] combined the residual dense network (RDN) with GAN to balance objective indicators and perceptual quality. In 2023, the MSRBGAN method proposed by

Zhao et al. [206] introduced multi-scale residual blocks and GAM attention to improve the performance of RSISR. The DRGAN method in recent work [112] proposed dynamic convolution and self-attention mechanism to further optimize feature extraction.

**Attention Mechanisms.** Attention mechanisms and multi-scale modeling are used in some studies. A typical example is that SCSE-GAN [207] first introduced spatial-channel attention into the generator to enhance feature representation. In addition, Li et al. [208] improved performance by capturing long-range dependencies based on local and global attention. Zhang et al. [209] proposed a coordinated attention mechanism and residual stacking strategy to optimize landslide scene reconstruction. Jia et al. [26] integrates pyramid convolution residuals, pixel attention, and branch attention to improve the performance of RSISR. Furthermore, Wang et al. [210] optimizes RSISR algorithm by combining multi-scale structure with channel-spatial attention. The CEEGAN proposed by Ren et al. [211] designs an edge feature enhancement module (EFEM) to fuse multi-scale contextual information and optimize edge recovery for RSISR. In 2024, MFFAGAN proposed by Tang et al. [212] developed a multi-level feature fusion module to enhance key information extraction through hybrid attention. The TDEGAN method [213] introduces Shuffle attention and artifact loss functions to effectively restore high-frequency textures. Similarly, SRDSRAN [99] and SRGAN-MSAM-DRC [214] use layered dense sampling and multi-scale attention mechanisms to significantly improve the performance of large-scale RSISR.

**Loss Functions and Training Strategies.** Some studies have focused on optimizing loss functions and training strategies to further improve the performance of RSISR. In 2019, Lei et al. [67] proposed a coupled discriminator to alleviate the low-frequency region discrimination ambiguity through a dual-path network and a random gate mechanism. In addition, Fan et al. [215] used a U-Net discriminator combined with a CBAM module to enhance detail discrimination for RSISR. Similarly, a RGTGAN method proposed by Tu et al. [27] designed a gradient-assisted texture enhancement module (GTEM) and a dense-intern deformable convolution (DID-Conv) to improve cross-view alignment for RSISR. On the other hand, the RWDM method [77] constructs a real degradation training dataset and combines it with the residual balanced attention network (RBAN) to improve the reconstruction effect of the actual scene. In addition, the BLG-GAN method [216] uses a two-stage training strategy to migrate real LR images to the bicubic degradation domain to alleviate the simulation data bias. MCWESRGAN method [217] uses Wasserstein loss and multi-column discriminator to accelerate training for RSISR. Zhu et al. [218] introduced the relative average GAN (RaGAN) reconstruction loss to optimize edge detail learning, and Guo et al. [219] improved texture fidelity based on Charbonnier loss and semantic perception loss.

**Cross-modal and Multi-task fusion.** Recently, cross-modal methods have been studied. For example, Kong et al. [220] combined Planet Fusion with Landsat data to generate high spatiotemporal resolution NDVI series. In addition, Sun et

al. [221] fused high-resolution optical images with digital surface models (DSM) to preserve terrain features through slope loss. The VHR-GAN method [222] uses PeruSat1 satellite data to achieve super-resolution of Sentinel-2 images. In addition, Huang Hejing [223] combines wavelet transform to optimize frequency domain feature expression. The MRSISR method [224] proposes a multi-frame super-resolution framework that uses temporal information to optimize video satellite image reconstruction. Some other examples are the Enlighten-GAN method [225] and recent work [226] which both integrate spatial image modality and frequency domain modality information, and optimize the RSISR algorithm by combining perceptual loss with pixel reconstruction loss.

### 3.2.3. Transformer-based RSISR

In recent years, Transformer has been widely applied in the field of natural language processing due to its unique self-attention mechanism and global modeling capabilities. Different from CNN, Transformer efficiently captures long-range dependencies and achieves global information interaction by dynamically calculating the correlation between all elements in the input sequence [227]. Furthermore, Vision Transformer (ViT) has proven that it can achieve competitive or even better performance than CNN in computer vision tasks such as image classification and object detection, especially in the ability to model complex textures and global structures [228].

In the field of RSISR, the conventional CNN-based methods still face challenges due to the inherent properties of remote sensing images, such as the coexistence of multi-scale targets, complex spectral-spatial coupling characteristics, and low processing efficiency of large-size images. In addition, the conventional CNN-based approaches often struggle to capture global contextual information due to their limited local receptive fields, frequently resulting in edge blurring or undesirable artifacts. In contrast, Transformer architecture's global attention mechanism offers a promising solution to address these limitations. To the best of our knowledge, Ye et al. [229] proposed the first Transformer-based RSISR method, which combines CNN and Transformer modules to achieve efficient super-resolution reconstruction of LR remote sensing images. Since then, various Transformer-based RSISR methods have been proposed, including transform-domain-based, multi-scale features, multi-modal fusion, special modality input, and improved self-attention mechanisms, and the detailed survey in this section is as follows:

**Multi-Scale Features.** Many studies considered the complexity of remote sensing image scenes and utilized multi-scale feature fusion to improve performance. Specifically, multi-scale feature fusion methods effectively balance the global structure coherence and local detail authenticity through dynamic weight allocation. Early studies such as TransENet proposed by Lei et al. [79] built a multi-stage enhanced structure based on Transformer, which embeds and fuses multi-scale high/low-dimensional features through an encoder-decoder architecture, breaking through the limitation of traditional models that rely on upsampling layers and ignore high-dimensional spatial features. In addition, the MSFNet proposed by Shi et

al. [230] achieved hierarchical feature propagation and adaptive cross-scale fusion across iteration stages based on multi-scale implicit constraints and row-column decoupling Transformer modules. Shang et al. [231] proposed a hybrid-scale hierarchical Transformer network (HSTNet) for RSISR, which explicitly modeled single-scale and cross-scale long-range dependencies via hybrid-scale recursive feature mining and enhanced the discriminative ability of high-dimensional features. In 2024, some studies have made breakthroughs in balancing computational efficiency and multi-scale perception. For example, SymSwin proposed by Jiao et al. [101] involved a symmetric multi-scale window mechanism (SyMW) and cross-receptive field adaptive attention (CRAA), which dynamically fuses contextual features of different sizes and enhances supervision through frequency domain wavelet transform loss (UWT). In addition, Lu et al. [232] proposed a Multi-Scale and Global Representation Enhancement-based Transformer (MSGFormer), which designed the dual-window self-attention (DWSA) and multi-scale deep convolutional attention (MDCA), and tracking back structure (TBS) to capture local-global multi-scale features at a lower computational cost. For geographic data, Wang et al. [102] introduced local-global deformable blocks (LGDB) to fuse the multi-scale heterogeneity of terrain, supplemented by spatial-channel coupled attention, which significantly alleviated the local smoothing problem in DEM reconstruction.

**Transform Domain.** The transform domain-based methods mainly separate the high- and low-frequency information of the image via frequency domain decomposition (such as wavelet transform and Fourier transform), and utilize the global attention mechanism of Transformer to strengthen the feature correlation. For example, the CFMB-T method proposed by Cao et al. [233] in 2023 employs SwinIR as the architecture, which separated the frequency domain features of infrared remote sensing images through wavelet decomposition, and adds degradation priors and recursive modules to improve performance. The dual SR framework [234] in 2024 further combined self-supervised learning with wavelet fusion, and modeled the long-range spatiotemporal dependency of remote sensing images through the Transformer attention mechanism, effectively solving the problem of periodic resolution degradation caused by the rotating synthetic aperture system. Recently, Xie et al. [235] proposed a RSISR framework based on Swin Transformer, named CFFormer, which enhances feature expression through frequency domain channel Fourier blocks (CFB) and global attention modules (GAB), and optimizes gradients by combining jump joint fusion mechanism. In addition, Liu and Yang [236] proposed a frequency domain feature hierarchical architecture based on discrete wavelet transform (DWT), which learns the correlation between full-band and high-frequency features through a self-attention mechanism. In summary, Transform-domain-based methods usually outperform pure spatial domain models, especially showing stronger detail reconstruction capabilities in complex degradation scenarios.

**Multi-modal Fusion.** Some studies have used the complementary information fusion method of hyperspectral (HSI) and multispectral (MSI) modalities to improve the performance

of RSISR. For example, Hu et al. [78] first proposed the Fusformer framework for the hyperspectral super-resolution (HISR) task. Specifically, the low-resolution hyperspectral image (LR-HSI) is used as the core to preserve the spectral integrity, and the spatial residual is estimated on the LR-HSI, thereby simplifying the complex mapping into small spatial residual learning. Li et al. [237] proposed a spectral learning based Transformer network (SLTN). Specifically, they designed a spectral response function (SRF) guided multi-level feature extraction module (MFEM) and a cascaded nonlinear mapping learning module (NMLM) to address the spectral complexity and degradation problems of remote sensing scenes.

**Special Modality-guided.** Recent studies have employed special modality input to improve the performance of Transformer in RSISR tasks. For example, Cai and Zhang [238] proposed a texture transfer transformer-based RSISR (T3SR) method, which first introduced the texture transfer paradigm into the remote sensing field, and solved the single image texture loss problem through a two-stage framework of shallow texture transfer and U-Transformer feature fusion, while greatly reducing the model’s dependence on reference images. In addition, the hybrid attention model proposed by Alireza and Mahdi [109] combines multi-head attention and spatial-channel attention mechanisms, which is optimized for the multispectral characteristics of Sentinel-2, and achieves SOTA performance. GeoSR framework for drone images proposed by Zhao and Li [103] pioneered a task-driven evaluation paradigm, which uses semantic segmentation accuracy as a supplementary modality to traditional PSNR/SSIM, and establishes a positive correlation between super-resolution quality and 8.6% accuracy of object classification. These studies further illustrated the potential of special modality-guided reconstruction such as texture/gradient/semantic maps in improving RSISR performance.

**Improved Self-attention Mechanisms.** In order to solve the problems of high computational complexity, insufficient local receptive field, and inefficient cross-stage feature fusion in the traditional global self-attention mechanism, some research based on improving the self-attention mechanism has been carried out to improve performance. Specifically, most of these studies are mainly based on enhancing context modeling capabilities, optimizing feature fusion efficiency, and reducing computational complexity. For example, Lu et al. [239] proposed a cross-spatial pixel integration and cross-stage feature fusion-based transformer network (SPIFFNet) for RSISR. Specifically, the spatial pixel integration attention (CSPIA) module is designed to introduce contextual information into the local window, and the cross-stage feature fusion attention (CSFFA) module is designed to achieve adaptive feature transfer. The ESSAformer method proposed by Zhang et al. [85] developed a kernelized self-attention (ESSA) based on spectral correlation coefficient, which reduces the computational complexity to linear and strengthens the interaction of spectral features. In addition, Mao et al. [240] proposed a distance-enhanced strip attention transformer (DESAT), which enhances spatial correlation by fusing strip window attention with distance prior, and designed an attention-enhanced upsampling module. Kang et al. [241] recently proposed an Aggregation Connection Trans-

former (ACT-SR) for RSISR, which constructs an aggregate connection attention block and uses a series-parallel hybrid connection to fuse spatial-channel features, supplemented by a gated feedforward network to enhance nonlinear expression capabilities. In addition, the scale-aware backprojection Transformer (SPT) proposed by Hao et al. [242] innovatively combined backprojection learning with Transformer to construct a scale-aware self-attention layer, thereby improving feature learning efficiency. Kang et al. [28] proposed an efficient Swin Transformer (ESTNet) via channel attention, which reduces the number of parameters by 83% by synergizing group attention with efficient channel attention. In recent work, Xiao et al. [29, 30] proposed a Top-k Token Selective Transformer (TTST) for RSISR, which designed a three-level self-attention optimization framework involving Residual Token Selective Group (RTSG), multi-scale feature fusion (MFL) and Global Context Attention (GCA), further solving the redundant calculation and single-scale modeling limitations of self-attention in specific tasks.

### 3.2.4. *Mamba-based RSISR*

Recently, empowered by state space model (SSM) involving near-linear complexity modeling long-distance dependencies, Mamba [243] has demonstrated superior performance compared to Transformer in natural language processing (NLP). Specifically, Mamba introduces a selective mechanism into the traditional SSM to improve computational efficiency and significantly enhance the ability to model long sequences. Building on success in sequence modeling, Mamba has recently demonstrated remarkable potential across diverse vision domains, achieving state-of-the-art performance in fundamental tasks, including image classification [244], object detection [245], and semantic segmentation [246]. However, the research on Mamba for low-level vision tasks is still in its infancy. In particular, a small number of studies have begun to use Mamba to perform RSISR tasks.

In recent work, Zhu et al. [104] proposed a ConvMambaSRF method that integrates SSM and CNN for RSISR. Specifically, they used SSM and CNN to model global dependencies and extract local details respectively, and realized multi-level feature fusion through the global-detail reconstruction module (GDRM). Besides, Zhi et al. [247] proposed a MambaFormerSR method combining Mamba and Transformer for RSISR. They designed a state-space-attention fusion module (SAFM) and combined it with a convolutional Fourier feedforward network (CTFFN) to strengthen frequency domain attention. The spatial-frequency dual-path framework proposed by Xiao et al. [105] for RSISR uses a frequency selection module (FSM) and a state space module (VSSM) to extract high-frequency details and capture long-range spatial correlations, respectively, and further designs a hybrid gating module (HGM) to dynamically fuse multi-level features, achieving outstanding performance. To improve computational efficiency, Zhang and Wang [248] combined SSM with residual connections to implement an equivalent attention mechanism with linear complexity, and experimentally demonstrated that it significantly enhances cross-region feature associations while preserving local textures.

Mamba-based RSISR method successfully solves the local receptive field limitations of traditional CNN and the high computational bottleneck of Transformer by leveraging the linear complexity global modeling capability of SSM, demonstrating a new paradigm for large-scale remote sensing image reconstruction. Although some studies, such as hybrid architecture design strategies [104, 247] and multi-modal feature collaboration [248], have significantly improved reconstruction performance, existing methods still face challenges such as blurred high-frequency details at extremely low-resolutions and insufficient temporal modeling of multi-phase images. In the future, the research on RSISR based on Mamba may focus on the following aspects: (a) lightweight 3D Mamba architecture design for time-series video RSISR and dynamic scene reconstruction, (b) physical degradation-aware SSM optimization, combined with imaging models to enhance the robustness of unknown degradation scenes, (c) cross-modal state space modeling, integrating multi-spectral, SAR and other multi-source remote sensing data to build a unified representation framework for heterogeneous features. With further breakthroughs in hardware perception algorithms and adaptive selectivity mechanisms, Mamba has the potential to become a universal model for RSISR tasks.

### 3.2.5. Diffusion Model-based RSISR

The diffusion model-based RSISR method iteratively reconstructs HR images from LR inputs through a conditional reverse diffusion process, leveraging probabilistic refinement to resolve ill-posedness of SR and geospatial ambiguities under sensor-specific degradation. In recent years, numerous diffusion model-based RSISR methods have been proposed.

To the best of our knowledge, Liu et al. [249] proposed the first diffusion model-based RSISR method, which uses LR images as conditional information to generate HR images. Wu et al. [84] proposed an HSR-Diff method for RSISR, which uses conditional Transformer to fuse HR images and LR images, and then optimizes the reconstruction through hierarchical feature iteration. The efficient hybrid conditional diffusion model (EHC-DMSR) for RSISR proposed by Han et al. [250] combines Transformer-CNN to extract conditional features and introduces Fourier high frequency constraints to accelerate reasoning. In addition, Meng et al. [94] proposed the FastDiffSR method to improve the sampling strategy and reduce the number of diffusion steps. An et al. [95] proposed a lightweight diffusion model LWTDM, which uses a cross-attention encoder-decoder to simplify the denoising network and integrates denoising diffusion implicit models (DDIMs) to accelerate sampling. The DiffALS method [251] introduces a noise discriminator (ND) through an adversarial learning strategy to enhance the diversity of detail generation. Furthermore, the TCDM method proposed by Zhang et al. [252] designs a conditional truncated noise generator (CTNG) for large-scale super-resolution, and embeds pixel-level constraints in combination with the texture consistency diffusion process to accelerate reasoning. Xiao et al. [98] proposed an EDiffSR method for RSISR, which improves efficiency by simplifying channel attention. Some methods focus on semantics and global opti-

mization. For example, Wang et al. [111] combined vector map semantic guidance and proposed a Semantic Guided Diffusion Model (SGDM). Zhu et al. [253] introduced low-rank adaptation (LoRA) to alleviate the distribution difference between natural images and RSI. Weng et al. [110] proposed an image reconstruction representation-diffusion model for RSISR, which uses a pre-trained encoder to guide high-frequency reconstruction.

### 3.2.6. Hybrid RSISR Methods

In recent years, some studies have adopted hybrid architectures to improve performance of RSISR. For example, He et al. [254] proposed a hybrid model (DsTer) that combines densely connected Transformer and ResNet, which enhances spectral super-resolution capabilities through multi-level Transformer feature fusion and demonstrates its advantages in long-range dependency modeling on natural and remote sensing datasets. In addition, Tu et al. [255] proposed a GAN method (SWCGAN) combining Swin Transformer and CNN for RSISR, which improves the multi-scale feature extraction capability through residual dense blocks and outperforms the traditional CNN method on the UCMerced dataset. However, the adversarial training of the SWCGAN method is prone to introduce artifacts. Wang et al. [256] proposed a dilated Transformer generative adversarial network (DTGAN), which introduced dilated convolution into the self-attention module of the Transformer and dynamically focused on local and global features of different scales, significantly improving the performance of land classification tasks.

In terms of lightweight design, Peng et al. [257] proposed a context-aware lightweight super-resolution network (CALSRN), which aggregated the global features of Swin Transformer and the local features of CNN by dynamic weights, reducing the number of parameters by 30% while ensuring the quality of reconstruction. However, the CALSRN method has limited modeling capabilities for complex ground structures. In addition, Lin et al. [258] proposed a distillation Transform-CNN Network (DTCNet), which employs a Transformer teacher network to guide a lightweight CNN student network and avoids zero-filling information loss through adaptive upsampling. For cross-sensor and frequency domain optimization, Hou et al. [259] proposed a CNN-Swin Transformer RSISR method (CSwT-SR) based on amplitude-phase learning, which jointly enhances spatial and frequency domain feature representation and outperforms prevailing degradation model methods in blind super-resolution tasks. Besides, Wang et al. [260] proposed a hybrid CNN-Transformer network named RepCHAT, which compresses the number of parameters through structural re-parameterization and introduces a frequency domain multi-scale feature extraction module to improve performance. In recent work, an improved SRGAN method named ViT-ISRGAN proposed by Yang et al. [114] employs Vision Transformer and spatial-spectral residual attention to improve performance for four typical ground objects (urban, water, farmland, and forest) in Sentinel-2. For infrared image super-resolution, Zhang et al. [261] designed the residual Swin Transformer block (RSTAB) and proposed a SwinAIR-GAN

method based on U-Net, which fuses multi-frequency features through average pooling and introduces artifact discrimination loss, greatly improving performance.

Recently, some studies have focused on exploring the generation ability and stability of hybrid architectures. For example, Guo et al. [262] proposed a sparse-activated sub-pixel transformer network (SSTNet), which enhances edge sharpness and texture details through sparse activation in sub-pixel space, but a sparse constraint term requires additional design. Besides, Liu et al. [263] proposed an improved RSISR method, which designs a multi-stage hybrid Transformer generator and combines Charbonnier loss with TV loss to improve training stability. The Fusing Transformers and CNN method (ConvFormerSR) for RSISR proposed by Li et al. [264] designed a cross-sensor feature fusion module (FFM) and spectral loss function, and achieved high-spectral consistency reconstruction of Landsat-8 and Sentinel-2 data by enhancing the high-order spatial interaction of Transformer. MSWAGAN method [265] designs a multi-scale sliding window attention (MSWA) to capture local multi-scale features, and combines the Transformer to model long-range pixel associations without increasing the number of parameters. Zhu et al. [108] proposed a Transformer-based Multi-modal Generative Adversarial Network (TMGAN) for multimodal data, which designed a global Transformer generator and fused depth and spectral information through self-attention to improve performance. The Enhanced Swin Transformer with U-Net GAN (ESTUGAN) proposed by Yu et al. [266] employs a Swin Transformer-based generator and a U-Net discriminator, which suppresses artifacts through region-aware adversarial learning. Specifically, ESTUGAN uses Best-buddy loss and Back-projection loss to enhance reconstruction fidelity. In the Trans-CNN GAN method proposed by Lin et al. [267], the global attention of the Transformer is used to compensate for the local defects of the generator. Huo et al. [268] proposed a STGAN model based on GANs and self-attention mechanism, which achieved better high-frequency detail recovery ability in RSISR through multi-CNN-Swin Transformer module (MCST) and improved association attention module (RAM-V).

## 4. Unsupervised RSISR Methods

Supervised RSISR methods usually need massive amounts of labeled training data, which face many challenges in practical applications, such as high cost of acquiring real HR data, poor annotation transferability across sensor scenarios, and difficulty in eliminating deviations between simulated data and real physical degradation models. In contrast, unsupervised methods alleviate the strict reliance on labeled data, which leverage the intrinsic characteristics of images, such as self-similarity, multi-source information complementarity, and domain-specific physical priors. Therefore, it is still necessary to conduct research on unsupervised RSISR methods. In this section, we conduct a detailed investigation on the unsupervised RSISR methods from the perspectives of traditional methods and deep learning.

### 4.1. Traditional RSISR Methods

Although deep learning has emerged as the dominant approach for RSISR, traditional unsupervised methods still hold significant research value due to their demonstrated advantages such as model robustness, physical interpretability, and cross-scenario generalization capabilities. In addition, these conventional techniques remain particularly promising in resource-constrained applications, particularly in scenarios involving small-sample learning, low-resource consumption, and specialized tasks like zero-shot super-resolution. Furthermore, their well-established theoretical frameworks provide valuable insights for advancing mainstream algorithms through improved architecture design and interpretability enhancement. Generally, traditional unsupervised RSISR mainly focuses on reconstruction-based methods, which involve the following aspects: interpolation-based, frequency domain-based, iterative back projection (IBP)-based, and regularization constraint-based.

#### 4.1.1. Interpolation-based Methods

As one of the most important basic technologies in the field of image reconstruction, interpolation-based methods predict the spatial distribution of LR pixels, and typical representatives are nearest neighbor interpolation, bilinear interpolation, and bicubic interpolation. Although these methods have limitations in reconstructing complex textures, it is still necessary to reveal their prior-guided spatial adaptive mechanisms for RSISR. In this section, we systematically review the classical RSISR algorithms based on interpolation.

In early work [269], wavelet transform and spatial interpolation were combined to improve reconstruction performance, which used a spectrum separation processing strategy to improve resolution while suppressing interpolation artifacts. In addition, Zhou et al. [44] proposed an interpolation super-resolution method based on multi-surface fitting, which focuses on spatial structure-driven surface modeling and maximum a posteriori probability fusion to achieve high-frequency detail preservation. To address the problems of blur and block effects caused by the loss of high-frequency information in conventional interpolation, Han et al. [270] proposed a RSISR framework that combines frequency domain segmentation enhancement with spatial domain interpolation optimization based on bicubic interpolation and discrete wavelet transform (DWT), which significantly improves the reconstruction performance and preserves the details of the ground objects. A similar work is the multi-band collaborative super-resolution framework based on dual-tree complex wavelet transform (DT-CWT) and improved edge-directed interpolation (INEDI) proposed by Solanki et al. [55]. In addition, Mareboyana and Moigne [271] proposed an edge-directed radial basis function (EDRBF) driven super-resolution method, which injects edge-constrained radial basis adaptive interpolation mechanism and co-optimizes sub-pixel registration, showing strong robustness to registration errors.

#### 4.1.2. POCS-based Methods

Projection onto Convex Sets (POCS) is an iterative optimization method based on convex set constraints, which approximates the feasible solution of RSISR reconstruction by alternately projecting onto a priori knowledge constraint sets of the degradation model. Earlier works [272, 273] have demonstrated that POCS has significant potential in improving super-resolution performance. A more concrete work is the two-stage regularization framework based on POCS proposed by Aguena and Mascarenhas [274] for multispectral-panchromatic fusion, which achieves spectral-spatial feature collaborative enhancement through sequential and parallel projection or least squares synthesis. In addition, Xie et al. [275] proposed a robust POCS iterative framework based on improved sub-pixel shift estimation for blind image super-resolution in 2009, but it has the disadvantage of slow convergence speed. In order to solve the problem of imbalanced image data of the Chang'e-1 three-line array, Zhang et al. [43] proposed a RSISR method based on global weighted POCS, which significantly improved the performance of lunar surface topography reconstruction. In 2016, Liu et al. [52] proposed an improved POCS algorithm based on visual mechanism for RSISR, which achieves infrared image target edge enhancement and background noise suppression through variable correction threshold consistency constraint and human visual contrast constraint. In order to solve the problem of inaccurate PSF estimation in traditional POCS, Fan et al. [276] proposed a slant-edge estimation strategy based on the linear relationship of PSF of LR images, which greatly improved the performance of image reconstruction. In addition, Dai et al. [277] proposed an improved POCS algorithm for RSISR, which employs iterative curvature-based interpolation (ICBI) to generate high-resolution initial estimates, effectively alleviating the edge blur and detail loss problems in POCS reconstruction. A similar work is that Wang et al. [75] proposed to use gradient interpolation instead of nearest neighbor interpolation to solve the problem of edge blur and iterative subjectivity in hyperspectral super-resolution, and designed an adaptive stopping criterion based on the mean square error of adjacent iterations to improve the quality of full-band reconstruction.

#### 4.1.3. IBP-based Methods

Iterative Back Projection (IBP)-based super-resolution methods mainly improve the resolution of remote sensing images through error feedback iterative optimization. To the best of our knowledge, IBP was first introduced as a multi-frame super-resolution algorithm in the work of Irani and Peleg et al. [278]. Early work in [279] proposed a sub-pixel migration multi-observation model, which established super-resolution equations and employed the IBP algorithm to obtain HR images. Besides, Li et al. [280] proposed an improved IBP algorithm for RSISR by integrating inverse-forward elastic registration with block-wise processing to address local affine transformations, which enhanced geometric adaptability and high-frequency preservation. Their subsequent work [281] further demonstrated the effectiveness in stereo image fusion of ALOS satellite's PRISM sensors. A similar work is that Yan and Lu

[282] combined IBP with the Papoulis-Gerchberg extrapolation method to solve the anisotropic resolution problem of MRI.

In order to deal with the inherent defects of IBP, many optimization strategy studies have been conducted. For example, Patel et al. [283] combined infinite symmetric exponential filter (ISEF) to suppress the checkerboard effect. Bareja and Modi [284] introduced Canny edge detection and error difference to enhance high-frequency reconstruction. In addition, Nayak et al. [285] innovatively combined the cuckoo search algorithm with IBP to achieve global optimization and improve super-resolution performance. Some studies utilize regularization strategies to improve performance. For example, Wang et al. [286] proposed a super-resolution method based on wavelet edge detection and principal component analysis (PCA), which improved the accuracy of face super-resolution recognition by 12% by extracting high-frequency information. Nayak et al. [287] designed a mathematical morphological edge regularization technique for the reconstruction task, which suppressed the ringing artifacts caused by IBP through adaptive weights and significantly improved the visual quality of strong edge areas.

In addition to the above, some related works focused on the research of algorithm efficiency and multimodal fusion. For example, Nayak and Patra [57] proposed an evolutionary edge-preserving IBP method (EEIBP) for super-resolution tasks. Specifically, EEIBP optimizes the initial estimate through non-uniform B-spline interpolation and combines an adaptive back-projection kernel driven by covariance, which greatly reduces the reconstruction time and effectively improves edge sharpness. Mutai et al. [80] incorporated a two-stage process of cubic B-spline approximation and discrete wavelet transform, which greatly improved the super-resolution performance by reducing blur through pre-filtering. In addition, Tao et al. [86] proposed a spatial-spectral joint back projection (SSBP) method to improve the quality of panchromatic sharpening while maintaining spectral consistency.

#### 4.1.4. Probability-based Methods

Probability-based methods mainly utilizes statistical modeling and probabilistic inference to perform image reconstruction. Specifically, these methods inherently incorporate prior knowledge of the imaging scene, enabling unsupervised reconstruction without relying on paired high-low-resolution training datasets. Generally, probabilistic RSISR methods can be systematically categorized into four paradigms: Bayesian inference, maximum a posteriori (MAP) estimation, maximum likelihood (ML) estimation, and Markov random field (MRF) modeling.

**Bayesian-based Methods.** Generally speaking, Bayesian-based methods transform the ill-posed problem of super-resolution reconstruction into a well-posed inversion model by combining image prior probability density with physical constraints. In the past two decades, Bayesian RSISR has been widely studied, and many Bayesian RSISR methods have been proposed. To the best of our knowledge, Tipping and Bishop [288] first proposed a Bayesian super-resolution method based on marginalization in 2002. Specifically, they modeled high-resolution images by injecting Gaussian process priors to

achieve joint estimation of point spread function and registration parameters. Besides, Molina et al. [289] integrated the sensor characteristics into the Bayesian framework and combined the observation process of multispectral and panchromatic images to effectively improve the spatial resolution of Landsat ETM+ while maintaining the spectral fidelity. Subsequently, Molina et al. [290, 291, 292] further constructed a hierarchical Bayesian model with parameter priors and used variational inference methods to achieve simultaneous estimation of HR multispectral images and model parameters. In addition, Babacan et al. [127] proposed a joint super-resolution reconstruction method based on variational Bayesian, which simultaneously estimates high-resolution images and motion parameters through probabilistic modeling to achieve adaptive robust reconstruction. For pancharpening, Wang et al. [293] proposed a Bayesian fusion model based on the geometric-spectral-spatial consistency hypothesis, which uses the alternating direction multiplier method (ADMM) to solve and verify the generalization ability of hyperspectral images. In order to solve the problem of parameter sensitivity, Armannsson et al. [294] innovatively introduced Bayesian optimization into Sentinel-2 super-resolution, and significantly improved the robustness of methods such as ATPRK and S2Sharp through a small-scale parameter optimization mechanism. Li et al. [295] proposed a multi-prior Bayesian model based on the fusion of TV and Laplace priors, which significantly improved the accuracy of target contour reconstruction in sea and land scenes. Furthermore, Tan et al. [296] established a two-dimensional spatial structure prior based on Markov random field (MRF), and characterized the spatial correlation of the scene through an n-order neighborhood system, which significantly improved the suppression of artifacts compared with previous methods. Besides, Ye et al. [81] proposed a Bayesian hyperspectral super-resolution method based on texture decomposition, which effectively suppressed spectral variation through Gaussian process spectral prior. In recent work, Shen et al. [297] and Guo et al. [113] achieved breakthroughs in RSISR of Bayesian forward-looking radar imaging in low signal-to-noise ratio and maneuvering scenarios by using gamma-normal conjugate model and structured Student's t prior, respectively.

**MAP-based Methods.** RSISR methods based on maximum a posteriori probability (MAP) have also been widely studied. For example, the early work of Chantas et al. [298] proposed a MAP framework with local adaptive edge-preserving priors, which achieved joint restoration and registration under degraded observations through a two-step reconstruction strategy. Subsequently, some studies began to optimize from the perspective of prior models. Wang et al. [299] proposed a MAP method based on high-frequency fusion of panchromatic images for RSISR, which introduced spectral fidelity prior constraints to iteratively optimize the framework. In addition, Belekos et al. [300] designed a multi-channel non-stationary Gaussian prior model to enhance the collaborative reconstruction capability of multispectral data. Li et al. [301] first introduced the Hidden Markov tree (HMT) into the MAP framework and used the multi-scale dependence of wavelet coefficients to improve the reconstruction performance. Improved methods for spe-

cific application scenarios have also emerged. For example, Guan et al. [302] proposed a MAP radar angle super-resolution method based on antenna pattern and target scattering convolution prior modeling. Zhang et al. [63] proposed a Rayleigh sparse MAP (RSMAP) algorithm for sea surface target imaging, which combines the distribution characteristics of sea clutter with the sparse prior of the target to improve the angular resolution. In terms of noise robustness, Vrigkas et al. designed a global M-estimation framework to achieve parameter adaptive adjustment. Besides, the regional adaptive total variation (RSATV) model proposed by Yuan et al. [303] for RSISR utilized spatial information classification to suppress artifacts. On the other hand, Li et al. [304] first achieved RSISR on short-time sequence images of the GF-4 geosynchronous satellite, verifying the feasibility of synchronous orbit observation data. In addition, some studies have constructed the MAP-MRF framework to perform hyperspectral super-resolution technology. Irmak et al. [305] achieved multi-frame reconstruction optimization through abundance map decomposition and end-member extraction. Further, the extended study [56] combined virtual dimension endmember determination with texture constrained secondary optimization, and its performance exceeded the mainstream method while maintaining spectral consistency, forming a complete technical chain for multi-source to single-source reconstruction.

**ML-based Methods.** Some studies use maximum likelihood (ML) methods to transform the ill-posed problem of RSISR into a well-posed problem. Different from the MAP method, the ML method omits explicit prior constraints and is more robust. Tan et al. [306] proposed a penalized ML method for I/Q dual-channel joint noise modeling for RSISR, which constructed a joint regularization term that integrated the square-Laplacian characteristic to suppress noise amplification. Furthermore, the extended study [307] proposed an I/Q channel joint probability model containing phase information, which achieved high-precision target estimation by maximizing the likelihood of complex signals. In addition, Wu et al. [308] proposed a fast ML algorithm with dynamic adjustment of adaptive acceleration factors, which significantly reduced the computational complexity while maintaining super-resolution performance.

**MRF-based Methods.** The Markov Random Field (MRF) based method mainly models the spatial dependencies between pixels and their neighborhoods, which performs effective integration of global spatial context information through the energy function of the local neighborhood. MRF-based RSISR has been studied for nearly two decades, and many MRF-based RSISR methods have been proposed. For example, Li et al. [309] proposed a spatial-temporal MRF super-resolution model (STMRF\_SRM), which integrates historical medium-resolution images with current coarse-resolution data to effectively enhance the spatiotemporal consistency of forest mapping. Aghighi et al. [310] further proposed a full-space adaptive MRF-SRM, which dynamically balances spectral and spatial weights based on endmember analysis and local energy matrix to achieve automatic parameter calibration. In the latest progress, Welikanna et al. [311] fused the fuzzy C-means and

spectral angle quantity to optimize the MRF posterior energy function, which reduces the influence of point spread effect.

#### 4.2. Deep learning-based RSISR Method

The majority of deep learning-based RSISR methods are supervised, which need a large amount of labeled training data. However, the ground truth is normally not available in RSISR, thus almost all supervised methods utilize synthetic degraded simulation datasets that are actually not realistic. Therefore, it is desirable to have unsupervised RSISR methods. In this section, we investigate the unsupervised deep learning RSISR methods, mainly involving self-supervised learning, contrastive learning, generative-based and zero-shot learning.

##### 4.2.1. Self-supervised Learning

Self-supervised RSISR methods are usually inspired by internal degradation modeling or cross-modal data association to generate pseudo-supervisory signals, thereby avoiding the reliance on external HR training data. In recent years, self-supervised RSISR methods have emerged. In 2018, Haut et al. [54] proposed the first unsupervised convolutional generation model, which learned the LR-HR feature relationship through stacked convolution and downsampling layers, and employed LR reconstruction loss to constrain the generation quality. In addition, Choi and Kim [312] proposed a new degradation model to generate LR samples, and combined it with morphological transformation to enhance HR images, thereby achieving super-resolution of KOMPSAT-3 images. Sheikholeslami et al. [68] proposed an efficient unsupervised super-resolution (EUSR) model for RSISR, which uses dense skip connections and bottleneck compression modules to reduce the amount of computation while maintaining reconstruction performance. For cross-modal data, Chen et al. [74] proposed a self-supervised spectral-spatial residual network (SSRN), which generates HR hyperspectral images through the mapping relationship between LR multispectral and hyperspectral images without HR ground truth supervision. In terms of multi-frame super-resolution, Nguyen et al. [313] proposed an frame-to-frame self-supervised framework that fuses satellite image sequence features and improves the resolution of SkySat satellite images. In the latest progress, Hong et al. [314] proposed a decoupled-and-coupled network (DC-Net) for RSISR, which effectively alleviated the distribution difference of hyperspectral and multispectral data through the decoupled-coupled structure and self-supervised constraints. Qian et al. [39] proposed a RSISR method based on deep image prior. Specifically, they used convolutional neural networks and 3D separable convolutions to perform super-resolution restoration on the coarse resolution band of Sentinel-2 satellite images without the need for additional training data, significantly improving the super-resolution performance. An interesting work is a self-supervised degradation guidance method proposed by Xiao et al. [89], which effectively adapts to various unknown degradations through contrastive learning and bidirectional feature modulation network, significantly improving the RSISR performance.

##### 4.2.2. Contrastive Learning

Traditional methods rely on bicubic downsampling to synthesize LR images for training, which is difficult to reflect the complex degradation patterns of real scenes. Contrastive learning, as a self-supervised learning method, unsupervisedly compares the degradation features and HR detail differences between samples to mine potential degradation representations, significantly improving the model's adaptability to unknown degradation and the physical consistency of super-resolution reconstruction. In recent years, some RSISR methods based on contrastive learning have been proposed. Mishra and Hadar [88] proposed a semi-supervised contrastive learning framework CLSR, which significantly reduced the reliance on large-scale diverse training samples by comparing the potential differences between real degradation and ideal bicubic degradation. Further, the extended research [315] proposed a two-stage contrast framework for RSISR. In the first stage, "artificial style images" with HR textures are generated through contrast training, and then neural style transfer is combined to achieve unsupervised super-resolution. An interesting contrastive learning-based RSISR method is the region-aware network (RAN) proposed by Liu et al. [87]. In RAN, they integrated the degradation prior extracted by contrastive learning with the regional structure analysis module, and captured cross-block self-similarity through graph neural networks and attention mechanisms, effectively improving the fidelity of texture reconstruction. In the latest progress, the EDRLN network proposed by Wang et al. [106] uses mutual affine convolution to replace the traditional convolution layer and integrates a lightweight pixel attention mechanism in the contrastive learning framework, which reduces the number of model parameters while maintaining excellent performance in multiple degradation scenarios.

##### 4.2.3. Generative-based Methods

Unsupervised generative methods establish data distribution mappings rather than relying on paired samples to perform RSISR. In recent years, some studies have used GAN or cyclic structures to learn the joint distribution of degradation and reconstruction, and achieve resolution enhancement through implicit image priors. For example, Wang et al. [316] proposed a Cycle-CNN based on a cyclic structure. They used two generative CNNs to model the downsampling and super-resolution processes respectively, and verified the effectiveness of unpaired training on GaoFen-2 satellite data. In 2021, the extended research [72] proposed a new Cycle-CNN that integrates the bidirectional mapping of the downsampling network and the SR network, achieving improved robustness on the UC Merced dataset, and further demonstrated the ability of the cyclic generative structure to suppress noise and blur. In addition, Wang et al. [73] proposed an enhanced image prior (EIP) method for RSISR, which encodes the reference image into the latent space based on GAN, and combines the cyclic update strategy to transfer texture features, achieving advanced performance. Similarly, the MIP method [71] constructs a transfer image prior and uses an implicit noise update mechanism to achieve feature transfer for RSISR. Zhang et al. [317] proposed

an unsupervised RSISR method based on GAN, which achieved competitive performance by reconstructing SR images through generator and then downsampling to train the discriminator. A recent work is TransCycleGAN proposed by Zhai et al. [107], which integrates the Transformer module into the CycleGAN framework and uses transposed self-attention to capture global context, effectively removing degenerate features in a pseudo-supervisory manner.

#### 4.2.4. Zero-shot Learning

Zero-shot learning-based RSISR method only uses the intrinsic features of the image to build a training set for super-resolution reconstruction. Yang and Wu [318] proposed an enhanced zero-shot super-resolution method, which generates enhanced images and builds training sets through a content adaptive resampler (CAR) network. In addition, they introduced a convolutional block attention module (CBAM) and a residual module, which significantly improved the quality of image detail reconstruction. In [319], the authors proposed a zero-shot RSISR framework based on self tessellations and cascaded attention sharing mechanism, which achieves high-quality reconstruction by exploiting the structural continuity of remote sensing images without pairing HR images. Self-FuseNet proposed by Mishra and Hadar [90] adopts a forward generation paradigm and accelerates image reconstruction through a UNet architecture with wide skip connections, demonstrating strong generalization capabilities in RSISR. Cha et al. [91] proposed a meta-learning based zero-shot remote sensing image super-resolution (ZSSR) method, which regards multiple LR image sets as a set of ZSSR tasks to learn general super-resolution meta-knowledge, significantly reducing the computational cost of large-scale image processing.

## 5. Recent Development Characteristics

This section summarizes some new characteristics of the RSISR field shown in recent years.

### 5.1. More and more types of deep learning models were being applied to RSISR

In 2015, CNN was first applied to SR tasks, and the milestone work SRCNN [32, 33] was proposed. Further, msiSRCNN [148] was proposed in 2016 for RSISR. Since then, various CNN-based RSISR methods [53, 60, 62] have emerged. In addition, GANs [198] and Transformer [229] were introduced into the RSISR field in 2018 and 2021, respectively. These architectural models have been widely studied and used in the field of RSISR. In 2022, diffusion models [249] are also introduced into RSISR, and many diffusion models-based RSISR methods have been proposed. Another new architecture is Mammab, which was introduced into RSISR in 2024. We anticipate that an increasing variety of deep learning models will be adopted for RSISR tasks, in order to further enhance performance.

### 5.2. Most RSISR methods are supervised

Most RSISR methods involving deep learning are supervised, because RSI usually has the characteristics of high geometric alignment accuracy, which means that paired training samples can be easily constructed by downsampling. In addition, mainstream evaluation metrics such as PSNR and SSIM require ground truth (i.e., real HR image) as a reference, which further demonstrates the advantages of supervised learning. Although unsupervised and self-supervised methods have emerged in recent years, they still face great limitations in the field of remote sensing, such as poor sample diversity and lack of transferable pre-training. Therefore, most RSISR methods still rely on the supervised paradigm to obtain stable reconstruction performance.

### 5.3. RSISR methods for different types of images

Most existing RSISR methods perform HR reconstruction on optical RSI, which is mainly collected from satellite images such as WorldView, Gaofen and Sentinel-2. Recently, some researchers started developing methods to conduct SR on different types of RSI. However, it is not uncommon to perform SR on different types of RSI. For example, in 2012, He et al. [20] proposed an SR method for SAR images. Specifically, they achieved SR reconstruction on a very small test set by combining multi-dictionary and sparse coding spatial pyramid machine training. Similar work includes RSMP [63] and Guo et al. [113].

Recently, many SR methods for HSI and MSI have been proposed. These images contain rich spectral information in a large number of bands and have broad research prospects. For example, from 2021 to 2024, many HSISR methods were proposed, covering Transformer-based [78, 85], Diffusion-based [84, 93] and self-supervised learning methods [39, 74, 89]. This diversity of RSISR tasks reflects the characteristics of different types of images, such as noise in SAR, spectral fidelity in HSI, and temporal consistency in satellite images, which require customized solutions. However, it is desirable to develop a general SR framework for different types of RSI, which may face great challenges in model generalization, cross-modal knowledge transfer, and computational efficiency.

### 5.4. Research on benchmarks

Although RSISR has made significant progress in recent years, benchmark research for RSISR still faces challenges. Unlike many basic tasks in computer vision, there are few studies on RSISR benchmarks, and there is a lack of general and high-quality RSISR benchmark datasets, which makes model performance comparisons unstable. In addition, most existing benchmarks [320, 321] rely on idealized downsampling degradation models, which limits the real-world adaptability of the methods.

Until recently, some researchers have started to create benchmarks in the field of RSISR. For example, Kowaleczko et al. [322] proposed the first benchmark dataset MuS2 based on real multi-temporal LR images and HR reference images, which breaks through the limitations of traditional simulated

data and enhances the practicality of RSISR. In addition, Wang et al. [323] constructed a real degradation benchmark dataset RRSISR based on spectral camera imaging to address the mismatch between simulated degradation and real scenes in RSISR, and proposed a reference table-based block exit (RPE) method to improve efficiency through dynamic calculation.

### 5.5. Application-oriented RSISR methods

Most existing RSISR methods do not consider downstream applications in the process of image reconstruction. Therefore, these RSISR methods generate visually-pleasing reconstructed images, but this may be suboptimal for downstream tasks. This leads to a growing gap between metric-based performance (e.g., PSNR, SSIM) and actual utility in downstream applications. Bridging this requires RSISR models aligned with task-specific objectives, not just perceptual quality.

In the past three years, some studies have started deeply coupling the SR process with specific remote sensing application tasks to achieve a paradigm shift from visual quality-oriented to application-oriented. For example, Zhang et al. [209] proposed an RSI reconstruction method based on SRGAN to construct a high-quality landslide training set from LR images. In addition, Kong et al. [220] proposed a dual RSS-GAN method to integrate high-resolution Planet Fusion data to spatially enhance NDVI and NIRv, significantly improving the temporal expression and estimation accuracy of the surface index. Recently, Sun et al. [234] proposed the RSISR framework based on Transformer and self-supervision mechanism to effectively improve the performance of image interpretation. Fan et al. [215] proposed a GAN-based RSISR method, which significantly improved the accuracy of vegetation index inversion and yield prediction by improving the spatial resolution of ginkgo tree RSIs. Compared with most RSISR methods, these methods directly consider the performance of downstream applications during the image reconstruction process, which provides reconstructed images that are more suitable for specific applications.

### 5.6. Programming frameworks

We conducted a systematic survey of existing RSISR methods and checked the programming frameworks used. The frequency of use of **PyTorch** has increased rapidly since 2017, becoming the mainstream framework, thanks to the flexibility of its dynamic graph mechanism, more convenient debugging, and an active open source community. In contrast, while TensorFlow's static computation graph demonstrated notable performance optimization in its early iterations, it has a high threshold for use in scientific research scenarios. MATLAB occasionally appears in some traditional image processing tasks, but is almost never used in deep learning RSISR methods.

## 6. Datasets and evaluation metrics

### 6.1. Available remote sensing image datasets

In the field of RS, due to the high cost of acquiring real HR images and the difficulty of registering corresponding LR

Table 2: Details of Existing Remote Sensing Image Datasets.

Name	Year	Data Source	Numbers	Resolution
UCMD	2010	Air-Spaceborne	2,100	256 × 256
WHU-RS19	2012	Google Earth	1,005	600 × 600
RSSCN7	2015	Google Earth	2,800	400 × 400
AID	2016	Aerial	10,000	400 × 400
KOSD	2016	Draper Satellite	1,620	3099 × 2329
SIRI-WHU	2016	Google Earth	2,400	200 × 200
NWPU-RESISC45	2017	Google Earth	31,500	256 × 256
PatternNet	2018	Google Earth	30,400	256 × 256
DOTA	2018	JL-1, GF-2	2,806	4000 × 4000
SpaceNet2	2018	WV-2	10,595	162 × 162
DFC2019	2019	WV-3	2,783	1024 × 1024
OPTIMAL-31	2019	Google Earth	1,860	256 × 256
RSI-CB	2020	Crowdsouce	60,000	128 × 128 256 × 256

images, there are few publicly available datasets for RSISR. To this end, most studies perform bicubic downscaling on RS datasets to generate RSISR datasets. In this section, we summarize the widely used datasets for RSISR in the literature, as shown in Table 2. Specifically, the details of these datasets are as follows:

- UCMD (UC Merced Land-Use Dataset)<sup>2</sup> [324]. This dataset is an RSI dataset for land use research, which is obtained from USGS National Map Urban Area Imagery. Besides, it contains images of 21 different land classes, with 100 images in each class. The pixel resolution of the public domain images is 1 foot (0.3 meters), and the image pixel size is 256 × 256.
- WHU-RS19<sup>3</sup> [325]. This dataset consists of HR satellite images exported from Google Earth, with a spatial resolution of up to 0.5 meters. It includes 19 classes of meaningful scenes in high-resolution satellite imagery. Each class contains approximately 50 image samples, providing a diverse and representative collection for research and analysis.
- RSSCN7<sup>4</sup> [326]. This dataset contains 2800 RS images, which are distributed across seven categories, each with 400 images sampled at four different scales. Each image is 400 × 400 pixels and obtained from Google Earth.
- AID (Aerial Image Dataset)<sup>5</sup> [327]. AID is a large-scale aerial image dataset, including 10,000 images of 30 different scene types collected from Google Earth, and all images are labeled by experts in the field of RSI interpretation.
- KOSD (Kaggle Open Source Dataset)<sup>6</sup> [328]. The dataset contains more than 1,000 HR aerial photographs from Southern California, consisting of 350 training images and 1,370 test images.

<sup>2</sup><http://weegee.vision.ucmerced.edu/datasets/landuse.html>

<sup>3</sup><https://captain-whu.github.io/BED4RS/>

<sup>4</sup><https://pan.baidu.com/s/1s1Sn6Vz>

<sup>5</sup><https://captain-whu.github.io/BED4RS/>

<sup>6</sup><https://www.kaggle.com/c/draper-satellite-image-chronology>

- NWPU-RESISC45<sup>7</sup> [329]. The dataset is a public RSI scene classification dataset created by Northwestern Polytechnical University (NWPU). It contains 31,500 images of 45 scene classes, involving 700 images with the size of  $256 \times 256$  pixels in each class.
- PatternNet<sup>8</sup> [330]. The dataset is a large-scale HR remote sensing dataset for RSI retrieval. It contains 30,400 images of 38 scene classes, involving 800 images with the size of  $256 \times 256$  pixels in each class. The images in PatternNet are collected from Google Earth images or through Google Map API for some cities in the United States.
- DOTA<sup>9</sup> [331]. DOTA is a large-scale public dataset collected from taken by Google Earth, GF-2 and JL-1 satellites for aerial image object detection. It contains a total of 2,806 HR images with resolutions ranging from  $800 \times 800$  to  $4000 \times 4000$  pixels.
- SpaceNet<sup>10</sup> [332]. SpaceNet is another large-scale satellite imagery dataset, obtained from the VHR WorldView-3(WV-3) satellite.
- DFC2019 (IEEE Data Fusion Contest 2019)<sup>11</sup> [333]. The dataset contains 2,783 multi-temporal HR satellite images taken by the WV-3 satellite as training sets and 50 test images. All images are provided in the form of regular tiles of  $1024 \times 1024$  pixels with a spatial resolution of sub-meter level.
- OPTIMAL-31<sup>12</sup> [334]. The dataset contains 1,860 images of 31 categories collected from Google Maps, each category consists of 60 images with a size of  $256 \times 256$  pixels.
- SIRI-WHU<sup>13</sup> [335]. The dataset includes 2,400 images covering 12 different categories of scenes, collected and produced by the RS-IDEA Research Group of Wuhan University (SIRI-WHU) from Google Earth, mainly covering urban areas in China. Each category contains 200 images, each with a size of  $200 \times 200$  pixels and a spatial resolution of 2m.
- RSI-CB<sup>14</sup> [336] The dataset constructs two sub-datasets of  $256 \times 256$  and  $128 \times 128$  pixel sizes (RSI-CB256 and RSI-CB128, respectively) with 0.3–3-m spatial resolutions. The former contains more than 24,000 images involving 35 categories, and the latter contains more than 36,000 images involving 45 categories.

## 6.2. Evaluation metrics

In the field of RSISR, evaluation metrics are crucial for measuring the performance of algorithms such as reconstruction accuracy and fidelity, which provides an objective reference for the performance comparison of algorithms through quantitative calculation. In this section, we summarize the commonly used quantitative evaluation indicators for RSISR, and the details are as follows:

(1) Structural Similarity Index Measure (SSIM): SSIM [337] is an important objective evaluation metric that measures the structural similarity between the reconstructed image and the real HR image. Specifically, SSIM simulates the perception of brightness, contrast, and structural information by the human visual system (HVS), which is more in line with subjective visual quality evaluation. Given a super-resolved image  $I_{SR}$  and a target image  $I_{HR}$ , SSIM can be calculated as:

$$SSIM = l(I_{SR}, I_{HR}) \cdot C(I_{SR}, I_{HR}) \cdot S(I_{SR}, I_{HR}) \quad (3)$$

where  $l(I_{SR}, I_{HR})$ ,  $C(I_{SR}, I_{HR})$  and  $S(I_{SR}, I_{HR})$  represent the similarity of luminance, contrast and structure respectively. In practice, SSIM is not sensitive enough to the high dynamic range (such as clouds, shadow areas) or complex textures (such as forests, farmlands) of remote sensing images. Therefore, some studies have proposed the mean structural similarity (MSSIM) and multi-scale structural similarity (MS-SSIM) to evaluate the super-resolution performance. A higher SSIM value implies that the super-resolution image has a higher similarity and better fidelity with the HR image.

(2) Peak-Signal-Noise-Ratio (PSNR): PSNR is another one of the most popular objective evaluation indicators, which is mainly used to quantify the pixel-level fidelity between super-resolved images and true HR images. Specifically, assuming that the size of the super-resolved image  $I_{SR}$  and the target image  $I_{HR}$  are  $M \times N$ , the mean square error (MSE) can be defined as:

$$MSE = \frac{1}{H \times W} \sum_{i=1}^H \sum_{j=1}^W (I_{HR}(i, j) - I_{SR}(i, j))^2 \quad (4)$$

Based on the MSE and the maximum value  $L$  of the dynamic range of image pixels, PSNR can be calculated as:

$$PSNR = 10 \cdot \log_{10} \left( \frac{L^2}{MSE} \right) \quad (5)$$

Generally speaking, a higher PSNR value indicates that the image has better visual quality.

(3) Learned Perceptual Image Patch Similarity (LPIPS): LPIPS [338] is a perceptual similarity metric based on deep learning, which is closer to HVS evaluation of image quality. Specifically, LPIPS quantifies the perceptual difference between the reconstructed image and the real image. Lower LPIPS means better image quality.

(4) Natural Image Quality Evaluator (NIQE): NIQE [339] is a no-reference image quality evaluation metric. This metric is based on natural image statistical modeling and measures the image visual quality by comparing the distance between the

<sup>7</sup>[https://1drv.ms/u/s!AmgKYzARB15ca3HNaH1zp\\_IXjs](https://1drv.ms/u/s!AmgKYzARB15ca3HNaH1zp_IXjs)  
<sup>8</sup><https://sites.google.com/view/zhouwx/dataset>  
<sup>9</sup><https://captain-whu.github.io/BED4RS/>  
<sup>10</sup><https://spacenet.ai/datasets/>  
<sup>11</sup><https://ieee-dataport.org/open-access/data-fusion-contest-2019-dfc2019>  
<sup>12</sup><https://drive.google.com/open?id=1Fk9a0DW8UyQsR8dP2Qdakmr69NVBhq9>  
<sup>13</sup>[http://www.lmars.whu.edu.cn/prof\\_web/zhongyanfei/e-code.html](http://www.lmars.whu.edu.cn/prof_web/zhongyanfei/e-code.html)  
<sup>14</sup><https://github.com/lehaifeng/RSI-CB>

local statistical features of the image and the statistical distribution. The lower the NIQE value, the better the image visual quality.

(5) Spectral Angle Mapper (SAM): SAM [340] evaluates spectral fidelity by calculating the angle between the test spectrum vector and the reference spectrum vector. Given a test spectrum  $v$  and a reference spectrum  $r$ , both with  $L$  layer, SAM is calculated as:

$$\text{SAM}(v, w) = \arccos \left( \frac{\sum_{i=1}^L v_i w_i}{\sqrt{\sum_{i=1}^L v_i^2} \sqrt{\sum_{i=1}^L w_i^2}} \right) \quad (6)$$

Smaller SAM values indicate a higher spectral fidelity. In particular, angles approaching  $0^\circ$  indicate a high degree of spectral consistency.

(6) Average Gradient (AG): AG [341] is used to measure the edge sharpness of image. It is evaluated by calculating the gradient magnitude of all pixels in the image and is defined as:

$$AG = \frac{1}{(h-1)(w-1)} \sum_{x=1}^{w-1} \sum_{y=1}^{h-1} \frac{|G(x, y)|}{\sqrt{2}} \quad (7)$$

where  $G(x, y)$  represents the gradient at the pixel  $(x, y)$ , and the denominator  $(h-1)(w-1)$  is used for normalization. The larger the AG value, the more details and sharper edges the image contains, and generally has higher clarity.

(7) Perceptual Index (PI): PI [342] was proposed by the 2018 PIRM Super-Resolution Challenge, which combines two no-reference image quality measures: Ma et al. [343] and NIQE [339]. Specifically, PI can be expressed as follows:

$$PI = \frac{1}{2} ((10 - Ma) + NIQE) \quad (8)$$

The smaller the PI value, the better the visual quality of the image.

In addition to the above evaluation metrics, there are some other metrics for quantitative evaluation of RSISR results, such as: ERGAS (Erreur Relative Globale Adimensionnelle de Synthèse) [344], Q-index [345], QNR [346], VIF [347], FSIM [348], spectral information divergence (SID) [349], correlation coefficient (CC) [350] and UIQI [345], etc. Here, we do not introduce them in detail.

## 7. Performance Evaluation Methods

This section summarizes the performance evaluation methods of RSISR. Generally speaking, most studies combine visual perception and objective metrics to conduct qualitative and quantitative evaluations of RSISR methods.

### 7.1. Qualitative Evaluation

Different from natural images, downstream tasks of RSISR often involve land cover classification, object detection, and change detection, etc. Therefore, the restoration of texture details and the preservation of spatial structure are particularly important, which is mainly evaluated manually and visually. The most common qualitative evaluation methods include the following aspects:

- *Visual Comparison*: Super-resolution images are displayed side by side with original images, HR reference images or other algorithm results to observe the reconstruction quality from the aspects of texture, edge sharpness, structural fidelity, etc.

- *Expert visual evaluation*: Experts with remote sensing interpretation experience make comprehensive judgments from the perspectives of object recognition, structure preservation, and edge integrity. This method is particularly suitable for the identifiable analysis of objects such as roads, buildings, and farmland boundaries in HR images.

- *Application-guided evaluation*: Super-resolution results participate in downstream tasks such as land cover classification, object detection, and change detection, etc. Furthermore, the visual quality and semantic preservation are indirectly evaluated through application performance. In addition, the analysis of some typical problems, such as color consistency, artifacts, and over-smoothing may also be involved. This method is highly subjective, and different people may have different standards when checking super-resolution images. To the best of our knowledge, there is not a good solution for these issues currently.

### 7.2. Quantitative Evaluation

Quantitative evaluation methods objectively check the quality of reconstructed images through metric values, which provides a unified standard for performance comparison among different algorithms. Many evaluation metrics, such as PSNR and SSIM and information entropy (EN), have been proposed. Specifically, PSNR measures the error between the reconstructed image and the reference image at the pixel level, while SSIM focuses more on the preservation of structural information, which is particularly suitable for the evaluation of highly structural targets such as building outlines and road networks in RSIs. In addition, EN is used to evaluate the richness of spatial information in super-resolution images.

On the other hand, some non-reference metrics, such as NIQE and PI, have also been proposed. They quantify the visual naturalness and quality degradation based on the statistical characteristics of the image, and are particularly suitable for real remote sensing scenes without HR ground truth. In current RSISR research, although quantitative evaluation provides a standardized and repeatable approach, they still face many challenges. Specifically, different evaluation metrics and test data sets are often used in different studies, which leads to a lack of consistency in experimental settings and result interpretation among various methods, making fair comparisons across methods difficult. In addition, each metric can usually only evaluate one aspect of image quality. Therefore, building a comprehensive and unified evaluation framework has become one of the most critical issues in the field of RSISR.

## 8. Future Prospects

### 8.1. Better Evaluation Metrics

Most RSISR methods are evaluated qualitatively by using visual performance and quantitatively by using evaluation metrics in existing papers. Existing metrics usually, such as PSNR and SSIM, can usually only evaluate one aspect of the super-resolved image, and different indicators are used for performance evaluation on different test datasets in different papers, making it difficult to compare algorithms fairly. Therefore, it is desirable to have better metrics. Ideal metrics should be consistent with visual performance and strongly correlated with performance evaluation on downstream tasks. In addition, it is also encouraging to propose evaluation metrics that adapt to diverse remote sensing data sources in the future.

### 8.2. Better Benchmarks

Although some benchmarks for RSISR have been proposed, the research on RSISR benchmark is still at an early stage. In 2023, Kowaleczko et al. [322] proposed a new benchmark, MuS2, for RSISR. However, the heterogeneity of MuS2 data leads to the inconsistencies between geometric and spectral, ground feature variations caused by large time spans, and inconsistencies between indicators and real perception. These challenges have greatly weakened the ability of the benchmark to fairly evaluate algorithm performance and slowed down the development of SR technology. In addition, Aybar et al. [320] proposed the OpenSR-test benchmark for optical RSISR. Although OpenSR-test focuses on same-day imaging and manual cleaning, the size of its dataset is still limited by the HR image acquisition and fine registration process. A more recent work is the RRSISR benchmark proposed by Wang et al. [323]. Although these benchmarks have made significant progress in real data collection, multi-temporal pairing, and evaluation mechanisms, these datasets rely on heterogeneous sensors, which makes it difficult to unify imaging geometry, spectral response, time span, and band consistency, resulting in insufficient evaluation generalization ability.

Furthermore, current mainstream metrics such as PSNR, SSIM and LPIPS fail to effectively measure multispectral consistency, structural fidelity and practical application performance. In addition, existing benchmarks face challenges in data acquisition costs and scale expansion, and it is difficult to meet the universality and scalability of large-scale, multi-task, and multi-source remote sensing. For this reason, it is urgent to build a benchmark for RSISR with authenticity, universality, and multi-task jointness to promote the model from synthetic optimization to real application.

### 8.3. Diffusion-Mamba Based RSISR Methods

Diffusion models and Mamba have demonstrated excellent performance in many computer vision tasks. However, the application of such models in RSISR is at a very early stage. The diffusion model generates high-fidelity details through iterative denoising, but its computational efficiency is low. In contrast, the Mamba model has high computational efficiency due to its

linear complexity long-range modeling ability, but it still needs to be optimized in recovering high-frequency details. In the future, we expect many RSISR methods based on the diffusion model and Mamba to emerge. Specifically, it is interesting to develop a hybrid architecture of diffusion and Mamba to synergize the advantages of both to improve application performance.

### 8.4. Application-Oriented RSISR Methods

One of the motivations of RSISR is to improve the performance of practical applications. However, it can be seen from our review that most studies ignore the deep requirements of downstream tasks for image quality. Specifically, existing methods generally use general metrics such as PSNR and SSIM, which may lead to suboptimal performance of downstream tasks. In the future, it is better to focus RSISR research on the application-oriented paradigm. To this end, we expect that the application-oriented RSISR methods will become the mainstream methods in this field. Specifically, it is desirable to conduct degradation modeling with application-oriented, downstream task-embedded evaluation and lightweight adaptive architectures.

### 8.5. Improving RSISR Efficiency

The efficiency of the RSISR algorithm greatly affects the deployment of real-time applications. Most studies significantly reduce the computational overhead through dynamic computing strategies and lightweight architectures, but still face the trade-off between detail recovery and efficiency. In the future, it is desirable to combine the local perception of CNN with the global modeling capabilities of Mamba or Transformer to reduce computation while maintaining accuracy.

## 9. Conclusion

In this paper, a detailed and comprehensive review of RSISR methods is presented, covering methodology, datasets, and evaluation metrics. Specifically, we carefully group the existing RSISR methods into supervised and unsupervised. Furthermore, representative methods in each category are analyzed and discussed in detail. We also discuss the recent developments in this field based on a survey of more than 300 papers. Through these reviews and analyses, we provide future perspectives on some issues we consider critical. We expect this survey to provide a suitable reference for researchers in the field of RSISR.

### CRedit authorship contribution statement

**Yunliang Qi**: Writing - original draft, Visualization, Validation, Methodology, Investigation. **Meng Lou**: Writing – review & editing, Visualization, Methodology. **Yimin Liu**: Supervision, Investigation. **Lu Li**: Writing – review & editing, Supervision, Investigation. **Zhen Yang**: Supervision, Investigation, **Wen Nie**: Supervision, Investigation.

## Declaration of competing interest

The authors declare that they have no known competing financial interests or personal relationships that could have appeared to influence the work reported in this paper.

## Acknowledgements

This work was jointly supported by the Natural Science Foundation of Gansu Province, China (No.22JR5RA492) and the Fundamental Research Funds for the Central Universities of China (No. lzujbky-2017-it72 and lzujbky- 2022-pd12).

## References

- [1] S. Farsiu, M. D. Robinson, M. Elad, P. Milanfar, Fast and robust multi-frame super resolution, *IEEE transactions on image processing* 13 (10) (2004) 1327–1344.
- [2] P. Wang, B. Bayram, E. Sertel, A comprehensive review on deep learning based remote sensing image super-resolution methods, *Earth-Science Reviews* 232 (2022) 104110.
- [3] W. Shi, J. Caballero, C. Ledig, X. Zhuang, W. Bai, K. Bhatia, A. M. S. M. de Marvao, T. Dawes, D. O'Regan, D. Rueckert, Cardiac image super-resolution with global correspondence using multi-atlas patchmatch, in: *Medical Image Computing and Computer-Assisted Intervention—MICCAI 2013: 16th International Conference, Nagoya, Japan, September 22–26, 2013, Proceedings, Part III 16*, Springer, 2013, pp. 9–16.
- [4] W. W. Zou, P. C. Yuen, Very low resolution face recognition problem, *IEEE Transactions on image processing* 21 (1) (2011) 327–340.
- [5] J. Xie, L. Fang, B. Zhang, J. Chanussot, S. Li, Super resolution guided deep network for land cover classification from remote sensing images, *IEEE Transactions on Geoscience and Remote Sensing* 60 (2021) 1–12.
- [6] X. Jia, X. Li, Z. Wang, Z. Hao, D. Ren, H. Liu, Y. Du, F. Ling, Enhancing cropland mapping with spatial super-resolution reconstruction by optimizing training samples for image super-resolution models, *Remote Sensing* 16 (24) (2024) 4678.
- [7] X. Fu, T. Kouyama, H. Yang, R. Nakamura, I. Yoshikawa, Toward faster and accurate post-disaster damage assessment: Development of end-to-end building damage detection framework with super-resolution architecture, in: *IGARSS 2022-2022 IEEE International Geoscience and Remote Sensing Symposium*, IEEE, 2022, pp. 1588–1591.
- [8] L. Li, T. Xu, Y. Chen, Improved urban flooding mapping from remote sensing images using generalized regression neural network-based super-resolution algorithm, *Remote Sensing* 8 (8) (2016) 625.
- [9] R. Fernandez-Beltran, P. Latorre-Carmona, F. Pla, Single-frame super-resolution in remote sensing: a practical overview, *International Journal of Remote Sensing*. 38 (2017) 314–354.
- [10] L. Loncan, L. B. de Almeida, J. M. Bioucas-Dias, X. Briottet, J. Chanussot, N. Dobigeon, S. Fabre, W. Liao, G. A. Licciardi, M. Simões, J.-Y. Tournet, M. A. Veganzones, G. Vivone, Q. Wei, N. Yokoya, Hyperspectral pansharpening: A review, *IEEE Geoscience and Remote Sensing Magazine* 3 (3) (2015) 27–46.
- [11] H. Chavez-Roman, V. Ponomaryov, Super resolution image generation using wavelet domain interpolation with edge extraction via a sparse representation, *IEEE Geoscience and remote sensing Letters* 11 (10) (2014) 1777–1781.
- [12] H. Demirel, G. Anbarjafari, Discrete wavelet transform-based satellite image resolution enhancement, *IEEE transactions on geoscience and remote sensing* 49 (6) (2011) 1997–2004.
- [13] P. Wang, E. Sertel, Channel–spatial attention-based pan-sharpening of very high-resolution satellite images, *Knowledge-Based Systems* 229 (2021) 107324.
- [14] D. Yang, Z. Li, Y. Xia, Z. Chen, Remote sensing image super-resolution: Challenges and approaches, in: *2015 IEEE international conference on digital signal processing (DSP)*, IEEE, 2015, pp. 196–200.
- [15] F. Ling, Y. Du, X. Li, W. Li, F. Xiao, Y. Zhang, Interpolation-based super-resolution land cover mapping, *Remote sensing letters* 4 (7) (2013) 629–638.
- [16] W. Ma, Z. Pan, J. Guo, B. Lei, Achieving super-resolution remote sensing images via the wavelet transform combined with the recursive res-net, *IEEE Transactions on Geoscience and Remote Sensing* 57 (6) (2019) 3512–3527.
- [17] Z. Wang, Y. Zhao, J. Chen, Multi-scale fast fourier transform based attention network for remote-sensing image super-resolution, *IEEE Journal of Selected Topics in Applied Earth Observations and Remote Sensing* 16 (2023) 2728–2740.
- [18] Z. Shao, L. Wang, Z. Wang, J. Deng, Remote sensing image super-resolution using sparse representation and coupled sparse autoencoder, *IEEE Journal of Selected Topics in Applied Earth Observations and Remote Sensing* 12 (8) (2019) 2663–2674.
- [19] J. Yang, Y.-Q. Zhao, J. C.-W. Chan, L. Xiao, A multi-scale wavelet 3d-cnn for hyperspectral image super-resolution, *Remote sensing* 11 (13) (2019) 1557.
- [20] C. He, L. Liu, L. Xu, M. Liu, M. Liao, Learning based compressed sensing for sar image super-resolution, *IEEE Journal of Selected Topics in Applied Earth Observations and Remote Sensing* 5 (4) (2012) 1272–1281.
- [21] W. Dong, F. Fu, G. Shi, X. Cao, J. Wu, G. Li, X. Li, Hyperspectral image super-resolution via non-negative structured sparse representation, *IEEE Transactions on Image Processing* 25 (5) (2016) 2337–2352.
- [22] W. Wu, X. Yang, K. Liu, Y. Liu, B. Yan, et al., A new framework for remote sensing image super-resolution: sparse representation-based method by processing dictionaries with multi-type features, *Journal of Systems Architecture* 64 (2016) 63–75.
- [23] C. Tuna, G. Unal, E. Sertel, Single-frame super resolution of remote-sensing images by convolutional neural networks, *International journal of remote sensing* 39 (8) (2018) 2463–2479.
- [24] M. Gargiulo, Advances on cnn-based super-resolution of sentinel-2 images, in: *IGARSS 2019-2019 IEEE International Geoscience and Remote Sensing Symposium*, IEEE, 2019, pp. 3165–3168.
- [25] X. Wang, L. Sun, A. Chehri, Y. Song, A review of gan-based super-resolution reconstruction for optical remote sensing images, *Remote Sensing* 15 (20) (2023) 5062.
- [26] S. Jia, Z. Wang, Q. Li, X. Jia, M. Xu, Multiattention generative adversarial network for remote sensing image super-resolution, *IEEE Transactions on Geoscience and Remote Sensing* 60 (2022) 1–15.
- [27] Z. Tu, X. Yang, X. He, J. Yan, T. Xu, Rgtgan: Reference-based gradient-assisted texture-enhancement gan for remote sensing super-resolution, *IEEE Transactions on Geoscience and Remote Sensing* (2024).
- [28] X. Kang, P. Duan, J. Li, S. Li, Efficient swin transformer for remote sensing image super-resolution, *IEEE Transactions on Image Processing* (2024).
- [29] Y. Xiao, Q. Yuan, K. Jiang, J. He, C.-W. Lin, L. Zhang, Ttst: A top-k token selective transformer for remote sensing image super-resolution, *IEEE Transactions on Image Processing* (2024).
- [30] Y. Xiao, Q. Yuan, Remote sensing image super-resolution with top-k token selective transformer, in: *IGARSS 2024-2024 IEEE International Geoscience and Remote Sensing Symposium*, IEEE, 2024, pp. 3159–3162.
- [31] R. Zhi, X. Fan, J. Shi, Mambaformers: A lightweight model for remote-sensing image super-resolution, *IEEE Geoscience and Remote Sensing Letters* (2024).
- [32] C. Dong, C. C. Loy, K. He, X. Tang, Image super-resolution using deep convolutional networks, *IEEE Transactions on Pattern Analysis and Machine Intelligence* 38 (2) (2016) 295–307. doi:[10.1109/TPAMI.2015.2439281](https://doi.org/10.1109/TPAMI.2015.2439281).
- [33] C. Dong, C. C. Loy, K. He, X. Tang, Learning a deep convolutional network for image super-resolution, in: *Computer Vision – ECCV 2014*, Springer International Publishing, Cham, 2014, pp. 184–199.
- [34] H. Liu, Y. Qian, X. Zhong, L. Chen, G. Yang, Research on super-resolution reconstruction of remote sensing images: A comprehensive review, *Optical Engineering* 60 (10) (2021) 100901–100901.
- [35] X. Wang, J. Yi, J. Guo, Y. Song, J. Lyu, J. Xu, W. Yan, J. Zhao, Q. Cai, H. Min, A review of image super-resolution approaches based on deep learning and applications in remote sensing, *Remote Sensing* 14 (21) (2022) 5423.

[36] K. Karwowska, D. Wierzbicki, Using super-resolution algorithms for small satellite imagery: A systematic review, *IEEE Journal of Selected Topics in Applied Earth Observations and Remote Sensing* 15 (2022) 3292–3312.

[37] D. C. Lepcha, B. Goyal, A. Dogra, V. Goyal, Image super-resolution: A comprehensive review, recent trends, challenges and applications, *Information Fusion* 91 (2023) 230–260.

[38] C. Chen, Y. Wang, N. Zhang, Y. Zhang, Z. Zhao, A review of hyperspectral image super-resolution based on deep learning, *Remote Sensing* 15 (11) (2023) 2853.

[39] X. Qian, T.-X. Jiang, X.-L. Zhao, Selfs2: Self-supervised transfer learning for sentinel-2 multispectral image super-resolution, *IEEE Journal of Selected Topics in Applied Earth Observations and Remote Sensing* 16 (2022) 215–227.

[40] J. Liu, Z. Wu, L. Xiao, A spectral diffusion prior for unsupervised hyperspectral image super-resolution, *IEEE Transactions on Geoscience and Remote Sensing* (2024).

[41] X. He, K. Cao, J. Zhang, K. Yan, Y. Wang, R. Li, C. Xie, D. Hong, M. Zhou, Pan-mamba: Effective pan-sharpening with state space model, *Information Fusion* 115 (2025) 102779.

[42] T.-M. Chan, J. Zhang, J. Pu, H. Huang, Neighbor embedding based super-resolution algorithm through edge detection and feature selection, *Pattern Recognition Letters* 30 (5) (2009) 494–502.

[43] Z. Zhang, X. Wang, J. Ma, G. Jia, Super resolution reconstruction of three view remote sensing images based on global weighted pocs algorithm, in: 2011 International Conference on Remote Sensing, Environment and Transportation Engineering, IEEE, 2011, pp. 3615–3618.

[44] F. Zhou, W. Yang, Q. Liao, Interpolation-based image super-resolution using multisurface fitting, *IEEE Transactions on Image Processing* 21 (7) (2012) 3312–3318.

[45] R. Timofte, V. De Smet, L. Van Gool, Anchored neighborhood regression for fast example-based super-resolution, in: Proceedings of the IEEE international conference on computer vision, 2013, pp. 1920–1927.

[46] S. Yang, Z. Wang, L. Zhang, M. Wang, Dual-geometric neighbor embedding for image super resolution with sparse tensor, *IEEE Transactions on Image Processing* 23 (7) (2014) 2793–2803.

[47] J. Ma, J. C.-W. Chan, F. Canters, Robust locally weighted regression for superresolution enhancement of multi-angle remote sensing imagery, *IEEE journal of selected topics in applied earth observations and remote sensing* 7 (4) (2014) 1357–1371.

[48] Y. Zhang, Y. Du, F. Ling, S. Fang, X. Li, Example-based super-resolution land cover mapping using support vector regression, *IEEE Journal of Selected Topics in Applied Earth Observations and Remote Sensing* 7 (4) (2014) 1271–1283.

[49] D. Dai, R. Timofte, L. Van Gool, Jointly optimized regressors for image super-resolution, in: Computer Graphics Forum, Vol. 34, Wiley Online Library, 2015, pp. 95–104.

[50] W. Xinglei, L. Naifeng, Super-resolution of remote sensing images via sparse structural manifold embedding, *Neurocomputing* 173 (2016) 1402–1411.

[51] L. Li, T. Xu, Y. Chen, Improved urban flooding mapping from remote sensing images using generalized regression neural network-based super-resolution algorithm, *Remote Sensing* 8 (8) (2016). [doi:10.3390/rs8080625](https://doi.org/10.3390/rs8080625).

[52] J. Liu, S. Dai, Z. Guo, D. Zhang, An improved pocs super-resolution infrared image reconstruction algorithm based on visual mechanism, *Infrared Physics & Technology* 78 (2016) 92–98.

[53] S. Lei, Z. Shi, Z. Zou, Super-resolution for remote sensing images via local-global combined network, *IEEE Geoscience and Remote Sensing Letters* 14 (8) (2017) 1243–1247.

[54] J. M. Haut, R. Fernandez-Beltran, M. E. Paoletti, J. Plaza, A. Plaza, F. Pla, A new deep generative network for unsupervised remote sensing single-image super-resolution, *IEEE Transactions on Geoscience and Remote sensing* 56 (11) (2018) 6792–6810.

[55] P. Solanki, D. Israni, A. Shah, An efficient satellite image super resolution technique for shift-variant images using improved new edge directed interpolation, *Statistics, Optimization & Information Computing* 6 (4) (2018) 619–632.

[56] H. Irmak, G. B. Akar, S. E. Yuksel, A map-based approach for hyperspectral imagery super-resolution, *IEEE Transactions on Image Processing* 27 (6) (2018) 2942–2951.

[57] R. Nayak, D. Patra, Enhanced iterative back-projection based super-resolution reconstruction of digital images, *Arabian Journal for Science and Engineering* 43 (12) (2018) 7521–7547.

[58] K. Jiang, Z. Wang, P. Yi, G. Wang, T. Lu, J. Jiang, Edge-enhanced gan for remote sensing image superresolution, *IEEE Transactions on Geoscience and Remote Sensing* 57 (8) (2019) 5799–5812.

[59] L. Li, Y. Chen, T. Xu, K. Shi, C. Huang, R. Liu, B. Lu, L. Meng, Enhanced super-resolution mapping of urban floods based on the fusion of support vector machine and general regression neural network, *IEEE Geoscience and Remote Sensing Letters* 16 (8) (2019) 1269–1273.

[60] J. Gu, X. Sun, Y. Zhang, K. Fu, L. Wang, Deep residual squeeze and excitation network for remote sensing image super-resolution, *Remote Sensing* 11 (15) (2019) 1817.

[61] J. M. Haut, R. Fernandez-Beltran, M. E. Paoletti, J. Plaza, A. Plaza, Remote sensing image superresolution using deep residual channel attention, *IEEE Transactions on Geoscience and Remote Sensing* 57 (11) (2019) 9277–9289.

[62] X. Dong, Z. Xi, X. Sun, L. Gao, Transferred multi-perception attention networks for remote sensing image super-resolution, *Remote Sensing* 11 (23) (2019) 2857.

[63] Y. Zhang, Q. Zhang, C. Li, Y. Zhang, Y. Huang, J. Yang, Sea-surface target angular superresolution in forward-looking radar imaging based on maximum a posteriori algorithm, *IEEE Journal of Selected Topics in Applied Earth Observations and Remote Sensing* 12 (8) (2019) 2822–2834.

[64] X. Li, D. Zhang, Z. Liang, D. Ouyang, J. Shao, Fused recurrent network via channel attention for remote sensing satellite image super-resolution, in: 2020 IEEE international conference on multimedia and expo (ICME), IEEE, 2020, pp. 1–6.

[65] S. Zhang, Q. Yuan, J. Li, J. Sun, X. Zhang, Scene-adaptive remote sensing image super-resolution using a multiscale attention network, *IEEE Transactions on Geoscience and Remote Sensing* 58 (7) (2020) 4764–4779.

[66] H. Wang, Q. Hu, C. Wu, J. Chi, X. Yu, Non-locally up-down convolutional attention network for remote sensing image super-resolution, *IEEE Access* 8 (2020) 166304–166319.

[67] S. Lei, Z. Shi, Z. Zou, Coupled adversarial training for remote sensing image super-resolution, *IEEE Transactions on Geoscience and Remote Sensing* 58 (5) (2019) 3633–3643.

[68] M. M. Sheikholeslami, S. Nadi, A. A. Naeini, P. Ghamisi, An efficient deep unsupervised superresolution model for remote sensing images, *IEEE Journal of Selected Topics in Applied Earth Observations and Remote Sensing* 13 (2020) 1937–1945.

[69] X. Dong, X. Sun, X. Jia, Z. Xi, L. Gao, B. Zhang, Remote sensing image super-resolution using novel dense-sampling networks, *IEEE Transactions on Geoscience and Remote Sensing* 59 (2) (2020) 1618–1633.

[70] D. Guo, Y. Xia, L. Xu, W. Li, X. Luo, Remote sensing image super-resolution using cascade generative adversarial nets, *Neurocomputing* 443 (2021) 117–130.

[71] J. Wang, Z. Shao, T. Lu, X. Huang, R. Zhang, Y. Wang, Unsupervised remote sensing super-resolution via migration image prior, in: 2021 IEEE International Conference on Multimedia and Expo (ICME), IEEE, 2021, pp. 1–6.

[72] H. Zhang, P. Wang, Z. Jiang, Nonpairwise-trained cycle convolutional neural network for single remote sensing image super-resolution, *IEEE Transactions on Geoscience and Remote Sensing* 59 (5) (2020) 4250–4261.

[73] J. Wang, Z. Shao, X. Huang, T. Lu, R. Zhang, J. Ma, Enhanced image prior for unsupervised remote sensing super-resolution, *Neural Networks* 143 (2021) 400–412.

[74] W. Chen, X. Zheng, X. Lu, Hyperspectral image super-resolution with self-supervised spectral-spatial residual network, *Remote Sensing* 13 (7) (2021) 1260.

[75] Y. Wang, X. He, Y. Shi, Q. Zhu, H. Yu, An improved hyperspectral image super resolution restoration algorithm based on pocs, in: 2021 IEEE International Geoscience and Remote Sensing Symposium IGARSS, IEEE, 2021, pp. 2460–2463.

[76] Z. Wang, L. Li, Y. Xue, C. Jiang, J. Wang, K. Sun, H. Ma, Fenet: Feature enhancement network for lightweight remote-sensing image super-resolution, *IEEE Transactions on Geoscience and Remote Sensing* 60

(2022) 1–12.

[77] J. Zhang, T. Xu, J. Li, S. Jiang, Y. Zhang, Single-image super-resolution of remote sensing images with real-world degradation modeling, *Remote Sensing* 14 (12) (2022) 2895.

[78] J.-F. Hu, T.-Z. Huang, L.-J. Deng, H.-X. Dou, D. Hong, G. Vivone, Fusformer: A transformer-based fusion network for hyperspectral image super-resolution, *IEEE Geoscience and Remote Sensing Letters* 19 (2022) 1–5.

[79] S. Lei, Z. Shi, W. Mo, Transformer-based multistage enhancement for remote sensing image super-resolution, *IEEE Transactions on Geoscience and Remote Sensing* 60 (2021) 1–11.

[80] V. K. Mutai, E. Mwangi, W. M. Ciira, A cubic b-splines approximation method combined with dwt and ibp for single image super-resolution (2022).

[81] F. Ye, Z. Wu, Y. Xu, H. Liu, Z. Wei, Bayesian hyperspectral image super-resolution in the presence of spectral variability, *IEEE Transactions on Geoscience and Remote Sensing* 60 (2022) 1–13.

[82] B. Deka, H. U. Mullah, T. Barman, S. Datta, Joint sparse representation-based single image super-resolution for remote sensing applications, *IEEE Journal of Selected Topics in Applied Earth Observations and Remote Sensing* 16 (2023) 2352–2365.

[83] J. Wang, B. Wang, X. Wang, Y. Zhao, T. Long, Hybrid attention-based u-shaped network for remote sensing image super-resolution, *IEEE Transactions on Geoscience and Remote Sensing* 61 (2023) 1–15.

[84] C. Wu, D. Wang, Y. Bai, H. Mao, Y. Li, Q. Shen, Hsr-diff: Hyperspectral image super-resolution via conditional diffusion models, in: *Proceedings of the IEEE/CVF International Conference on Computer Vision*, 2023, pp. 7083–7093.

[85] M. Zhang, C. Zhang, Q. Zhang, J. Guo, X. Gao, J. Zhang, Essaformer: Efficient transformer for hyperspectral image super-resolution, in: *Proceedings of the IEEE/CVF International Conference on Computer Vision*, 2023, pp. 23073–23084.

[86] J. Tao, W. Ni, C. Song, X. Wang, Fssbp: Fast spatial–spectral back projection based on pan-sharpening iterative optimization, *Remote Sensing* 15 (18) (2023) 4543.

[87] B. Liu, L. Zhao, S. Shao, W. Liu, D. Tao, W. Cao, Y. Zhou, Ran: Region-aware network for remote sensing image super-resolution, *IEEE Transactions on Geoscience and Remote Sensing* 61 (2023) 1–13.

[88] D. Mishra, O. Hadar, Clsr: Contrastive learning for semi-supervised remote sensing image super-resolution, *IEEE Geoscience and Remote Sensing Letters* 20 (2023) 1–5.

[89] Y. Xiao, Q. Yuan, K. Jiang, J. He, Y. Wang, L. Zhang, From degrade to upgrade: Learning a self-supervised degradation guided adaptive network for blind remote sensing image super-resolution, *Information Fusion* 96 (2023) 297–311.

[90] D. Mishra, O. Hadar, Self-fusenet: Data free unsupervised remote sensing image super-resolution, *IEEE Journal of Selected Topics in Applied Earth Observations and Remote Sensing* 16 (2023) 1710–1727.

[91] Z. Cha, D. Xu, Y. Tang, Z. Jiang, Meta-learning for zero-shot remote sensing image super-resolution, *Mathematics* 11 (7) (2023) 1653.

[92] J. Wang, Y. Lu, S. Wang, B. Wang, X. Wang, T. Long, Two-stage spatial-frequency joint learning for large-factor remote sensing image super-resolution, *IEEE Transactions on Geoscience and Remote Sensing* 62 (2024) 1–13.

[93] B. Chen, L. Liu, C. Liu, Z. Zou, Z. Shi, Spectral-cascaded diffusion model for remote sensing image spectral super-resolution, *IEEE Transactions on Geoscience and Remote Sensing* (2024).

[94] F. Meng, Y. Chen, H. Jing, L. Zhang, Y. Yan, Y. Ren, S. Wu, T. Feng, R. Liu, Z. Du, A conditional diffusion model with fast sampling strategy for remote sensing image super-resolution, *IEEE Transactions on Geoscience and Remote Sensing* (2024).

[95] T. An, B. Xue, C. Huo, S. Xiang, C. Pan, Efficient remote sensing image super-resolution via lightweight diffusion models, *IEEE Geoscience and Remote Sensing Letters* 21 (2023) 1–5.

[96] Y. Zhong, X. Wu, Z. Cao, H.-X. Dou, L.-J. Deng, Ssdiff: Spatial-spectral integrated diffusion model for remote sensing pansharpening, *Advances in Neural Information Processing Systems* 37 (2024) 77962–77986.

[97] X. Lu, J. Zhang, R. Yang, Q. Yang, M. Chen, H. Xu, P. Wan, J. Guo, F. Liu, Effective variance attention-enhanced diffusion model for crop field aerial image super resolution, *ISPRS Journal of Photogrammetry and Remote Sensing* 218 (2024) 50–68.

[98] Y. Xiao, Q. Yuan, K. Jiang, J. He, X. Jin, L. Zhang, Ediffr: An efficient diffusion probabilistic model for remote sensing image super-resolution, *IEEE Transactions on Geoscience and Remote Sensing* 62 (2024) 1–14. [doi:10.1109/TGRS.2023.3341437](https://doi.org/10.1109/TGRS.2023.3341437).

[99] F. Meng, S. Wu, Y. Li, Z. Zhang, T. Feng, R. Liu, Z. Du, Single remote sensing image super-resolution via a generative adversarial network with stratified dense sampling and chain training, *IEEE Transactions on Geoscience and Remote Sensing* 62 (2024) 1–22. [doi:10.1109/TGRS.2023.3344112](https://doi.org/10.1109/TGRS.2023.3344112).

[100] X. Kang, P. Duan, J. Li, S. Li, Efficient swin transformer for remote sensing image super-resolution, *IEEE Transactions on Image Processing* 33 (2024) 6367–6379. [doi:10.1109/TIP.2024.3489228](https://doi.org/10.1109/TIP.2024.3489228).

[101] D. Jiao, N. Su, Y. Yan, Y. Liang, S. Feng, C. Zhao, G. He, Symswin: Multi-scale-aware super-resolution of remote sensing images based on swin transformers, *Remote Sensing* 16 (24) (2024) 4734.

[102] Y. Wang, S. Jin, Z. Yang, H. Guan, Y. Ren, K. Cheng, X. Zhao, X. Liu, M. Chen, Y. Liu, et al., Ttsr: A transformer-based topography neural network for digital elevation model super-resolution, *IEEE Transactions on Geoscience and Remote Sensing* 62 (2024) 1–19.

[103] R. Li, X. Zhao, Lswinsr: Uav imagery super-resolution based on linear swin transformer, *IEEE Transactions on Geoscience and Remote Sensing* 62 (2024) 1–13. [doi:10.1109/TGRS.2024.3463204](https://doi.org/10.1109/TGRS.2024.3463204).

[104] Q. Zhu, G. Zhang, X. Zou, X. Wang, J. Huang, X. Li, Convmmabasr: Leveraging state-space models and cnns in a dual-branch architecture for remote sensing imagery super-resolution, *Remote Sensing* 16 (17) (2024) 3254.

[105] Y. Xiao, Q. Yuan, K. Jiang, Y. Chen, Q. Zhang, C.-W. Lin, Frequency-assisted mamba for remote sensing image super-resolution, *IEEE Transactions on Multimedia* (2024) 1–14. [doi:10.1109/TMM.2024.3521798](https://doi.org/10.1109/TMM.2024.3521798).

[106] X. Wang, L. Sun, J. Yi, Y. Song, Q. Zheng, A. Chehri, Efficient degradation representation learning network for remote sensing image super-resolution, *Computer Vision and Image Understanding* 249 (2024) 104182.

[107] L. Zhai, Y. Wang, S. Cui, Y. Zhou, Transcyclegan: An approach for remote sensing image super-resolution, in: *2024 IEEE Southwest Symposium on Image Analysis and Interpretation (SSIAI)*, IEEE, 2024, pp. 61–64.

[108] J. Zhu, V. K. Z. Koh, Z. Lin, B. Wen, Tm-gan: A transformer-based multi-modal generative adversarial network for guided depth image super-resolution, *IEEE Journal on Emerging and Selected Topics in Circuits and Systems* 14 (2) (2024) 261–274. [doi:10.1109/JETCAS.2024.3394495](https://doi.org/10.1109/JETCAS.2024.3394495).

[109] A. Sharifi, M. M. Safari, Enhancing the spatial resolution of sentinel-2 images through super-resolution using transformer-based deep-learning models, *IEEE Journal of Selected Topics in Applied Earth Observations and Remote Sensing* 18 (2025) 4805–4820. [doi:10.1109/JSTARS.2025.3526260](https://doi.org/10.1109/JSTARS.2025.3526260).

[110] W.-D. Weng, C.-W. Zheng, J.-N. Su, G.-Y. Chen, M. Gan, Efficient high-frequency texture recovery diffusion model for remote sensing image super-resolution, *IEEE Transactions on Instrumentation and Measurement* 74 (2025) 1–14. [doi:10.1109/TIM.2025.3556898](https://doi.org/10.1109/TIM.2025.3556898).

[111] C. Wang, W. Sun, Semantic guided large scale factor remote sensing image super-resolution with generative diffusion prior, *ISPRS Journal of Photogrammetry and Remote Sensing* 220 (2025) 125–138.

[112] Y. Song, L. Sun, J. Bi, S. Quan, X. Wang, Drgan: A detail recovery-based model for optical remote sensing images super-resolution, *IEEE Transactions on Geoscience and Remote Sensing* 63 (2025) 1–13. [doi:10.1109/TGRS.2024.3512528](https://doi.org/10.1109/TGRS.2024.3512528).

[113] Y. Guo, Y. Liang, Y. Liang, X. Sun, Structured bayesian super-resolution forward-looking imaging for maneuvering platforms based on enhanced sparsity model, *Remote Sensing* 17 (5) (2025) 775.

[114] Y. Yang, H. Zhao, X. Huangfu, Z. Li, P. Wang, Vit-isrgan: A high-quality super-resolution reconstruction method for multispectral remote sensing images, *IEEE Journal of Selected Topics in Applied Earth Observations and Remote Sensing* 18 (2025) 3973–3988. [doi:10.1109/JSTARS.2025.3527226](https://doi.org/10.1109/JSTARS.2025.3527226).

[115] J. Yang, J. Wright, T. Huang, Y. Ma, Image super-resolution as sparse representation of raw image patches, in: *2008 IEEE conference on computer vision and pattern recognition*, IEEE, 2008, pp. 1–8.

[116] J. Yang, J. Wright, T. S. Huang, Y. Ma, Image super-resolution via sparse

representation, *IEEE transactions on image processing* 19 (11) (2010) 2861–2873.

[117] Z. Zhihui, W. Bo, S. Kang, Single remote sensing image super-resolution and denoising via sparse representation, in: 2011 international workshop on multi-platform/multi-sensor remote sensing and mapping, IEEE, 2011, pp. 1–5.

[118] Y. Zhang, W. Wu, Y. Dai, X. Yang, B. Yan, W. Lu, Remote sensing images super-resolution based on sparse dictionaries and residual dictionaries, in: 2013 IEEE 11th International Conference on Dependable, Autonomic and Secure Computing, IEEE, 2013, pp. 318–323.

[119] S. Gou, S. Liu, S. Yang, L. Jiao, Remote sensing image super-resolution reconstruction based on nonlocal pairwise dictionaries and double regularization, *IEEE Journal of Selected Topics in Applied Earth Observations and Remote Sensing* 7 (12) (2014) 4784–4792.

[120] S. T. Roweis, L. K. Saul, Nonlinear dimensionality reduction by locally linear embedding, *science* 290 (5500) (2000) 2323–2326.

[121] H. Chang, D.-Y. Yeung, Y. Xiong, Super-resolution through neighbor embedding, in: Proceedings of the 2004 IEEE Computer Society Conference on Computer Vision and Pattern Recognition, 2004. CVPR 2004., Vol. 1, IEEE, 2004, pp. I–I.

[122] J. Xu, Y. Gao, J. Xing, J. Fan, Q. Gao, S. Tang, Two-direction self-learning super-resolution propagation based on neighbor embedding, *Signal Processing* 183 (2021) 108033. [doi:<https://doi.org/10.1016/j.sigpro.2021.108033>](https://doi.org/10.1016/j.sigpro.2021.108033).

[123] M. Bevilacqua, A. Roumy, C. Guillemot, M. L. Alberi-Morel, Low-complexity single-image super-resolution based on nonnegative neighbor embedding (2012).

[124] H. Zhang, B. Huang, Scale conversion of multi sensor remote sensing image using single frame super resolution technology, in: 2011 19th International Conference on Geoinformatics, IEEE, 2011, pp. 1–5.

[125] F. Zhou, T. Yuan, W. Yang, Q. Liao, Single-image super-resolution based on compact kpca coding and kernel regression, *IEEE Signal Processing Letters* 22 (3) (2014) 336–340.

[126] S. Kanakaraj, M. S. Nair, S. Kalady, Adaptive importance sampling unscented kalman filter with kernel regression for sar image super-resolution, *IEEE Geoscience and Remote Sensing Letters* 19 (2020) 1–5.

[127] S. D. Babacan, R. Molina, A. K. Katsaggelos, Variational bayesian super resolution, *IEEE Transactions on Image Processing* 20 (4) (2010) 984–999.

[128] N. Akhtar, F. Shafait, A. Mian, Bayesian sparse representation for hyperspectral image super resolution, in: Proceedings of the IEEE conference on computer vision and pattern recognition, 2015, pp. 3631–3640.

[129] L. Liebel, M. Körner, Single-image super resolution for multispectral remote sensing data using convolutional neural networks, *The International Archives of the Photogrammetry, Remote Sensing and Spatial Information Sciences* 41 (2016) 883–890.

[130] C. Dong, C. C. Loy, K. He, X. Tang, Learning a deep convolutional network for image super-resolution, in: Computer Vision–ECCV 2014: 13th European Conference, Zurich, Switzerland, September 6–12, 2014, Proceedings, Part IV 13, Springer, 2014, pp. 184–199.

[131] K. I. Kim, Y. Kwon, Single-image super-resolution using sparse regression and natural image prior, *IEEE transactions on pattern analysis and machine intelligence* 32 (6) (2010) 1127–1133.

[132] H. He, W.-C. Siu, Single image super-resolution using gaussian process regression, in: CVPR 2011, IEEE, 2011, pp. 449–456.

[133] K. Zhang, X. Gao, J. Li, H. Xia, Single image super-resolution using regularization of non-local steering kernel regression, *Signal Processing* 123 (2016) 53–63.

[134] K. Zhang, X. Gao, D. Tao, X. Li, Single image super-resolution with non-local means and steering kernel regression, *IEEE Transactions on Image Processing* 21 (11) (2012) 4544–4556.

[135] S. Kanakaraj, M. S. Nair, S. Kalady, Adaptive importance sampling unscented kalman filter with kernel regression for sar image super-resolution, *IEEE Geoscience and Remote Sensing Letters* 19 (2022) 1–5. [doi:\[10.1109/LGRS.2020.3031600\]\(https://doi.org/10.1109/LGRS.2020.3031600\)](https://doi.org/10.1109/LGRS.2020.3031600).

[136] Y. Zhang, Y. Du, F. Ling, X. Li, Improvement of the example-regression-based super-resolution land cover mapping algorithm, *IEEE Geoscience and Remote Sensing Letters* 12 (8) (2015) 1740–1744.

[137] D. F. Specht, et al., A general regression neural network, *IEEE transactions on neural networks* 2 (6) (1991) 568–576.

[138] C.-Y. Yang, M.-H. Yang, Fast direct super-resolution by simple functions, in: Proceedings of the IEEE international conference on computer vision, 2013, pp. 561–568.

[139] X. Yang, W. Wu, K. Liu, K. Zhou, B. Yan, Fast multisensor infrared image super-resolution scheme with multiple regression models, *Journal of Systems Architecture* 64 (2016) 11–25.

[140] D. Gao, Z. Hu, R. Ye, Self-dictionary regression for hyperspectral image super-resolution, *Remote Sensing* 10 (10) (2018) 1574.

[141] Y. Lecun, L. Bottou, Y. Bengio, P. Haffner, Gradient-based learning applied to document recognition, *Proceedings of the IEEE* 86 (11) (1998) 2278–2324. [doi:\[10.1109/5.726791\]\(https://doi.org/10.1109/5.726791\)](https://doi.org/10.1109/5.726791).

[142] A. Krizhevsky, I. Sutskever, G. Hinton, Imagenet classification with deep convolutional neural networks, in: NIPS, 2012.

[143] K. Simonyan, A. Zisserman, Very deep convolutional networks for large-scale image recognition, in: International Conference on Learning Representations, 2015.

[144] K. He, X. Zhang, S. Ren, J. Sun, Deep residual learning for image recognition, in: Proceedings of the IEEE Conference on Computer Vision and Pattern Recognition (CVPR), 2016.

[145] S. Minaee, Y. Boykov, F. Porikli, A. Plaza, N. Kehtarnavaz, D. Terzopoulos, Image segmentation using deep learning: A survey, *IEEE Transactions on Pattern Analysis and Machine Intelligence* 44 (7) (2022) 3523–3542. [doi:\[10.1109/TPAMI.2021.3059968\]\(https://doi.org/10.1109/TPAMI.2021.3059968\)](https://doi.org/10.1109/TPAMI.2021.3059968).

[146] S. Ren, K. He, R. Girshick, J. Sun, Faster r-cnn: Towards real-time object detection with region proposal networks, *IEEE Transactions on Pattern Analysis and Machine Intelligence* 39 (6) (2017) 1137–1149. [doi:\[10.1109/TPAMI.2016.2577031\]\(https://doi.org/10.1109/TPAMI.2016.2577031\)](https://doi.org/10.1109/TPAMI.2016.2577031).

[147] Y. Qi, Z. Yang, W. Sun, M. Lou, J. Lian, W. Zhao, X. Deng, Y. Ma, A comprehensive overview of image enhancement techniques, *Archives of Computational Methods in Engineering* 29 (2022) 583–607. [doi:\[10.1007/s11831-021-09587-6\]\(https://doi.org/10.1007/s11831-021-09587-6\)](https://doi.org/10.1007/s11831-021-09587-6).

[148] L. Liebel, M. Körner, Single-image super resolution for multispectral remote sensing data using convolutional neural networks, *The International Archives of the Photogrammetry, Remote Sensing and Spatial Information Sciences* 41 (2016) 883–890.

[149] J. Fu, Y. Liu, F. Li, in: IGARSS 2018 - 2018 IEEE International Geoscience and Remote Sensing Symposium, 2018, pp. 8014–8017. [doi:\[10.1109/IGARSS.2018.8518584\]\(https://doi.org/10.1109/IGARSS.2018.8518584\)](https://doi.org/10.1109/IGARSS.2018.8518584).

[150] H. M. Keshk, X.-C. Yin, Obtaining super-resolution satellites images based on enhancement deep convolutional neural network, *International Journal of Aeronautical and Space Sciences* 22 (1) (2021) 195–202.

[151] Q. Ran, X. Xu, S. Zhao, W. Li, Q. Du, Remote sensing images super-resolution with deep convolution networks, *Multimedia Tools and Applications* 79 (13) (2020) 8985–9001.

[152] T. Lu, J. Wang, Y. Zhang, Z. Wang, J. Jiang, Satellite image super-resolution via multi-scale residual deep neural network, *Remote Sensing* 11 (13) (2019) 1588.

[153] X. Dong, L. Wang, X. Sun, X. Jia, L. Gao, B. Zhang, Remote sensing image super-resolution using second-order multi-scale networks, *IEEE Transactions on Geoscience and Remote Sensing* 59 (4) (2021) 3473–3485. [doi:\[10.1109/TGRS.2020.3019660\]\(https://doi.org/10.1109/TGRS.2020.3019660\)](https://doi.org/10.1109/TGRS.2020.3019660).

[154] X. Wang, Y. Wu, Y. Ming, H. Lv, Remote sensing imagery super-resolution based on adaptive multi-scale feature fusion network, *Sensors* 20 (4) (2020) 1142.

[155] H. Huan, N. Zou, Y. Zhang, Y. Xie, C. Wang, Remote sensing image reconstruction using an asymmetric multi-scale super-resolution network, *The Journal of Supercomputing* 78 (17) (2022) 18524–18550. [doi:\[10.1007/s11227-022-04617-x\]\(https://doi.org/10.1007/s11227-022-04617-x\)](https://doi.org/10.1007/s11227-022-04617-x).

[156] K. Jiang, Z. Wang, P. Yi, J. Jiang, J. Xiao, Y. Yao, Deep distillation recursive network for remote sensing imagery super-resolution, *Remote Sensing* 10 (11) (2018) 1700.

[157] Z. Yin, Y. Wu, P. Wu, Z. Hao, F. Ling, Super-resolution mapping with a fraction error eliminating cnn model, *IEEE Transactions on Geoscience and Remote Sensing* 61 (2023) 1–18.

[158] H. Huan, P. Li, N. Zou, C. Wang, Y. Xie, Y. Xie, D. Xu, End-to-end super-resolution for remote-sensing images using an improved multi-scale residual network, *Remote Sensing* 13 (4) (2021) 666.

[159] F. Deeba, Y. Zhou, F. A. Dharejo, Y. Du, X. Wang, S. Kun, Multi-scale single image super-resolution with remote-sensing application using transferred wide residual network, *Wireless Personal Communications* 120 (1) (2021) 323–342.

[160] W. Ye, B. Lin, J. Lao, Y. Liu, Z. Lin, Mra-idn: A lightweight super-

resolution framework of remote sensing images based on multiscale residual attention fusion mechanism, *IEEE Journal of Selected Topics in Applied Earth Observations and Remote Sensing* 17 (2024) 7781–7800. [doi:10.1109/JSTARS.2024.3381653](https://doi.org/10.1109/JSTARS.2024.3381653).

[161] T. Wu, R. Zhao, M. Lv, Z. Jia, L. Li, Z. Wang, H. Ma, Lightweight remote sensing image super-resolution via background-based multiscale feature enhancement network, *IEEE Geoscience and Remote Sensing Letters* 21 (2024) 1–5. [doi:10.1109/LGRS.2024.3481645](https://doi.org/10.1109/LGRS.2024.3481645).

[162] D. Kong, L. Gu, X. Li, F. Gao, Multiscale residual dense network for the super-resolution of remote sensing images, *IEEE Transactions on Geoscience and Remote Sensing* 62 (2024) 1–12. [doi:10.1109/TGRS.2024.3370826](https://doi.org/10.1109/TGRS.2024.3370826).

[163] H. Xiao, X. Chen, L. Luo, C. Lin, A dual-path feature reuse multi-scale network for remote sensing image super-resolution, *The Journal of Supercomputing* 81 (1) (2025) 1–28.

[164] X. Chen, Y. Wu, T. Lu, Q. Kong, J. Wang, Y. Wang, Remote sensing image super-resolution with residual split attention mechanism, *IEEE Journal of Selected Topics in Applied Earth Observations and Remote Sensing* 16 (2023) 1–13.

[165] Z. Chen, X. Han, X. Ma, Combining contextual information by integrated attention mechanism in convolutional neural networks for digital elevation model super-resolution, *IEEE Transactions on Geoscience and Remote Sensing* 62 (2024) 1–16. [doi:10.1109/TGRS.2024.3423716](https://doi.org/10.1109/TGRS.2024.3423716).

[166] Y. Peng, X. Wang, J. Zhang, S. Liu, Pre-training of gated convolution neural network for remote sensing image super-resolution, *IET Image Processing* 15 (5) (2021) 1179–1188.

[167] K. Zhao, T. Lu, Y. Zhang, J. Jiang, Z. Wang, Z. Xiong, Structure-texture dual preserving for remote sensing image super resolution, *IEEE Journal of Selected Topics in Applied Earth Observations and Remote Sensing* 17 (2024) 5527–5540.

[168] W. Wang, T. Mu, Q. Li, H. Li, Q. Yang, A hybrid spectral attention-enabled multiscale spatial-spectral learning network for hyperspectral image superresolution, *IEEE Journal of Selected Topics in Applied Earth Observations and Remote Sensing* 17 (2024) 11016–11033. [doi:10.1109/JSTARS.2024.3407953](https://doi.org/10.1109/JSTARS.2024.3407953).

[169] L. Chen, H. Liu, M. Yang, Y. Qian, Z. Xiao, X. Zhong, Remote sensing image super-resolution via residual aggregation and split attentional fusion network, *IEEE Journal of Selected Topics in Applied Earth Observations and Remote Sensing* 14 (2021) 9546–9556.

[170] Y. Ma, P. Lv, H. Liu, X. Sun, Y. Zhong, Remote sensing image super-resolution based on dense channel attention network, *Remote Sensing* 13 (15) (2021) 2966.

[171] A. Patnaik, M. K. Bhuyan, K. F. MacDorman, A two-branch multiscale residual attention network for single image super-resolution in remote sensing imagery, *IEEE Journal of Selected Topics in Applied Earth Observations and Remote Sensing* 17 (2024) 6003–6013. [doi:10.1109/JSTARS.2024.3371710](https://doi.org/10.1109/JSTARS.2024.3371710).

[172] D. Zhang, J. Shao, X. Li, H. T. Shen, Remote sensing image super-resolution via mixed high-order attention network, *IEEE Transactions on Geoscience and Remote Sensing* 59 (6) (2020) 5183–5196.

[173] B. Huang, B. He, L. Wu, Z. Guo, Deep residual dual-attention network for super-resolution reconstruction of remote sensing images, *Remote Sensing* 13 (14) (2021) 2784.

[174] J. Wang, Y. Wu, L. Wang, L. Wang, O. Alfarraj, A. Tolba, Lightweight feedback convolution neural network for remote sensing images super-resolution, *IEEE Access* 9 (2021) 15992–16003.

[175] C. Ren, X. He, L. Qing, Y. Wu, Y. Pu, Remote sensing image recovery via enhanced residual learning and dual-luminance scheme, *Knowledge-Based Systems* 222 (2021) 107013.

[176] T. Wang, W. Sun, H. Qi, P. Ren, Aerial image super resolution via wavelet multiscale convolutional neural networks, *IEEE Geoscience and Remote Sensing Letters* 15 (5) (2018) 769–773.

[177] J. Yang, Y.-Q. Zhao, J. C.-W. Chan, Hyperspectral image super-resolution based on multi-scale wavelet 3d convolutional neural network, in: *IGARSS 2019-2019 IEEE International Geoscience and Remote Sensing Symposium*, IEEE, 2019, pp. 2770–2773.

[178] N. Aburaed, A. Panthakkan, M. Al-Saad, M. C. El Rai, S. Al Mansoori, H. Al-Ahmad, S. Marshall, Super-resolution of satellite imagery using a wavelet multiscale-based deep convolutional neural network model, in: *Image and Signal Processing for Remote Sensing XXVI*, Vol. 11533, SPIE, 2020, pp. 305–311.

[179] F. Deeba, Y. Zhou, F. A. Dharejo, M. A. Khan, B. Das, X. Wang, Y. Du, A plexus-convolutional neural network framework for fast remote sensing image super-resolution in wavelet domain, *IET Image Processing* 15 (8) (2021) 1679–1687.

[180] K. Thool, S. Deivalakshmi, et al., Combined wavelet and multiwavelet-based convolutional neural network (cwm-cnn) for remote sensing image super resolution, in: *International Conference on Computer Vision and Internet of Things 2023 (ICCVIoT'23)*, Vol. 2023, IET, 2023, pp. 102–107.

[181] C. Lanaras, J. Bioucas-Dias, S. Galliani, E. Baltsavias, K. Schindler, Super-resolution of sentinel-2 images: Learning a globally applicable deep neural network, *ISPRS Journal of Photogrammetry and Remote Sensing* 146 (2018) 305–319.

[182] Z. Yin, F. Ling, X. Li, X. Cai, H. Chi, X. Li, L. Wang, Y. Zhang, Y. Du, A cascaded spectral-spatial cnn model for super-resolution river mapping with modis imagery, *IEEE Transactions on Geoscience and Remote Sensing* 60 (2021) 1–13.

[183] P. V. Arun, K. M. Buddhiraju, A. Porwal, J. Chanussot, Cnn based spectral super-resolution of remote sensing images, *Signal Processing* 169 (2020) 107394.

[184] L. Wagner, L. Liebel, M. Körner, Deep residual learning for single-image super-resolution of multi-spectral satellite imagery, *ISPRS Annals of the Photogrammetry, Remote Sensing and Spatial Information Sciences* 4 (2019) 189–196.

[185] V. Vasilescu, M. Datcu, D. Faur, A cnn-based sentinel-2 image super-resolution method using multiobjective training, *IEEE Transactions on Geoscience and Remote Sensing* 61 (2023) 1–14.

[186] C. Chen, Y. Wang, Y. Zhang, Z. Zhao, H. Feng, Remote sensing hyperspectral image super-resolution via multidomain spatial information and multiscale spectral information fusion, *IEEE Transactions on Geoscience and Remote Sensing* 62 (2024) 1–16. [doi:10.1109/TGRS.2024.3388531](https://doi.org/10.1109/TGRS.2024.3388531).

[187] S. Mei, R. Jiang, X. Li, Q. Du, Spatial and spectral joint super-resolution using convolutional neural network, *IEEE Transactions on Geoscience and Remote Sensing* 58 (7) (2020) 4590–4603.

[188] M. Müller, N. Ekhtiari, R. Almeida, C. Rieke, Super-resolution of multispectral satellite images using convolutional neural networks, *ISPRS Annals of the Photogrammetry, Remote Sensing and Spatial Information Sciences* 1 (2020) 33–40.

[189] W. Xu, X. Guangluan, Y. Wang, X. Sun, D. Lin, W. Yirong, High quality remote sensing image super-resolution using deep memory connected network, in: *IGARSS 2018-2018 IEEE International Geoscience and Remote Sensing Symposium*, IEEE, 2018, pp. 8889–8892.

[190] Y. Chang, B. Luo, Bidirectional convolutional lstm neural network for remote sensing image super-resolution, *Remote Sensing* 11 (20) (2019) 2333.

[191] X. Zhu, H. Talebi, X. Shi, F. Yang, P. Milanfar, Super-resolving commercial satellite imagery using realistic training data, in: *2020 IEEE International Conference on Image Processing (ICIP)*, IEEE, 2020, pp. 498–502.

[192] F. Deeba, F. A. Dharejo, Y. Zhou, A. Ghaffar, M. H. Memon, S. Kun, Single image super-resolution with application to remote-sensing image, in: *2020 Global Conference on Wireless and Optical Technologies (GCWOT)*, IEEE, 2020, pp. 1–6.

[193] Z. Wei, Y. Liu, Construction of super-resolution model of remote sensing image based on deep convolutional neural network, *Computer Communications* 178 (2021) 191–200.

[194] K. Zhao, T. Lu, J. Wang, Y. Zhang, J. Jiang, Z. Xiong, Hyper-laplacian prior for remote sensing image super-resolution, *IEEE Transactions on Geoscience and Remote Sensing* 62 (2024) 1–14. [doi:10.1109/TGRS.2024.3434998](https://doi.org/10.1109/TGRS.2024.3434998).

[195] Z. Yin, P. Wu, X. Li, Z. Hao, X. Ma, R. Fan, C. Liu, F. Ling, Super-resolution water body mapping with a feature collaborative cnn model by fusing sentinel-1 and sentinel-2 images, *International Journal of Applied Earth Observation and Geoinformation* 134 (2024) 104176.

[196] L.-Y. Dai, M.-D. Li, S.-W. Chen, Pccn: Polarimetric contexture convolutional network for polar satellite image super-resolution, *IEEE Journal of Selected Topics in Applied Earth Observations and Remote Sensing* 18 (2025) 4664–4679. [doi:10.1109/JSTARS.2025.3530136](https://doi.org/10.1109/JSTARS.2025.3530136).

[197] C. Ledig, L. Theis, F. Huszár, J. Caballero, A. Cunningham, A. Acosta,

A. Aitken, A. Tejani, J. Totz, Z. Wang, et al., Photo-realistic single image super-resolution using a generative adversarial network, in: Proceedings of the IEEE conference on computer vision and pattern recognition, 2017, pp. 4681–4690.

[198] W. Ma, Z. Pan, J. Guo, B. Lei, Super-resolution of remote sensing images based on transferred generative adversarial network, in: IGARSS 2018-2018 IEEE International Geoscience and Remote Sensing Symposium, IEEE, 2018, pp. 1148–1151.

[199] W. Ma, Z. Pan, F. Yuan, B. Lei, Super-resolution of remote sensing images via a dense residual generative adversarial network, *Remote Sensing* 11 (21) (2019) 2578.

[200] Z. Wang, K. Jiang, P. Yi, Z. Han, Z. He, Ultra-dense gan for satellite imagery super-resolution, *Neurocomputing* 398 (2020) 328–337.

[201] Y.-Z. Chen, T.-J. Liu, K.-H. Liu, Super-resolution of satellite images based on two-dimensional rrd and edge-enhanced generative adversarial network, in: 2022 IEEE International Conference on Consumer Electronics (ICCE), IEEE, 2022, pp. 1–4.

[202] B. Pang, S. Zhao, Y. Liu, The use of a stable super-resolution generative adversarial network (ssrgan) on remote sensing images, *Remote Sensing* 15 (20) (2023) 5064.

[203] B. Liu, H. Li, Y. Zhou, Y. Peng, A. Elazab, C. Wang, A super resolution method for remote sensing images based on cascaded conditional wasserstein gans, in: 2020 IEEE 3rd International Conference on Information Communication and Signal Processing (ICICSP), IEEE, 2020, pp. 284–289.

[204] M. Guo, Z. Zhang, H. Liu, Y. Huang, Ndsgan: A novel dense generative adversarial network for real aerial imagery super-resolution reconstruction, *Remote Sensing* 14 (7) (2022) 1574.

[205] R. Sustika, A. B. Suksmono, D. Danudirdjo, K. Wikantika, Generative adversarial network with residual dense generator for remote sensing image super resolution, in: 2020 International Conference on Radar, Antenna, Microwave, Electronics, and Telecommunications (ICRAMET), IEEE, 2020, pp. 34–39.

[206] Y. Zhao, S. Zhang, J. Hu, Forest single-frame remote sensing image super-resolution using gans, *Forests* 14 (11) (2023) 2188.

[207] M. S. Moustafa, S. A. Sayed, Satellite imagery super-resolution using squeeze-and-excitation-based gan, *International journal of aeronautical and space sciences* 22 (6) (2021) 1481–1492.

[208] Y. Li, S. Mavromatis, F. Zhang, Z. Du, J. Sequeira, Z. Wang, X. Zhao, R. Liu, Single-image super-resolution for remote sensing images using a deep generative adversarial network with local and global attention mechanisms, *IEEE Transactions on Geoscience and Remote Sensing* 60 (2021) 1–24.

[209] H. Zhang, C. Ye, Y. Zhou, R. Tang, R. Wei, A super-resolution network for high-resolution reconstruction of landslide main bodies in remote sensing imagery using coordinated attention mechanisms and deep residual blocks, *Remote Sensing* 15 (18) (2023) 4498.

[210] C. Wang, X. Zhang, W. Yang, X. Li, B. Lu, J. Wang, Msagan: a new super-resolution algorithm for multispectral remote sensing image based on a multiscale attention gan network, *IEEE Geoscience and Remote Sensing Letters* 20 (2023) 1–5.

[211] Z. Ren, L. He, J. Lu, Context aware edge-enhanced gan for remote sensing image super-resolution, *IEEE Journal of Selected Topics in Applied Earth Observations and Remote Sensing* 17 (2023) 1363–1376.

[212] Y. Tang, T. Wang, D. Liu, Mffagan: Generative adversarial network with multilevel feature fusion attention mechanism for remote sensing image super-resolution, *IEEE Journal of Selected Topics in Applied Earth Observations and Remote Sensing* 17 (2024) 6860–6874. [doi:10.1109/JSTARS.2024.3373764](https://doi.org/10.1109/JSTARS.2024.3373764).

[213] M. Guo, F. Xiong, B. Zhao, Y. Huang, Z. Xie, L. Wu, X. Chen, J. Zhang, Tdegan: A texture-detail-enhanced dense generative adversarial network for remote sensing image super-resolution, *Remote Sensing* 16 (13) (2024) 2312.

[214] W. Hu, L. Ju, Y. Du, Y. Li, A super-resolution reconstruction model for remote sensing image based on generative adversarial networks, *Remote Sensing* 16 (8) (2024) 1460.

[215] K. Fan, M. Hu, M. Zhao, L. Qi, W. Xie, H. Zou, B. Wu, S. Zhao, X. Wang, Rmsrgan: A real multispectral imagery super-resolution reconstruction for enhancing ginkgo biloba yield prediction, *Forests* 15 (5) (2024) 859.

[216] M. Chung, M. Jung, Y. Kim, Enhancing remote sensing image super-resolution guided by bicubic-downsampled low-resolution image, *Remote Sensing* 15 (13) (2023) 3309.

[217] K. Karwowska, D. Wierzbicki, Mcwesrgan: Improving enhanced super-resolution generative adversarial network for satellite images, *IEEE Journal of Selected Topics in Applied Earth Observations and Remote Sensing* 16 (2023) 9459–9479.

[218] F. Zhu, C. Wang, B. Zhu, C. Sun, C. Qi, An improved generative adversarial networks for remote sensing image super-resolution reconstruction via multi-scale residual block, *The Egyptian Journal of Remote Sensing and Space Science* 26 (1) (2023) 151–160.

[219] J. Guo, F. Lv, J. Shen, J. Liu, M. Wang, An improved generative adversarial network for remote sensing image super-resolution, *IET Image Processing* 17 (6) (2023) 1852–1863.

[220] J. Kong, Y. Ryu, S. Jeong, Z. Zhong, W. Choi, J. Kim, K. Lee, J. Lim, K. Jang, J. Chun, et al., Super resolution of historic landsat imagery using a dual generative adversarial network (gan) model with cubesat constellation imagery for spatially enhanced long-term vegetation monitoring, *ISPRS Journal of Photogrammetry and Remote Sensing* 200 (2023) 1–23.

[221] G. Sun, Y. Chen, J. Huang, Q. Ma, Y. Ge, Digital surface model super-resolution by integrating high-resolution remote sensing imagery using generative adversarial networks, *IEEE Journal of Selected Topics in Applied Earth Observations and Remote Sensing* 17 (2024) 10636–10647. [doi:10.1109/JSTARS.2024.3399544](https://doi.org/10.1109/JSTARS.2024.3399544).

[222] F. Pineda, V. Ayma, C. Beltran, A generative adversarial network approach for super-resolution of sentinel-2 satellite images, *The International Archives of the Photogrammetry, Remote Sensing and Spatial Information Sciences* 43 (2020) 9–14.

[223] Z.-X. Huang, C.-W. Jing, Super-resolution reconstruction method of remote sensing image based on multi-feature fusion, *Ieee Access* 8 (2020) 18764–18771.

[224] P. Wang, E. Sertel, Multi-frame super-resolution of remote sensing images using attention-based gan models, *Knowledge-Based Systems* 266 (2023) 110387.

[225] Y. Gong, P. Liao, X. Zhang, L. Zhang, G. Chen, K. Zhu, X. Tan, Z. Lv, Enlighten-gan for super resolution reconstruction in mid-resolution remote sensing images, *Remote Sensing* 13 (6) (2021) 1104.

[226] X. Wang, Z. Ao, R. Li, Y. Fu, Y. Xue, Y. Ge, Super-resolution image reconstruction method between sentinel-2 and gaoen-2 based on cascaded generative adversarial networks, *Applied Sciences* 14 (12) (2024) 5013.

[227] A. Vaswani, N. Shazeer, N. Parmar, J. Uszkoreit, L. Jones, A. N. Gomez, Ł. Kaiser, I. Polosukhin, Attention is all you need, *Advances in neural information processing systems* 30 (2017).

[228] A. Dosovitskiy, L. Beyer, A. Kolesnikov, D. Weissenborn, X. Zhai, T. Unterthiner, M. Dehghani, M. Minderer, G. Heigold, S. Gelly, et al., An image is worth 16x16 words: Transformers for image recognition at scale, *arXiv preprint arXiv:2010.11929* (2020).

[229] C. Ye, L. Yan, Y. Zhang, J. Zhan, J. Yang, J. Wang, A super-resolution method of remote sensing image using transformers, in: 2021 11th IEEE International Conference on Intelligent Data Acquisition and Advanced Computing Systems: Technology and Applications (IDAACS), Vol. 2, IEEE, 2021, pp. 905–910.

[230] M. Shi, Y. Gao, L. Chen, X. Liu, Multisource information fusion network for optical remote sensing image super-resolution, *IEEE Journal of Selected Topics in Applied Earth Observations and Remote Sensing* 16 (2023) 3805–3818.

[231] J. Shang, M. Gao, Q. Li, J. Pan, G. Zou, G. Jeon, Hybrid-scale hierarchical transformer for remote sensing image super-resolution, *Remote Sensing* 15 (13) (2023) 3442.

[232] Y. Lu, S. Wang, B. Wang, X. Zhang, X. Wang, Y. Zhao, Enhanced window-based self-attention with global and multi-scale representations for remote sensing image super-resolution, *Remote Sensing* 16 (15) (2024) 2837.

[233] Y. Cao, L. Li, B. Liu, W. Zhou, Z. Li, W. Ni, Cfmb-t: A cross-frequency multi-branch transformer for low-quality infrared remote sensing image super-resolution, *Infrared Physics & Technology* 133 (2023) 104861.

[234] Y. Sun, X. Zhi, S. Jiang, G. Fan, T. Shi, X. Yan, Transformer-based self-supervised image super-resolution method for rotating synthetic aperture system via multi-temporal fusion, *Information Fusion* 108 (2024) 102372.

[235] Z. Xie, J. Wang, W. Song, Y. Du, H. Xu, Q. Yang, Cfformer: Channel fourier transformer for remote sensing super resolution, *IEEE Journal of Selected Topics in Applied Earth Observations and Remote Sensing* 18 (2025) 569–583. [doi:10.1109/JSTARS.2024.3492044](https://doi.org/10.1109/JSTARS.2024.3492044).

[236] J. Liu, X. Yang, Wtt: combining wavelet transform with transformer for remote sensing image super-resolution, *Machine Vision and Applications* 36 (2) (2025) 1–14.

[237] Z. Li, L. Li, B. Liu, Y. Cao, W. Zhou, W. Ni, Z. Yang, Spectral-learning-based transformer network for the spectral super-resolution of remote-sensing degraded images, *IEEE Geoscience and Remote Sensing Letters* 20 (2023) 1–5.

[238] D. Cai, P. Zhang, T<sup>3</sup>SR: Texture transfer transformer for remote sensing image superresolution, *IEEE Journal of Selected Topics in Applied Earth Observations and Remote Sensing* 15 (2022) 7346–7358.

[239] Y. Lu, L. Min, B. Wang, L. Zheng, X. Wang, Y. Zhao, L. Yang, T. Long, Cross-spatial pixel integration and cross-stage feature fusion-based transformer network for remote sensing image super-resolution, *IEEE Transactions on Geoscience and Remote Sensing* 61 (2023) 1–16.

[240] Y. Mao, G. He, G. Wang, R. Yin, Y. Peng, B. Guan, Desat: A distance-enhanced strip attention transformer for remote sensing image super-resolution, *Remote Sensing* 16 (22) (2024) 4251.

[241] Y. Kang, X. Wang, X. Zhang, S. Wang, G. Jin, Act-sr: Aggregation connection transformer for remote sensing image super-resolution, *IEEE Journal of Selected Topics in Applied Earth Observations and Remote Sensing* (2024) 1–12 [doi:10.1109/JSTARS.2024.3506717](https://doi.org/10.1109/JSTARS.2024.3506717).

[242] J. Hao, W. Li, Y. Lu, Y. Jin, Y. Zhao, S. Wang, B. Wang, Scale-aware backprojection transformer for single remote sensing image super-resolution, *IEEE Transactions on Geoscience and Remote Sensing* 62 (2024) 1–13. [doi:10.1109/TGRS.2024.3499363](https://doi.org/10.1109/TGRS.2024.3499363).

[243] A. Gu, T. Dao, Mamba: Linear-time sequence modeling with selective state spaces, *arXiv preprint arXiv:2312.00752* (2023).

[244] Y. Liu, Y. Tian, Y. Zhao, H. Yu, L. Xie, Y. Wang, Q. Ye, J. Jiao, Y. Liu, Vmamba: Visual state space model, *Advances in neural information processing systems* 37 (2024) 103031–103063.

[245] W. Dong, H. Zhu, S. Lin, X. Luo, Y. Shen, X. Liu, J. Zhang, G. Guo, B. Zhang, Fusion-mamba for cross-modality object detection, *arXiv preprint arXiv:2404.09146* (2024).

[246] J. Ma, F. Li, B. Wang, U-mamba: Enhancing long-range dependency for biomedical image segmentation, *arXiv preprint arXiv:2401.04722* (2024).

[247] R. Zhi, X. Fan, J. Shi, Mambaformersr: A lightweight model for remote-sensing image super-resolution, *IEEE Geoscience and Remote Sensing Letters* 21 (2024) 1–5. [doi:10.1109/LGRS.2024.3453428](https://doi.org/10.1109/LGRS.2024.3453428).

[248] G. Zhao, F. Wang, Mamba-based residual network for remote sensing image super-resolution, in: 2024 7th International Conference on Pattern Recognition and Artificial Intelligence (PRAI), IEEE, 2024, pp. 316–321.

[249] J. Liu, Z. Yuan, Z. Pan, Y. Fu, L. Liu, B. Lu, Diffusion model with detail complement for super-resolution of remote sensing, *Remote Sensing* 14 (19) (2022) 4834.

[250] L. Han, Y. Zhao, H. Lv, Y. Zhang, H. Liu, G. Bi, Q. Han, Enhancing remote sensing image super-resolution with efficient hybrid conditional diffusion model, *Remote Sensing* 15 (13) (2023) 3452.

[251] J. Sui, Q. Wu, M.-O. Pun, Denoising diffusion probabilistic model with adversarial learning for remote sensing super-resolution, *Remote Sensing* 16 (7) (2024) 1219.

[252] Y. Zhang, H. Liu, Z. Li, X. Gao, G. Shi, J. Jiang, Tcdm: Effective large-factor image super-resolution via texture consistency diffusion, *IEEE Transactions on Geoscience and Remote Sensing* 62 (2024) 1–13.

[253] C. Zhu, Y. Liu, S. Huang, F. Wang, Taming a diffusion model to revitalize remote sensing image super-resolution, *Remote Sensing* 17 (8) (2025) 1348.

[254] J. He, Q. Yuan, J. Li, Y. Xiao, X. Liu, Y. Zou, Dster: A dense spectral transformer for remote sensing spectral super-resolution, *International Journal of Applied Earth Observation and Geoinformation* 109 (2022) 102773.

[255] J. Tu, G. Mei, Z. Ma, F. Piccialli, Swgan: Generative adversarial network combining swin transformer and cnn for remote sensing image super-resolution, *IEEE Journal of Selected Topics in Applied Earth Observations and Remote Sensing* 15 (2022) 5662–5673.

[256] C. Wang, X. Zhang, W. Yang, G. Wang, Z. Zhao, X. Liu, B. Lu, Landsat-8 to sentinel-2 satellite imagery super-resolution-based multi-scale dilated transformer generative adversarial networks, *Remote Sensing* 15 (22) (2023) 5272.

[257] G. Peng, M. Xie, L. Fang, Context-aware lightweight remote-sensing image super-resolution network, *Frontiers in Neurorobotics* 17 (2023) 1220166.

[258] C. Lin, X. Mao, C. Qiu, L. Zou, Dtcnet: Transformer-cnn distillation for super-resolution of remote sensing image, *IEEE Journal of Selected Topics in Applied Earth Observations and Remote Sensing* 17 (2024) 11117–11133. [doi:10.1109/JSTARS.2024.3409808](https://doi.org/10.1109/JSTARS.2024.3409808).

[259] M. Hou, Z. Huang, Z. Yu, Y. Yan, Y. Zhao, X. Han, Cswt-sr: Conv-swin transformer for blind remote sensing image super-resolution with amplitude-phase learning and structural detail alternating learning, *IEEE Transactions on Geoscience and Remote Sensing* 62 (2024) 1–14. [doi:10.1109/TGRS.2024.3416495](https://doi.org/10.1109/TGRS.2024.3416495).

[260] J. Wang, H. Li, Y. Li, Z. Qin, A lightweight cnn-transformer implemented via structural re-parameterization and hybrid attention for remote sensing image super-resolution, *ISPRS International Journal of Geo-Information* 14 (1) (2024) 8.

[261] F. Huang, Y. Li, X. Ye, J. Wu, Infrared image super-resolution network utilizing the enhanced transformer and u-net, *Sensors* 24 (14) (2024) 4686.

[262] Y. Guo, C. Gong, J. Yan, Activated sparsely sub-pixel transformer for remote sensing image super-resolution, *Remote Sensing* 16 (11) (2024) 1895.

[263] D. Liu, L. Zhong, H. Wu, S. Li, Y. Li, Remote sensing image super-resolution reconstruction by fusing multi-scale receptive fields and hybrid transformer, *Scientific Reports* 15 (1) (2025) 2140.

[264] J. Li, Y. Meng, C. Tao, Z. Zhang, X. Yang, Z. Wang, X. Wang, L. Li, W. Zhang, Convformersr: Fusing transformers and convolutional neural networks for cross-sensor remote sensing imagery super-resolution, *IEEE Transactions on Geoscience and Remote Sensing* 62 (2024) 1–15. [doi:10.1109/TGRS.2023.3340043](https://doi.org/10.1109/TGRS.2023.3340043).

[265] C. Wang, X. Zhang, W. Yang, G. Wang, X. Li, J. Wang, B. Lu, Mswagan: Multispectral remote sensing image super-resolution based on multiscale window attention transformer, *IEEE Transactions on Geoscience and Remote Sensing* 62 (2024) 1–15. [doi:10.1109/TGRS.2024.3385752](https://doi.org/10.1109/TGRS.2024.3385752).

[266] C. Yu, L. Hong, T. Pan, Y. Li, T. Li, Estugan: enhanced swin transformer with u-net discriminator for remote sensing image super-resolution, *Electronics* 12 (20) (2023) 4235.

[267] Z. Lin, B. Lin, W. Ye, Y. Liu, Trans-cnn gan: Self-attention generative adversarial network for remote sensing image super-resolution, in: 2024 4th International Conference on Neural Networks, Information and Communication (NNICE), IEEE, 2024, pp. 456–459.

[268] W. Huo, X. Zhang, S. You, Y. Zhang, Q. Zhang, N. Hu, Stgan: Swin transformer-based gan to achieve remote sensing image super-resolution reconstruction, *Applied Sciences* 15 (1) (2024) 305.

[269] H. Tao, X. Tang, J. Liu, J. Tian, Superresolution remote sensing image processing algorithm based on wavelet transform and interpolation, in: Image Processing and Pattern Recognition in Remote Sensing, Vol. 4898, SPIE, 2003, pp. 259–263.

[270] S. Y. Han, N. H. Park, K. H. Joo, Wavelet transform based image interpolation for remote sensing image, *International Journal of Software Engineering and Its Applications* 9 (2) (2015) 59–66.

[271] M. Mareboyana, J. Le Moigne, Super-resolution of remote sensing images using edge-directed radial basis functions, in: Signal processing, sensor/information fusion, and target recognition XXVII, Vol. 10646, SPIE, 2018, pp. 216–221.

[272] A. J. Patti, M. I. Sezan, A. M. Tekalp, Superresolution video reconstruction with arbitrary sampling lattices and nonzero aperture time, *IEEE transactions on image processing* 6 (8) (1997) 1064–1076.

[273] A. J. Patti, M. I. Sezan, A. M. Tekalp, Robust methods for high-quality stills from interlaced video in the presence of dominant motion, *IEEE Transactions on Circuits and Systems for Video Technology* 7 (2) (1997) 328–342.

[274] M. L. Aguena, N. D. Mascarenhas, Multispectral image data fusion using pocs and super-resolution, *Computer Vision and Image Understanding* 102 (2) (2006) 178–187.

[275] W. Xie, F. Zhang, H. Chen, Q. Qin, Blind super-resolution image reconstruction based on pocs model, in: 2009 international conference

on measuring technology and mechatronics automation, Vol. 1, IEEE, 2009, pp. 437–440.

[276] C. Fan, C. Wu, G. Li, J. Ma, Projections onto convex sets super-resolution reconstruction based on point spread function estimation of low-resolution remote sensing images, *Sensors* 17 (2) (2017) 362.

[277] S. Dai, J. Cui, D. Zhang, Q. Liu, X. Zhang, Study on infrared image super-resolution reconstruction based on an improved pocs algorithm, *Journal of Semiconductors* 38 (4) (2017) 044010.

[278] M. Irani, S. Peleg, Improving resolution by image registration, *CVGIP: Graphical models and image processing* 53 (3) (1991) 231–239.

[279] Y. Lu, M. Imamura, Pyramid-based super-resolution of the undersampled and subpixel shifted image sequence, *International journal of imaging systems and technology* 12 (6) (2002) 254–263.

[280] F. Li, D. Fraser, X. Jia, Improved ibp for super-resolving remote sensing images, *Geographic Information Sciences* 12 (2) (2006) 106–111.

[281] F. Li, D. Fraser, X. Jia, Efficient ibp with super resolution for alos imagery, in: *Geoinformatics 2007: Remotely Sensed Data and Information*, Vol. 6752, SPIE, 2007, pp. 1423–1430.

[282] Z. Yan, Y. Lu, Super resolution of mri using improved ibp, in: *2009 International Conference on Computational Intelligence and Security*, Vol. 1, IEEE, 2009, pp. 643–647.

[283] V. Patel, C. K. Modi, C. N. Paunwala, S. Patnaik, Hybrid approach for single image super resolution using isef and ibp, in: *2011 International Conference on Communication Systems and Network Technologies*, IEEE, 2011, pp. 495–499.

[284] M. N. Bareja, C. K. Modi, An effective iterative back projection based single image super resolution approach, in: *2012 international conference on communication systems and Network technologies*, IEEE, 2012, pp. 95–99.

[285] R. Nayak, S. Monalisa, D. Patra, Spatial super resolution based image reconstruction using hibp, in: *2013 Annual IEEE India Conference (INDICON)*, IEEE, 2013, pp. 1–6.

[286] W. Cong, L. Weifeng, W. Longbiao, L. Qingming, An effective framework of ibp for single facial image super resolution, in: *3rd International Conference on Multimedia Technology (ICMT-13)*, Atlantis Press, 2013, pp. 986–993.

[287] R. Nayak, S. Harshavardhan, D. Patra, Morphology based iterative back-projection for super-resolution reconstruction of image, in: *2014 2nd international conference on emerging technology trends in electronics, communication and networking*, IEEE, 2014, pp. 1–6.

[288] M. Tipping, C. Bishop, Bayesian image super-resolution, *Advances in neural information processing systems* 15 (2002).

[289] R. Molina, J. Mateos, A. K. Katsaggelos, R. Zurita-Milla, S. Liang, J. Liu, X. Li, R. Liu, M. Schaepman, A new super resolution bayesian method for pansharpening landsat etm+ imagery, in: *9th International Symposium on Physical Measurements and Signatures in Remote Sensing (ISPMSRS), ISPRS WG VII/1*, 2005, pp. 280–283.

[290] R. Molina, M. Vega, J. Mateos, A. K. Katsaggelos, Variational posterior distribution approximation in bayesian super resolution reconstruction of multispectral images, *Applied and Computational Harmonic Analysis* 24 (2) (2008) 251–267.

[291] R. Molina, M. Vega, J. Mateos, A. K. Katsaggelos, Parameter estimation in bayesian reconstruction of multispectral images using super resolution techniques, in: *2006 International Conference on Image Processing*, IEEE, 2006, pp. 1749–1752.

[292] R. Molina, M. Vega, J. Mateos, A. K. Katsaggelos, Hierarchical bayesian super resolution reconstruction of multispectral images, in: *2006 14th European Signal Processing Conference*, IEEE, 2006, pp. 1–5.

[293] T. Wang, F. Fang, F. Li, G. Zhang, High-quality bayesian pansharpening, *IEEE Transactions on Image Processing* 28 (1) (2018) 227–239.

[294] S. E. Armannsson, M. O. Ulfarsson, J. Sigurdsson, H. V. Nguyen, J. R. Sveinsson, A comparison of optimized sentinel-2 super-resolution methods using wald's protocol and bayesian optimization, *Remote Sensing* 13 (11) (2021) 2192.

[295] W. Li, M. Li, L. Zuo, H. Sun, H. Chen, Y. Li, Forward-looking super-resolution imaging for sea-surface target with multi-prior bayesian method, *Remote Sensing* 14 (1) (2021) 26.

[296] K. Tan, X. Lu, J. Yang, W. Su, H. Gu, A novel bayesian super-resolution method for radar forward-looking imaging based on markov random field model, *Remote Sensing* 13 (20) (2021) 4115.

[297] J. Shen, D. Mao, Y. Zhang, Y. Huang, H. Yang, J. Yang, Super-resolution imaging method for forward-looking scanning radar based on two-layer bayesian model, in: *2024 IEEE Radar Conference (RadarConf24)*, IEEE, 2024, pp. 1–6.

[298] G. K. Chantas, N. P. Galatsanos, N. A. Woods, Super-resolution based on fast registration and maximum a posteriori reconstruction, *IEEE Transactions on Image Processing* 16 (7) (2007) 1821–1830.

[299] S. Wang, L. Zhuo, X. Li, Spectral imagery super resolution by using of a high resolution panchromatic image, in: *2010 3rd International Conference on Computer Science and Information Technology*, Vol. 4, IEEE, 2010, pp. 220–224.

[300] S. P. Belekos, N. P. Galatsanos, A. K. Katsaggelos, Maximum a posteriori video super-resolution using a new multichannel image prior, *IEEE transactions on image processing* 19 (6) (2010) 1451–1464.

[301] F. Li, X. Jia, D. Fraser, A. Lambert, Super resolution for remote sensing images based on a universal hidden markov tree model, *IEEE Transactions on Geoscience and Remote Sensing* 48 (3) (2009) 1270–1278.

[302] J. Guan, J. Yang, Y. Huang, W. Li, Maximum a posteriori-based angular superresolution for scanning radar imaging, *IEEE Transactions on Aerospace and Electronic Systems* 50 (3) (2014) 2389–2398.

[303] Q. Yuan, L. Yan, J. Li, L. Zhang, Remote sensing image super-resolution via regional spatially adaptive total variation model, in: *2014 IEEE Geoscience and Remote Sensing Symposium*, IEEE, 2014, pp. 3073–3076.

[304] F. Li, L. Xin, Y. Guo, D. Gao, X. Kong, X. Jia, Super-resolution for gaofen-4 remote sensing images, *IEEE Geoscience and Remote Sensing Letters* 15 (1) (2017) 28–32.

[305] H. Irmak, G. B. Akar, S. E. Yuksel, H. Ayaylan, Super-resolution reconstruction of hyperspectral images via an improved map-based approach, in: *2016 IEEE International Geoscience and Remote Sensing Symposium (IGARSS)*, IEEE, 2016, pp. 7244–7247.

[306] K. Tan, W. Li, Q. Zhang, Y. Huang, J. Wu, J. Yang, Penalized maximum likelihood angular super-resolution method for scanning radar forward-looking imaging, *Sensors* 18 (3) (2018) 912.

[307] K. Tan, W. Li, J. Pei, Y. Huang, J. Yang, An i/q-channel modeling maximum likelihood super-resolution imaging method for forward-looking scanning radar, *IEEE Geoscience and Remote Sensing Letters* 15 (6) (2018) 863–867.

[308] X. Wu, Y. Fang, D. Wu, Super-resolution imaging method based on fast maximum likelihood, in: *2021 IEEE 5th Advanced Information Technology, Electronic and Automation Control Conference (IAEAC)*, IEEE, 2021, pp. 1545–1548.

[309] X. Li, Y. Du, F. Ling, Super-resolution mapping of forests with bitemporal different spatial resolution images based on the spatial-temporal markov random field, *IEEE Journal of Selected Topics in Applied Earth Observations and Remote Sensing* 7 (1) (2013) 29–39.

[310] H. Aghighi, J. Trinder, S. Lim, Y. Tarabalka, Fully spatially adaptive smoothing parameter estimation for markov random field super-resolution mapping of remotely sensed images, *International Journal of Remote Sensing* 36 (11) (2015) 2851–2879.

[311] D. Welikanna, M. Tamura, Fuzzy parameters integrated markov random field (mrf) model for super resolution mapping (srm) over vague land cover regions, *Journal of Geospatial Surveying* 4 (1) (2024).

[312] Y. Choi, Y. Kim, A no-reference super resolution for satellite image quality enhancement for kompsat-3, in: *IGARSS 2020-2020 IEEE International Geoscience and Remote Sensing Symposium*, IEEE, 2020, pp. 220–223.

[313] N. L. Nguyen, J. Anger, A. Davy, P. Arias, G. Facciolo, Self-supervised multi-image super-resolution for push-frame satellite images, in: *Proceedings of the IEEE/CVF Conference on Computer Vision and Pattern Recognition*, 2021, pp. 1121–1131.

[314] D. Hong, J. Yao, C. Li, D. Meng, N. Yokoya, J. Chanussot, Decoupled-and-coupled networks: Self-supervised hyperspectral image super-resolution with subpixel fusion, *IEEE Transactions on Geoscience and Remote Sensing* 61 (2023) 1–12.

[315] D. Mishra, O. Hadar, Accelerating neural style-transfer using contrastive learning for unsupervised satellite image super-resolution, *IEEE Transactions on Geoscience and Remote Sensing* 61 (2023) 1–14.

[316] P. Wang, H. Zhang, F. Zhou, Z. Jiang, Unsupervised remote sensing image super-resolution using cycle cnn, in: *IGARSS 2019-2019 IEEE International Geoscience and Remote Sensing Symposium*, IEEE, 2019, pp. 3117–3120.

[317] N. Zhang, Y. Wang, X. Zhang, D. Xu, X. Wang, An unsupervised remote sensing single-image super-resolution method based on generative adversarial network, *IEEE Access* 8 (2020) 29027–29039.

[318] Y. Yang, Y. Wu, Enhanced zero-shot learning algorithm for super-resolution reconstruction of remote sensing images, in: 2022 IEEE 8th International Conference on Computer and Communications (ICCC), IEEE, 2022, pp. 1994–1998.

[319] R. Bose, V. Rangnekar, B. Banerjee, S. Chaudhuri, Zero-shot remote sensing image super-resolution based on image continuity and self tessellations, in: DAGM German Conference on Pattern Recognition, Springer, 2021, pp. 649–662.

[320] C. Aybar, D. Montero, S. Donike, F. Kalaitzis, L. Gómez-Chova, A comprehensive benchmark for optical remote sensing image super-resolution, *IEEE Geoscience and Remote Sensing Letters* (2024).

[321] Y. Wang, S. M. A. Bashir, M. Khan, Q. Ullah, R. Wang, Y. Song, Z. Guo, Y. Niu, Remote sensing image super-resolution and object detection: Benchmark and state of the art, *Expert Systems with Applications* 197 (2022) 116793.

[322] P. Kowaleczko, T. Tarasiewicz, M. Ziaja, D. Kostrzewa, J. Nalepa, P. Rokita, M. Kawulok, A real-world benchmark for sentinel-2 multi-image super-resolution, *Scientific Data* 10 (1) (2023) 644.

[323] J. Wang, L. Xiang, L. Liu, J. Xu, P. Li, Q. Xu, Z. He, Toward real-world remote sensing image super-resolution: A new benchmark and an efficient model, *IEEE Transactions on Geoscience and Remote Sensing* 63 (2025) 1–13. [doi:10.1109/TGRS.2024.3516538](https://doi.org/10.1109/TGRS.2024.3516538).

[324] Y. Yang, S. Newsam, Bag-of-visual-words and spatial extensions for land-use classification, in: Proceedings of the 18th SIGSPATIAL international conference on advances in geographic information systems, 2010, pp. 270–279.

[325] D. Dai, W. Yang, Satellite image classification via two-layer sparse coding with biased image representation, *IEEE Transactions on Geoscience and Remote Sensing* 8 (1) (2011) 173–176.

[326] Q. Zou, L. Ni, T. Zhang, Q. Wang, Deep learning based feature selection for remote sensing scene classification, *IEEE Geoscience and remote sensing letters* 12 (11) (2015) 2321–2325.

[327] G.-S. Xia, J. Hu, F. Hu, B. Shi, X. Bai, Y. Zhong, L. Zhang, X. Lu, Aid: A benchmark data set for performance evaluation of aerial scene classification, *IEEE Transactions on Geoscience and Remote Sensing* 55 (7) (2017) 3965–3981.

[328] troylau, W. Cukierski, Draper Satellite Image Chronology, <https://kaggle.com/competitions/draper-satellite-image-chronology>, accessed: [Insert Access Date] (2016).

[329] G. Cheng, J. Han, X. Lu, Remote sensing image scene classification: Benchmark and state of the art, *Proceedings of the IEEE* 105 (10) (2017) 1865–1883.

[330] W. Zhou, S. Newsam, C. Li, Z. Shao, Patternnet: A benchmark dataset for performance evaluation of remote sensing image retrieval, *ISPRS journal of photogrammetry and remote sensing* 145 (2018) 197–209.

[331] G.-S. Xia, X. Bai, J. Ding, Z. Zhu, S. Belongie, J. Luo, M. Datcu, M. Pelillo, L. Zhang, Dota: A large-scale dataset for object detection in aerial images, in: Proceedings of the IEEE conference on computer vision and pattern recognition, 2018, pp. 3974–3983.

[332] SpaceNet on AWS, The SpaceNet Catalog, <https://spacenet.ai/datasets/>, accessed: August 1, 2021 (2018).

[333] Data Fusion Contest 2019 (DFC2019), <https://ieee-dataport.org/open-access/data-fusion-contest-2019-dfc2019>, accessed: [Insert Access Date] (2019).

[334] Q. Wang, S. Liu, J. Chanussot, X. Li, Scene classification with recurrent attention of vhr remote sensing images, *IEEE Transactions on Geoscience and Remote Sensing* 57 (2) (2018) 1155–1167.

[335] B. Zhao, Y. Zhong, G.-S. Xia, L. Zhang, Dirichlet-derived multiple topic scene classification model for high spatial resolution remote sensing imagery, *IEEE Transactions on Geoscience and Remote Sensing* 54 (4) (2015) 2108–2123.

[336] H. Li, X. Dou, C. Tao, Z. Wu, J. Chen, J. Peng, M. Deng, L. Zhao, Rscb: A large-scale remote sensing image classification benchmark using crowdsourced data, *Sensors* 20 (6) (2020) 1594. [doi:doi.org/10.3390/s20061594](https://doi.org/10.3390/s20061594).

[337] Z. Wang, A. C. Bovik, H. R. Sheikh, E. P. Simoncelli, Image quality assessment: from error visibility to structural similarity, *IEEE transactions on image processing* 13 (4) (2004) 600–612.

[338] R. Zhang, P. Isola, A. A. Efros, E. Shechtman, O. Wang, The unreasonable effectiveness of deep features as a perceptual metric, in: Proceedings of the IEEE conference on computer vision and pattern recognition, 2018, pp. 586–595.

[339] A. Mittal, R. Soundararajan, A. C. Bovik, Making a “completely blind” image quality analyzer, *IEEE Signal processing letters* 20 (3) (2012) 209–212.

[340] R. H. Yuhas, A. F. Goetz, J. W. Boardman, Discrimination among semi-arid landscape endmembers using the spectral angle mapper (sam) algorithm, in: JPL, Summaries of the Third Annual JPL Airborne Geoscience Workshop, Volume 1: AVIRIS Workshop, 1992.

[341] A. A. Chen, X. Chai, B. Chen, R. Bian, Q. Chen, A novel stochastic stratified average gradient method: Convergence rate and its complexity, in: 2018 International Joint Conference on Neural Networks (IJCNN), IEEE, 2018, pp. 1–8.

[342] Y. Blau, R. Mechrez, R. Timofte, T. Michaeli, L. Zelnik-Manor, The 2018 pirm challenge on perceptual image super-resolution, in: Proceedings of the European Conference on Computer Vision (ECCV) Workshops, 2018.

[343] C. Ma, C.-Y. Yang, X. Yang, M.-H. Yang, Learning a no-reference quality metric for single-image super-resolution, *Computer Vision and Image Understanding* 158 (2017) 1–16.

[344] L. Wald, Quality of high resolution synthesised images: Is there a simple criterion?, in: Third conference “Fusion of Earth data: merging point measurements, raster maps and remotely sensed images”, SEE/URISCA, 2000, pp. 99–103.

[345] Z. Wang, A. C. Bovik, A universal image quality index, *IEEE signal processing letters* 9 (3) (2002) 81–84.

[346] L. Alparone, B. Aiazzi, S. Baronti, A. Garzelli, F. Nencini, M. Selva, Multispectral and panchromatic data fusion assessment without reference, *Photogrammetric Engineering & Remote Sensing* 74 (2) (2008) 193–200.

[347] H. R. Sheikh, A. C. Bovik, Image information and visual quality, *IEEE Transactions on image processing* 15 (2) (2006) 430–444.

[348] L. Zhang, L. Zhang, X. Mou, D. Zhang, Fsim: A feature similarity index for image quality assessment, *IEEE transactions on Image Processing* 20 (8) (2011) 2378–2386.

[349] C.-I. Chang, Spectral information divergence for hyperspectral image analysis, in: IEEE 1999 International Geoscience and Remote Sensing Symposium. IGARSS’99 (Cat. No. 99CH36293), Vol. 1, IEEE, 1999, pp. 509–511.

[350] Q. Du, O. Gungor, J. Shan, Performance evaluation for pan-sharpening techniques, in: Proceedings. 2005 IEEE International Geoscience and Remote Sensing Symposium, 2005. IGARSS ’05., Vol. 6, 2005, pp. 4264–4266. [doi:10.1109/IGARSS.2005.1525860](https://doi.org/10.1109/IGARSS.2005.1525860).